NANYANG TECHNOLOGICAL UNIVERSITY

INJECTABLE AND BIOMIMETIC POLY (ETHYLENE GLYCOL) HYDROGEL SYSTEMS FOR *IN SITU* THERAPEUTIC CELL DELIVERY

CAO YE

SCHOOL OF MATERIALS SCIENCE AND ENGINEERING

2017

INJECTABLE AND BIOMIMETIC POLY (ETHYLENE GLYCOL) HYDROGEL SYSTEMS FOR IN SITU THERAPEUTIC CELL DELIVERY

CAO YE

SCHOOL OF MATERIALS SCIENCE AND ENGINEERING

A thesis submitted to the Nanyang Technological University in partial fulfilment of the requirement for the degree of Doctor of Philosophy

2017

Statement of Originality

I hereby certify that the work embodied in this thesis is the result of original research and has not been submitted for a higher degree to any other University or Institution.

. . . . . .
Date

. . . . . .
CAO YE

Abstract

Biomimetic poly (ethylene glycol) (PEG)-based hydrogels have been widely explored as extracellular matrix (ECM) mimicking hydrogels as they conserve the advantages of both ECM (cell-responsive molecules) and synthetic hydrogels (controllable structure and mechanical properties), but did not mimic natural ECM well enough due to limited instructive cues. The aim of this work is to synthesize and characterize a novel and facile prepared multi ECM proteins incorporated PEG hydrogel system that can better mimic natural ECM and innately guide cell behavior. Gelatin, elastin and PEG diacrylate (PEGDA) were designed to synthesize biomimetic hydrogels in this study for developing ECM-mimicking synthetic hydrogels. In this thesis, the thiolation of ECM proteins were finished first; thiolated ECM protein was then conjugated to one end of PEGDA by Michael type addition reaction. Two kinds of elastin-PEG hydrogels were fabricated and encapsulated with smooth muscle cells (SMCs), but SMCs were not able to attach in 3-dimensional (3-D), presumably due to lack of strong cell adhesion peptides or sequences. Therefore, gelatin was considered that combining other biological cues with elastin to support ADCs attachment and growth. Two kinds of gelatin-PEG precursors, GP30 and GP60, were synthesized by adjusting the amount of Traut's reagent. FRP (NHDFs) were encapsulated into the gelatin-PEG hydrogel by crosslinking the remaining double bonds of precursor under UV light *in situ* with high cell viability. In particular, this study proved that a minimum amount of cell-binding motifs (gelatin > 2.3 wt/v %) are required for attachment; and appropriate initial mechanical properties (storage modulus <~100 Pa or mesh size >~150 nm) can accelerate the attachment of cells and improve cell viability. Therefore, this gelatin-PEG hydrogel system with tunable mechanical properties (storage modulus: 40~2000Pa) can support cell attachment, growth and help to rebuild a new ECM in 3-D microenvironments. Further studies of gelatin-PEG hydrogels on better mimicking natural ECM were done by covalently conjugating soluble elastin. Elastin has been conjugated into gelatin-PEG hydrogel to innately guide cell behavior and help the remolding of new ECM in 3-D microenvironment for better mimicking natural ECM. To evaluate the benefits of covalently-bound elastin, NHDFs were encapsulated into

the hybrid hydrogel systems *in situ* and demonstrated high viability (>95%). This work showed that covalently conjugating elastin to gelatin-PEG hydrogel is more effective in guiding fibroblast behavior by promoting the spreading and proliferation of NHDFs and finally to secret their-own ECM protein in 3-D. Results from NHDFs studies showed that proliferation rate of NHDFs in GEP45 (13.5%) and GEP30 (11.4%) were higher than that of control (7.3%) on day 9. Live/dead staining showed that NHDFs in GEP45 and GEP30 could form extensive intercellular networks, while NHDFs in GPE control showed limited spreading and networks. Besides, F-actin and ECM proteins (collagen type I and elastin) staining revealed that cells in GPE45 and GPE30 showed significant cytoplasmic spreading and F-actin bundling compared with GPE control hydrogels. Taken together, the ability of elastin to alter the biological response of gelatin-PEG hydrogel in 3-D has led to a better ECM-mimicking construct highly suitable for soft tissues (especially dermal substitutes). To the best of our knowledge, this is the first injectable and multiple ECM-proteins incorporated ECM-mimicking PEG hydrogel with tunable mechanical properties that can effectively help to rebuild new ECM for the specific application of soft tissue replacement.

Acknowledgements

I would like to express my utmost gratitude to my supervisors, Professor Subbu Venkatraman and Professor Havazelet Bianco-Peled, for their continuous support, patience and valuable advice throughout these years. I would also like to thank my thesis advisory committee members, Assistant Professor Fong Wen Mei, Eileen and Assistant Professor Terry W.J. Steele for their advices on this work.

Next, I would like to thank my senior, Dr Lee Bae Hoon, who is highly skillful and patient when guiding me during my early days of research. Without his kindest help, it would have taken me much more time to learn various techniques. Also, I would like to show my appreciation to Dr Wong Yee Shan, Dr Huang Yingying, Dr Susan Liao, Dr Xiong Minru Gordon, Dr Sow Wan Ting, Mr. Lui Yuan Siang, Ms. Chua Hui Yee, Ms. Chan Jing Ni, Mr. Tan Yang Fei, Ms. Tan Wei Ni Dulcia, Ms. Seah Xin Ying, Ms. Chaw Su Yin, Ms. Joseph Rini Rachel, for their tremendous support and friendship. My appreciation also extends to my friends in Technion-Israel Institute of Technology, Ms. Yulia Poshumensky, Ms. Shaked Eliyahu, and Ms. Gefen Adi.

I would also like to take this opportunity to thank Nanyang Technological University and Technion-Israel Institute of Technology for supporting the author under NTU-Technion Joint PhD degree programme.

Last but not least, I would like to dedicate this thesis to my parents and all of my friends for their powerful support and help.

Table Captions

Figure Captions

primary amine groups;(B) The disulfide bonds of protein can be cleaved by DTT, while the byproduct can be removed by dialysis method; (C) Ellman's reagents react with a thiol and then produce the chromogenic TNB anion, which can be measured by its absorbance at 412 nm.

Figure 3.3 The reduction reaction of TCEP and disulfides.

Figure 3.4 Two molecules of BCA react with one copper ion that produced from a protein -mediated biuret reaction.

Figure 4.1 The fabrication routine of Elastin-PEG hydrogel.

Figure 4.2 The relationship between EDC amount and sulfhydryl group amount (n=4)

Figure 4.3 FTIR spectra of ES, ES-PEG, EP, EP EP-SS, EP-PEG and PEGDA.

Figure 4.4 ^{1}H-NMR figure: A:6.1 (dd,-CH=CH_2); B:5.8 and 6.4 (dd,-CH=CH_2).

Figure 4.5 The electrophoresis results of elastin and modification elastin. (There were 7 wells. Well 1: ES; well 2: EP; well 3: ES-SS; well 4: EP-SS, well 5: Maker; well 6: ES-PEG; well 7: EP-PEG. The elastin concentration was lower in Elastin-PEG comparing with Elastin or Elastin-SS, so the samples in wells of ES-PEG and EP-PEG were increased about ten times than the others. The protein concentrations would be explained in the BCA part.)

Figure 4.6 FBs and SMCs were seeding into cell culture medium with the existing of ES-PEG (100mg/mL), EP-PEG (100mg/mL), respectively.

Figure 4.7 Morphology of SMCs encapsulated in ES-PEG, EP-PEG and PEGDA hydrogel.

Figure 5.1 (A) The synthesis method of gelatin-PEG precursor. Sulfhydryl groups were conjugated with the primary amine groups of gelatin *via* reacting with Traut's reagent. (B) Cells were encapsulated into gelatin-PEG hydrogel *via* photo-polymerization with Irgacure 2959.

Figure 5.2 ^{1}H NMR spectrums of original gelatin, PEGDA, and gelatin-PEG.

Figure 5.3 Shear storage modulus and loss modulus data (A) and damping factor-tan δ (B) from rheological experiments that were determined during photo-polymerization of all the hydrogels. The UV light was turned on after 60 seconds.

Figure 5.4 Initial mesh sizes of gelatin-PEG hydrogels after photo-crosslinking.

Figure 5.5 Swelling properties of gelatin-PEG hydrogel (A: GP30 hydrogels; B: GP 60 hydrogels) and control PEG hydrogel (n=4).

Figure 5.6 The mesh size change (mesh size at each time point divided by initial mesh size) of various cell encapsulated gelatin-PEG hydrogels at day 1, day 3 and day7 (n=3, $p<0.05$).

Figure 5.7 3-D cell encapsulation in GP30-45, GP30-55 and control PEG hydrogels. Live/dead staining reveals the survival and morphology of cells within the gel (Live: green/Dead: red). The red scale bar at the bottom right side is 50μm.

Figure 5.8 Cell morphology of 3-D cell encapsulation in GP30-45, GP30-55, GP60-45 and GP60-55 at day 16.

Figure 5.9 Schematic illustrations of interactions between cells and the hydrogel networks. (The dotted line means the broken network of hydrogel, while the solid line is network of hydrogel. And then the red rectangle means gelatin molecules.)

levels for flow cytometry data was used to estimate the percentage of proliferation cells during 24hours EdU incubation. (Non pro represents the percentage of non-proliferation cells, while pro means the percentage of proliferation cells.)

Figure 6.9 (A) Immunofluorescence staining for elastin, collagen type I, F-actin in GEP45, GEP30 and GPE control at day 10. Scale bar=250μm.The antibodies are only reactive with human specific collagen type I and elastin. (B) Immunofluorescence staining for elastin (green) and collagen type I A (yellow) in cell free GEP45, GEP30 and GPE control. Scale bar=250μm.

Figure 6.10 Effect of elastin addition on ECM proteins (collagen 1A and elastin) gene expression at day 9. Elastin addition resulted in a significant increase in collagen 1A and elastin at day 9. Gene expression was normalized to the housekeeping gene GAPDH and expressed as fold change versus NHDFs seeded GPE control hydrogels (considered as 1) at day 9. * denote $p<0.05$.n=4.

Abbreviations

2-D	2- Dimension
3-D	3- Dimension
AAc	Acrylic acid
AAm	Acrylamide
ADCs	Anchorage-dependent cells
BSA	Bovine Serum Albumin
BCA	Bicinchoninic acid
DAPI	4', 6-diamidino-2-phenylindole
DCM	Dichloride methylene
DTT	Dithiothreitol
EBP	Elastin-binding protein
EDC	1-ethyl-3-(3-dimethylamino) propyl carbodiimide, hydrochloride
EdU	5-ethynyl-2'-deoxyuridine
GAGs	Glycosaminoglycans
FTIR	Fourier Transform Infrared Spectroscopy
FBS	Fetal Bovine Serum
FRP	Free radical polymerization
HA	Hyaluronic acid
HCl	Hydrochloride Acid
HPLC	High Performance Liquid Chromatography
HUVECs	Human Umbilical Vein Endothelial Cells
MA	Methacrylamide
MMPs	Matrix metalloproteinases
MSCs	Human mesenchymal stem cells
MWCO	Molecular weight cut off
NHS	N- hydroxysuccinimide
NIPAm	N-isopropylacrylamide
NHDFs	Neonatal human dermal fibroblasts

NMR	Nuclear magnetic resonance
PBS	Phosphate Buffer Saline
PNIPAm	Poly NIPAm
PEG	Polyethylene glycol
PEGDA	PEG diacrylate
PEO	Poly (ethyleneoxide)
PPO	Poly (propylene oxide)
PFA	Paraformaldehyde
PGs	Proteoglycans
PGA	Poly (glycolic acid)
PLA	Poly (lactic acid)
PCL	Poly (ε-caprolactone)
RGD	Arginine - glycine- aspartic acid
SMCs	Artery smooth muscle cells
TCEP	Tris (2-caboxyethyl) Phosphine
TFF	Tangential flow filtration
VIS	Visible light
UV	Ultraviolet light
Q	Swelling ratio
Q_m	Mass swelling ratio
Q_v	Volume swelling ratio
$\upsilon_{2,s}$	The polymer volume fraction in the swollen state
M_c	Number average molecular weight of the chain between two cross-links
ξ	The network mesh size

Chapter 1

Introduction

This chapter briefly introduces the status of the art of tissue engineering and the current shortcomings of this discipline. Extracellular matrix (ECM) based natural hydrogel and synthetic hydrogels have been explored to face the challenges in tissue engineering, and the advantages and disadvantages of both hydrogels have been analyzed. Inspired by nature, ECM-derived proteins incorporated in synthetic hydrogels may be a promising and alternative approach to overcome these limitations for cell delivery based tissue regeneration. In summary, this chapter contains several sections to introduce the background, problem statement, hypothesis, objective and scope.

1.1 Background

Tissue engineering utilizes methods from chemistry, materials, engineering and life sciences to fabricate artificial and living substitutes to guide the regeneration of tissue or to improve tissue function.[1, 2] In order to deliver the cells to the appropriate location in the body, many cellular delivery systems have been explored. The two dominant methods are an injectable system incorporating replacement cells, or a solid scaffold incorporating cells and needed bioactive molecules. A variety of materials have been explored as scaffolds by combing cells, proteins, genes, or other biological molecules into an artificial porous bioactive scaffold.[3] In particular, hydrogels have been extensively explored as tissue engineering scaffolds because of their high water retaining capacity, biological similarity to natural extracellular matrix (ECM), ability to deliver cells *in situ*, host tissue adhesive properties and non-invasive method of delivery.[4] The natural ECM has been an attractive model for biomimetic scaffolds. Therefore, ECM-derived proteins such as gelatin and collagen have been fabricated into natural hydrogels and shown excellent cell behaviors.[5] However, ECM-derived natural hydrogels is often limit used due to relatively poor mechanical properties, inability to control their structure and degradation, and potential immunogenic infection and variability of properties based on source.[5] Compared with ECM-derived natural hydrogels, synthetic hydrogels is a good choice for hydrogel scaffolds because of tunable mechanical properties, controllable structure and compositions. Therefore, rational design of biomimetic scaffolds is based on the combination of natural ECM-derived proteins and synthetic hydrogel, which provide cells with both essential biological cues and tunable mechanical properties. Hence, to create an ideal cellular microenvironment conducive to the regeneration of tissue, biomimetic constructs with cell adhesion, biodegradability and tunable mechanical properties are required.

Injectable biopolymer hydrogels display great promise for cell delivery due to their high water retaining capacity, host tissue adhesive properties, biological similarity to natural extracellular matrix, tunable mechanical characteristics, controllable porosity, and minimally invasive method of delivery. Furthermore, after having served as a temporary scaffold, hydrogels can be degraded into non-toxic soluble by-products that can be

cleared or metabolized without surgery.[6] Polyethylene glycol (PEG) hydrogel, an important type of synthetic hydrogel, is attractive and promising synthetic scaffolds to construct three-dimensional (3-D) structures in aqueous environments for tissue engineering because they have several merits including biocompatibility, hydrophilicity, controllable mechanical properties and degradation.[5] Despite these advantages, pure PEG hydrogel suffers from the inability to incorporated cells due to lack of biological cues to interact with cell-surface molecules, particularly integrin. Another problem arising from using pure PEG hydrogel for tissue engineering is that it is not naturally degradable. Yet the degradation can be enhanced by conjugating degradable polymer, functional groups or biological cues.[4, 7, 8] To overcome these disadvantages, a variety of bioactive modified PEG hydrogels were fabricated by tailoring biological cues to mimic the natural ECM, such as Arg-Gly-Asp (RGD) and matrix metalloproteinases (MMPs).[5] Extensive chemical modifications have been explored to fabricate a biological response and cell compatible PEG hydrogel, while cells can be encapsulated in to the hydrogel simultaneously. In this thesis, the research was focusing on developing an injectable cellular delivery system based on photo-polymerized hydrogels. Photo-polymerization, which triggers the polymerization of liquid PEG monomer (normally acrylate) solutions to form solid hydrogels by UV at physiological temperature and pH, is one of the most common and easy approaches to fabricate PEG hydrogels.[9-11] For tissue engineering, the cells are added into the protein-polymer precursor solution; the cells are homogeneously encapsulated inside the PEG hydrogel scaffold after photo-polymerization. Despite these advantages, photo-polymerization of cell loaded hydrogel process can be done *in situ*, which means that cell encapsulated constructs can be transplant to injury tissue through minimally invasive surgery.[5, 6, 12] Thus, this method can provide a convenient way to fabricate cell-encapsulated injuectables which form hydrogels *in situ* with controllable structure and mechanical properties. Previous studies proved that aqueous solutions of acrylate and bioactive modified PEG could be photo-polymerized directly while contacting cells and tissues without harmful effects.[4, 13] In this thesis, PEG diacrylate (PEGDA) was conjugated with biological cues through Michael-type addition reaction and then fabricated into hydrogel via photo-polymerization. In addition, the ester bonds in PEGDA and the structure of –S-CH_2-

(thiol-acrylate based Michael-type addition reaction) have been introduced to PEG hydrogel in this thesis to enhance the degradation of PEG-based hydrogels according to previous studies.[5, 14, 15]

Natural tissue is assembled from different kinds of cell embedded in ECM hydrogels, which are complex networks and secreted by the cells.[16, 17] The natural ECM not only provides mechanical support for tissue, but also guides cell behaviors to satisfy the specify needs of different tissue.[5] Therefore, ECM components play a crucial and meaningful role in tissue remodeling because they can modulate cell behaviors including cell adhesion, spreading, phenotype type, proteolytic degradation and differentiation innately. Natural ECM proteins, such as gelatin,[18] collagen,[19] fibrin[20] and hyaluronic acid[21] have been used as natural hydrogels due to excellent cell adhesion and biodegradation properties.[5] But the uses of the natural ECM proteins as natural hydrogels are limited due to their poor mechanical properties and potential immunogen problems. Taking cues from the natural ECM, several ECM-derived proteins or peptides sequences were conjugated into PEG hydrogels to guide cell behaviors in 3-D. Substantial challenges remain in the design and fabrication of ECM-mimicking hydrogels with high cell viability and controlled behavior in situ. Currently, biomimetic PEG hydrogels do not mimic natural ECM well enough due to limited biological or instructive cues. Consequently, this led to low cell viability, unsatisfactory cell behaviors and compromised the effect of delivered therapeutic-cells. To overcome those multiple challenges and afterwards enhance controlling cell behavior in a more effective way, there is a need to develop hybrid hydrogels that can mimic multiple functions of ECM with tunable mechanical properties and finally provide predictable control over cell fate while allowing facile delivery of the cells to injury tissue. In this thesis, the thiol-acrylate based Michael-type addition reaction was explored to achieve a hybrid hydrogel system by crosslinking of ECM-derived proteins and PEGDA.

1.2 Problem statement

It has been demonstrated that cells behave more natively when cultured in 3-D microenvironment.[22, 23] In order to truly mimic the biological microenvironment in 3-

D, gelatin and elastin were conjugated into PEG hydrogels to modulate the cell behaviors in 3-D. Gelatin, denatured from collagen, is easily achieved, bio-degradable, widely-used material in tissue engineering which proved to have good biocompatibility *in vivo*. Moreover, gelatin processes cell-adhesive peptides such as RGD and MMP-sensitive degradation sequences, which is important for encapsulated cells. A variety of researches have investigated gelatin-related hydrogels fabricated *via* Michael type addition reaction or photo-polymerization for tissue regeneration.[24-26] An interpenetrating gelatin methacrylamide (MA) - PEG hydrogel was fabricated by photo-polymerization of gelatin-MA, PEG tetra-thiol and PEG tetra-alkyne. Though 90% of the encapsulated endothelial cells were alive after 7 days, most cells were still round-shape and showed delayed proliferation probably due to the improper initial mechanical properties (modulus from 10.8 to 327.7 kPa) of the hydrogel and limit biological cues(inefficient gelatin dissolution).[18] Another kind of gelatin-PEG diacrylate hydrogel fabricated by photo-polymerization of cysteine conjugated gelatin-PEG and PEGDA exhibited similar cell culture results as gelatin-MA PEG hydrogel mentioned above.[27] Fu Yao et al. investigated a gelatin-PEG hydrogel system, while thiolation of gelatin was finished in a three-step reaction, followed by lyophilization of the thiolated gelatin and photo-polymerization with PEGDA to encapsulate cells at pH 8.5. [28] As we all know, thiols are susceptible to be oxidized and formation of disulfide bonds,[29] which is a challenge to preserve and finally affect the repeatability and consistency of protein and hydrogel. Another disadvantage is that its cell encapsulation was done at pH 8.5 for 30mins, which has potential side effect to cells. In summary, substantial challenges remain in the incorporation of gelatin into PEG hydrogels with high cell viability and controlled behavior *in situ*, such as well-designed conjugation between gelatin and PEG, suitable initial mechanical properties, and maintaining enough biological cues for cell attachment. To overcome these challenges, in this study a facile, cytocompatible and effective synthesis approach was explored to fabricate a gelatin-PEG hydrogel for 3-D cell encapsulation.

Elastin is the major insoluble protein existing in elastic tissue, contributing to elasticity of the skin and promoting a number of cellular responses including chemotaxis, proliferation and differentiation.[30, 31] Elastin is historically underrepresented in

commercial dermal substitutes and playing a crucial role in skin healing and regeneration. Because elastic fibers are not readily replaced after injury due to difficulties in resynthesize of tropoelastin (precursor of elastin fiber), thus seriously decrease the regeneration of new tissue and the speed of full healing.[30] Therefore, burn survivors often experience excessive scarring and skin contractures which significantly affect their health and quality of life.[30] Despite the need, however, there is a dearth of research on elastin-based dermal substitutes with tunable mechanical property, while elastin is historically underrepresented in commercial dermal substitutes. Previous researches on elastin have mainly focused on loading methods (chemical conjugation or physical blending) [32-34] leading to a 2-Dimensionnal (2-D) cell study or evaluation *in vivo*. Substantial challenges remain in the incorporation of elastin into scaffolds with high cell viability and controlled behavior *in situ*. Thus, this study attempted to mimic and combine multiple ECM-derived proteins into PEG hydrogel to render a mechanical tunable and cytocompatible hydrogel for tissue engineering.

1.3 Hypotheses

Hypothesis 1:

Elastin, one of the structure ECM proteins, has been widely explored as biological cues to modulate cell behavior in biomaterials; therefore, covalent conjugating elastin into PEG hydrogel can effectively support cell attachment and growth in 3-D microenvironment.

Hypothesis 2:

Traut’s reagent based thiolation method can be used to conjugate gelatin into PEG hydrogel with less dissolution; thus, this new method fabricated gelatin-PEG hydrogel would markedly enhance the cellular activity in PEG hydrogel, including cell's spreading, migration and proliferation, while retaining the ability to fine-tune mechanical properties.

Hypothesis 3:

Covalent crosslinking of elastin into the gelatin-PEG hydrogel would further fine-tune cellular behavior and improve cell's biological responses, and would be beneficial for skin tissue engineering and wound healing.

1.4 Objectives and Scope

The overall objective of this thesis is to design and synthesize novel biomimetic PEG hydrogels, which are able to encapsulate cell, support the adhesion of cells, promote proliferation of cells and innately guide cells to rebuild their-own new ECM. More specifically, the objectives of this research were:

1. Design a novel and facile synthesis of elastin-PEG and gelatin-PEG precursors, which can be used to encapsulate cells *in situ* and modulate cell behaviors in 3-D microenvironment.
2. Fabricate hydrogels with tunable mechanical properties and protein amount to investigate the influence on cell behaviors including spreading, morphology, proliferation, secretion of new 3-D cellular network of encapsulated cells inside the 3-D microenvironment.
3. Characterize elastin-PEG precursor, gelatin-PEG precursor, elastin-PEG hydrogel, gelatin-PEG hydrogel and hybrid crosslinked gelatin/elastin PEG hydrogels.
4. Investigate cell behavior within elastin-PEG, gelatin-PEG and hybrid crosslinked gelatin/elastin PEG hydrogels in 3-D microenvironment.

The scope of this thesis includes:

1. Comparing and optimizing different thiolation method to achieve thiolated ECM-derived proteins.
2. Investigating and optimizing the Michael addition reaction between thiolated ECM-derived proteins and PEGDA.
3. Characterizing chemical properties of ECM-derived proteins conjugated PEG precursor through Fourier Transform infrared spectroscopy (FTIR), Nuclear magnetic resonance (NMR), or Electrophoresis.
4. Characterizing the mechanical properties of elastin-PEG, gelatin-PEG and hybrid

crosslinked gelatin/elastin PEG hydrogels.

5. Investigating cell behaviors including viability, spreading, morphology, proliferation and secretion of new ECM proteins inside the 3-D microenvironment.
6. Exploring a new method to analysis and quantify the proliferation of cells inside the 3-D microenvironment.

1.5 Dissertation Overview

The dissertation is organized into the following 7 chapters.

Chapter 1 summarized the current research progress of ECM-derived proteins conjugated PEG hydrogel for cell therapy, in particular, the challenges existing in design and fabrication of ECM-derived proteins conjugated PEG hydrogels and hybrid hydrogels, precisely control the fate of encapsulated cells. The facile synthesis of ECM-derived proteins conjugated PEG hydrogels and hybrid hydrogels presented in this thesis were highlighted to be able to guide cell behavior innately. The hypothesis, objective and scope of this thesis were presented.

Chapter 2 reviews reported literature in five sections: (1) tissue engineering, (2) cell encapsulation, (3) cell encapsulated hydrogel for tissue engineering applications, (4) PEG hydrogel for cell encapsulation, and (5) ECM derived PEG hydrogel. The review not only focused on the statement of advantages of this field, but also highlights some unresolved crucial issues and challenges, which make the rational design of this thesis to be reasonable and meaningful.

Chapter 3 presents the materials and methods used in this thesis.

Chapter 4 investigates the covalently conjugation between elastin and PEGDA. The capacity of elastin-PEG hydrogel to support 2-D and 3-D attachment was studied. The characterization of elastin-PEG was also performed to study physical and chemical properties.

Chapter 5 describes the covalent conjugation between gelatin and PEGDA; cell encapsulations were performed to study effect of 3-D cell culture. Cell viability, morphology, proliferation and 3-D cellular networks were investigated. Specifically, gelatin-PEG hydrogels with tunable mechanical properties (shear storage modulus which

ranges from 100 to 2000 Pa) and gelatin amount (varies from 2.30 wt/v % to 3.32 wt/v %) were fabricated to investigate the influence on cell behaviors including spreading, morphology, proliferation, secretion of new 3-D cellular network of encapsulated cells inside the 3-D microenvironment. The characterization of gelatin-PEG was also performed to study physical and chemical properties.d

Chapter 6 reports a multiple ECM-derived proteins (gelatin/elastin) hybrid-crosslinked PEG hydrogel system. This hybrid system is designed to mimic multiple functions of ECM and finally provide predictable control over cell fate while allowing facile delivery of the cells to injury tissue. Gelatin and elastin hybrid PEG hydrogels were tested for 3-D cell encapsulation and culture, with assessment of cellular morphology, proliferation, F-actin expression, and remolding of their own ECM proteins in the 3-D culture systems. The characterization of hybrid hydrogel was studied in order to analysis its physical and chemical properties.

Chapter 7 presents discussion and conclusions from all the above findings and proposes possible future work.

1.6 Findings and Outcomes

This research led to several novel outcomes:

1. Establishing a time-saving and effective thiolation method for ECM proteins.
2. Designing a novel and facile synthesis of elastin-PEG and gelatin-PEG precursor to better mimic natural ECM for cell encapsulation.
3. Encapsulated human artery smooth muscle cells cannot grow in elastin-PEG hydrogel (without gelatin) probably due to lack of strong adhesive peptides.
4. Human dermal fibroblasts can be encapsulated into gelatin-PEG hydrogel with controllable cell behavior (such as cell growth and morphology) by adjusting stiffness of hydrogel.
5. Finding the minimum requirements for the attachment of human dermal fibroblast in 3-D hydrogels: gelatin content > 2.30 wt % and gel mesh size mesh size >~150nm.

6. Fabricating an injectable and multiple ECM-protein (gelatin/elastin) conjugated PEG hydrogel system with tunable mechanical properties that can effectively help to rebuild new ECM for the specific application of soft tissue replacement.

7. Establishing a new analysis method for the proliferation of encapsulated cells (3-D) *via* labeling DNA of proliferated cell, releasing the cells from hydrogels and measuring the florescence intensity by flow cytometry.

8. Encapsulating human dermal fibroblasts into gelatin / elastin based hybrid PEG hydrogel with controllable cell behavior (such as cell proliferation, morphology and new ECM deposition) via adjusting the amount of elastin.

References

[1] A. Atala, F. K. Kasper, A. G. Mikos. Science translational medicine. 2012, 4, 160rv112-160rv112.

[2] N. Lee, J. Robinson, H. Lu. Current opinion in biotechnology. 2016, 40, 64-74.

[3] J. F. Mano, G. A. Silva, H. S. Azevedo, P. B. Malafaya, R. A. Sousa, S. S. Silva, L. F. Boesel, J. M. Oliveira, T. C. Santos, A. P. Marques, N. M. Neves, R. L. Reis. Journal of The Royal Society Interface. 2007, 4, 999-1030.

[4] D. Seliktar. Science. 2012, 336, 1124-1128.

[5] J. Zhu. Biomaterials. 2010, 31, 4639-4656.

[6] H. Tan, K. G. Marra. Materials. 2010, 3, 1746-1767.

[7] D. L. Elbert, A. B. Pratt, M. P. Lutolf, S. Halstenberg, J. A. Hubbell. Journal of Controlled Release. 2001, 76, 11-25.

[8] A. N. Buxton, J. Zhu, R. Marchant, J. L. West, J. U. Yoo, B. Johnstone. Tissue engineering. 2007, 13, 2549-2560.

[9] P. M. Kharkar, M. Rehmann, K. M. Skeens, E. Maverakis, A. Kloxin. ACS Biomaterials Science & Engineering. 2016.

[10] L. Oss-Ronen, D. Seliktar. Advanced Engineering Materials. 2010, 12, B45-B52.

[11] S. Devasani, A. Dev, S. R. Rathod, G. Deshmukh. Pharmaceutical and Biological Evaluations. 2016, 3, 60-69.

[12] T. Billiet, M. Vandenhaute, J. Schelfhout, S. Van Vlierberghe, P. Dubruel. Biomaterials. 2012, 33, 6020-6041.

[13] I. Mironi-Harpaz, D. Y. Wang, S. Venkatraman, D. Seliktar. Acta Biomaterialia. 2012, 8, 1838-1848.

[14] C. N. Salinas, K. S. Anseth. Macromolecules. 2008, 41, 6019-6026.

[15] A. E. Rydholm, K. S. Anseth, C. N. Bowman. Acta biomaterialia. 2007, 3, 449-455.

[16] E. H. Chung, M. Gilbert, A. S. Virdi, K. Sena, D. R. Sumner, K. E. Healy. Journal of Biomedical Materials Research Part A. 2006, 79, 815-826.

[17] A. Shekaran, A. J. Garcia. Biochimica et Biophysica Acta (BBA) - General Subjects. 2011, 1810, 350-360.

[18] M. A. Daniele, A. A. Adams, J. Naciri, S. H. North, F. S. Ligler. Biomaterials. 2014, 35, 1845-1856.

[19] L. A. Reis, L. L. Chiu, Y. Liang, K. Hyunh, A. Momen, M. Radisic. Acta biomaterialia. 2012, 8, 1022-1036.

[20] H. Hall. Current pharmaceutical design. 2007, 13, 3597-3607.

[21] H. Tan, C. M. Ramirez, N. Miljkovic, H. Li, J. P. Rubin, K. G. Marra. Biomaterials. 2009, 30, 6844-6853.

[22] C. S. Chen, M. Mrksich, S. Huang, G. M. Whitesides, D. E. Ingber. Science. 1997, 276, 1425-1428.

[23] K. M. Mabry, S. Z. Payne, K. S. Anseth. Biomaterials. 2016, 74, 31-41.

[24] Y. Fu, K. Xu, X. Zheng, A. J. Giacomin, A. W. Mix, W. J. Kao. Biomaterials. 2012, 33, 48-58.

[25] K. Xu, Y. Fu, W. Chung, X. Zheng, Y. Cui, I. C. Hsu, W. J. Kao. Acta Biomaterialia. 2012, 8, 2504-2516.

[26] K. Xu, D. A. Cantu, Y. Fu, J. Kim, X. Zheng, P. Hematti, W. J. Kao. Acta Biomaterialia. 2013, 9, 8802-8814.

[27] A. Girotti, J. Reguera, J. C. Rodr ́guez-Cabello, F. J. Arias, M. Alonso, A. M. Testera. Journal of Materials Science: Materials in Medicine. 2004, 15, 479-484.

[28] K. Xu, D. A. Cantu, Y. Fu, J. Kim, X. Zheng, P. Hematti, W. J. Kao. Acta biomaterialia. 2013, 9, 8802-8814.

[29] G. T. Hermanson. Bioconjugate techniques, Academic press, 2013.

[30] J. Rnjak, S. G. Wise, S. M. Mithieux, A. S. Weiss. Tissue Engineering Part B: Reviews. 2011, 17, 81-91.

[31] A. Vasconcelos, A. C. Gomes, A. Cavaco-Paulo. Acta Biomaterialia. 2012, 8, 3049-3060.

[32] L. Buttafoco, P. Engbers‐Buijtenhuijs, A. Poot, P. Dijkstra, W. Daamen, T. Van Kuppevelt, I. Vermes, J. Feijen. Journal of Biomedical Materials Research Part B: Applied Biomaterials. 2006, 77, 357-368.

[33] C. N. Grover, R. E. Cameron, S. M. Best. Journal of the Mechanical Behavior of Biomedical Materials. 2012, 10, 62-74.

[34] A. J. Ryan, F. J. O'Brien. Biomaterials. 2015, 73, 296-307.

Chapter 2

Literature Review

This chapter summarizes the background and current research progress related to the work investigated in the thesis. It provides a review on the current research and challenges of tissue engineering, 3-D cell culture, ECM, cell encapsulation, fabrication methods of hydrogels and ECM-mimicking hydrogels. It also discusses the understanding of ECM-mimicking hydrogels for 3-D cell encapsulation and the mesh-size effect on cell activity in 3-D. The last section summarizes gelatin-based hydrogel and elastin-based hydrogel and reviews on the fabrication mechanisms, crosslinking methods and cell response after encapsulation.

2.1 Tissue engineering

2.1.1 Overview of tissue engineering

The main aim of tissue engineering strategies is to rebuild the function of injured tissues by delivering a combination of biological cues, cells and bio-responsive construct on which these cells can attach, spread, proliferate and finally regenerate a new tissue(Figure 2.1).[1] The field of tissue engineering has been developed to satisfy the increasing need for new organs and tissues. It is important for artificial biomaterials to facilitate tissue engineering through incorporation of proteins or peptides. Therefore, a variety of biological cues incorporated biomaterials have been used to repair and promote regeneration of a variety of tissues, such as cartilage, bone, cardiac and vasculature [2-4].

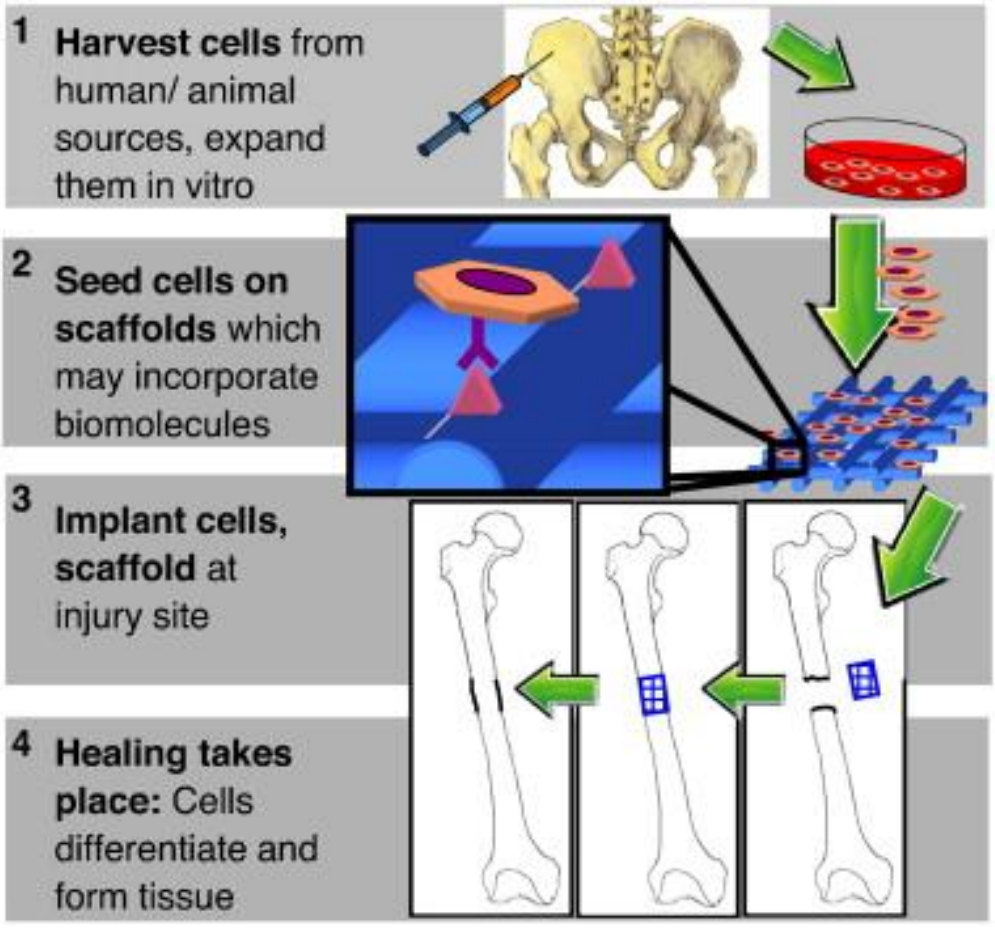

Figure 2.1 Schematic illustration of tissue engineering.[1]

It is well known that microenvironment for cell survival should satisfy several confirmed requirements: biodegradability, high porosity, biocompatibility and lack of immunogenicity. Tissue engineering scaffolds should allow diffusion of oxygen and nutrients into cells as well as signaling molecules and waste flow out. Secondly, a specific physical substrate is fundamental requirement for anchorage-dependent cells (ADCs) as the survival of ADCs is highly depending on the cell adhesion and spreading.[5] The majority of cells are ADCs thus can spread only after attachment to a proper material(Figure 2.2),[5]. ADCs comprise of endothelial, epithelial, smooth muscle cells, fibroblasts, osteoblasts - all of which are frequently used in tissue engineering. However, cells encapsulated into 3-D environment often do not attach and maintain a spheroidal shape, which is different from the situation in 2-D culture and thus more challenging. Consequently, encapsulated and round-shape ADCs showed poor attachment in synthetic 3-D environment, accompanied with cell apoptosis and death.[5] Since the aim of tissue engineering is to fabricate a reliable and effective cell survival environment,[6] the primary challenge of 3-D cell culture for tissue engineering is the adhesion of ADCs. Thirdly, the degradation speed of biomaterials is another one of the most important considerations and it is crucial to assure that the speed of degradation matches with the regeneration of new tissue at the damaged site. Otherwise, fast degradation of the scaffolds will lose their designed effect on the growth of cell; on the contrary, slow degradation of the scaffolds will hamper the regeneration of new tissue.

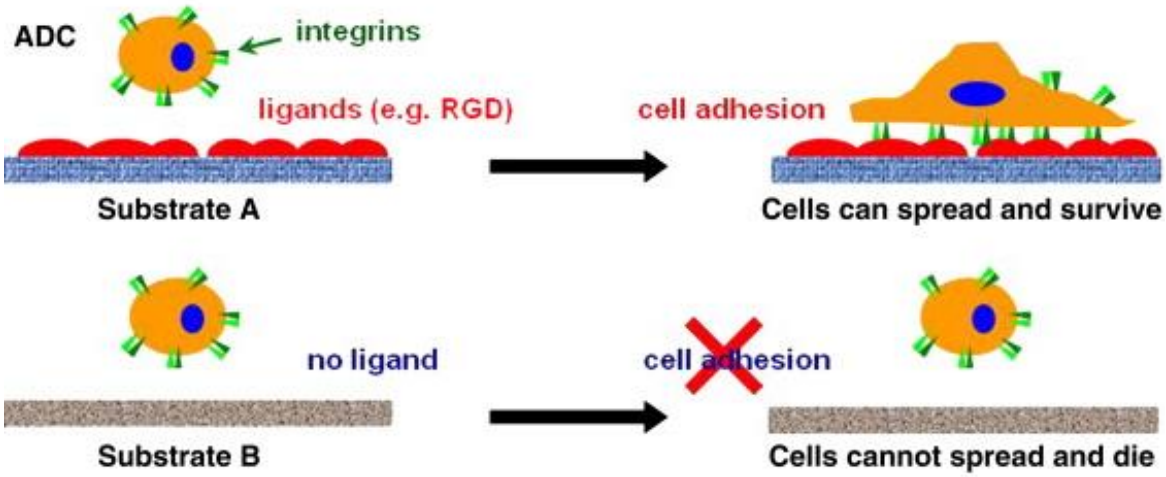

Figure 2.2 Illustration of the relationship among cell adhesion, integrins and substrate.[5]

Therapeutics cell delivery has emerged as one of the most possible and widely used approach for tissue engineering and regenerative medicine. Its effectiveness depends on successful delivery of the cells to injured tissue, where the newly delivered cells can repair damaged tissue or promote the regeneration of new tissue. Therefore, the scaffolds for 3-D tissue engineering should consider several aspects such as cell adhesion, degradation, and mechanical property. The aim of such design is to fabricate a reliable, functional structure for cell survival.

2.1.2 2-D and 3-D cell culture

Flat, 2-D culture have been the most popular approach for studying cell behaviors in the past and is still a standard and basic method for cell culture *in vitro*. This method, involving culturing cells on 2-D substrates or the surface of tissue, provides a feasible platform for studying the physiology and pathophysiology of cells and tissue *in vitro*. 2-D cell cultures experiments not only have been used to study the base of complex biological activates, such as stem cell differentiation[7] and tissue morphogenesis,[8] but also to investigate the dynamic interactions between cell and the cellular microenvironment. For instance, previous studies demonstrated that the stiffness of the 2-D culture substance can affect the differentiation of human mesenchymal stem cells (hMSCs).[9] Moreover, the same research group has proven that the growth and apoptotic rates of cells cultured on 2-D scaffold could be influenced by the stiffness of the scaffold.[10] Therefore, 2-D cell culture experiments can be used to investigate how biological phenomena are influenced by the epigenetic factors.

Recent studies have demonstrated that cells often behave unnaturally when they are extracted from native 3-D tissues and cultured as a monolayer. 2-D cell culture can polarize cells since only part of the cell membrane can communicate with the neighboring cells and interact with ECM components. The rest of the cells cultured in 2-D planar are immersing in the bulk culture media, which may led to unnatural, inherent polarized binding and finally influence the cellular signaling and phenotype.[11] Accordingly, previous studies also proved that cellular responses were similar to those *in vivo*, when the cells were cultured in artificial 3-D environment.[12] For example, Bissell et al.

showed that human breast epithelial cells transformed to tumor cells when culture in 2-D, but behaved similarly to the normal cells (from native tissue) in 3-D environment.[13] Cancer researchers have explored several complex 3-D cell culture models[14] to study the paracrine signal of cells,[15] the influence of matrix on cancer cell phonotype,[16, 17] and select potential therapeutic approach[18]. Similarly, embryonic stem cells expressed more chondrogenesis when culture in 3-D compared to monolayer culture.[19] Birgers et al. demonstrated that the microenvironment of cells plays a dominant role in modulating cell phenotype by altering the expression the gene and protein.[20] The differences in cell behavior between 2-D and 3-D cell cultures are due to the permutations in the expression of gene as the cells recognize its surroundings differently (2-D and 3-D microenvironment, shown in Figure 2.3). Therefore, there were some considerations on what features should be contained in designing a 3-D scaffold for cells therapy.

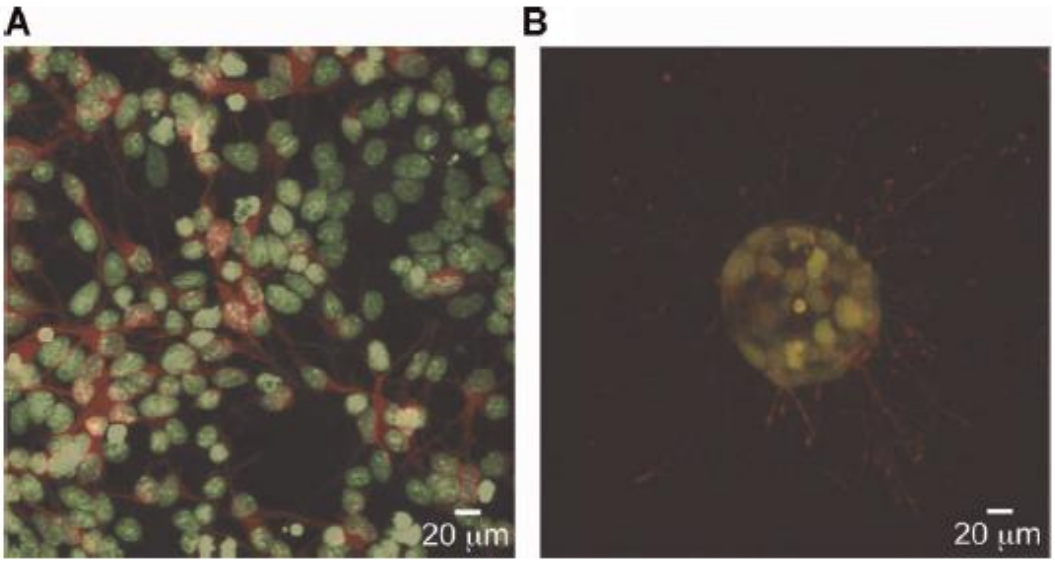

Figure 2.3 Cells behave in a different manner in 2D and 3D culture. Neural cells cultured in 2-D (A) extensively spread in the plane (cytoskeleton was stained green and b-tubulin were stained red). When cultured within hydrolytically degradable PEG hydrogels in 3-D (B) the same neural cells spread isotopically.[21]

2.1.3 Natural ECM structure and functions

The rapid increase in the understanding of ECM function and structure has provided opportunities to mimic the natural ECM for design and fabrication of bio-inspired scaffolds. Natural tissues contain cells secreted ECM molecules, which organize cells into tissue, guide cell behaviors and provide the mechanical support for tissue (Figure 2.4). This complex, organized and heterogeneous network of proteins, polysaccharides and growth factors facilitates the anchorage of cells, interactions between cells and the formation of tissue. As a result, scientists have investigated a variety of 3-D scaffolds that possess benefits of the native 3-D ECM microenvironment.

Figure 2.4 shows the structure of ECM and the interactions between ECM and cells. Generally, the natural ECM contains three major biological cues that are useful for design and fabrication of biomaterials, including: (1) Insoluble ECM fibrous macromolecules, (2) soluble molecules, and (3) cell-cell receptors.[1] There are several insoluble ECM fibrous macromolecules such as collagens, elastin and fibrin. Collagen, the most abundant protein in mammals, provides mechanical support for the tissue, while other proteins, such as elastin, offers elasticity for the tissue.[22] There are several different types of collagen. For example, Type I collagen is most abundant in several tissues such as bone, skin and tendons. Type II collagen has similar fibrillary structure which offers high tensile strength to cartilage.[23] Fibronectin (FN, shown in Figure 2.4) and laminin (LN) in natural ECM provide the several binding domains for cells. Glycans including glycosaminoglycans (GAGs) and proteoglycans (PGs) are linear polymers of hyaluronic acid (HA), chondroitin, heparin and so on. Both GAGs and PGs swell in the aqueous environment and fill the interstitial space of structure fibers to absorb compressive force and also prevent tissue collapse. They are the reservoirs of biomolecules (growth factors, ECM proteins) and also allow the diffusion of nutrients and wastes.[24] The attachment of cell to ECM is crucial for the proliferation, migration and phenotype of cells. Integrins interacting with ECM peptide ligands play major roles in cell attachment to ECM by offering anchorage and signals that guide cell behavior and affect the gene and protein expression. Although ECM macromolecules contain thousands of amino acids, integrins only can recognize and bind to a few peptide ligands, such as arginine - glycine- aspartic acid (RGD), REDV, and LDV.[21] Thus, incorporation of ECM-derived molecules such

as collagen, LN and FN or their incorporation into scaffold is crucial for cell survival in 3-D.

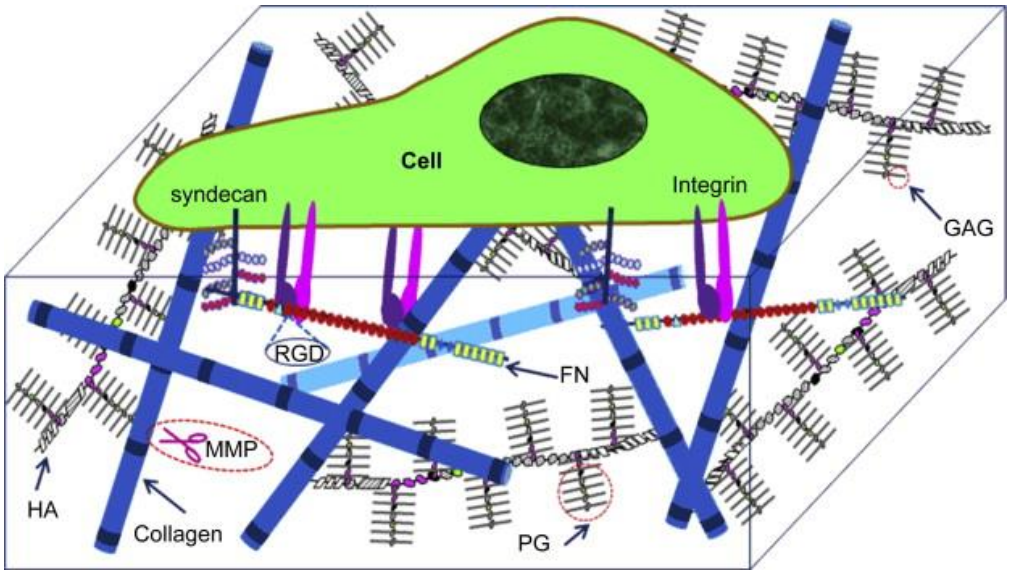

Figure 2.4 Schematic illustration of a 3-D ECM model.

2.1.4 Challenges in 3-D scaffold design and fabrication

Bio-responsive scaffolds for 3-D cell culture have been extensive investigated by the following methods: 1) pre-fabrication of ECM-derived protein incorporated scaffolds and seeding cells on the surface of scaffolds before transplanting to injured tissue; and 2) *in situ* formation of hydrogel through physical or covalent crosslinking. In general, pre-fabricated scaffolds are introduced into injured tissue after seeding target cells to the surface of scaffolds and culturing for several days. However, they are not completely recapitulating the 3-D environment of the ECM, since most of the cells are growing on the surface of the scaffolds. Traditional biomaterial scaffold fabrication methods, such as solution-casting, electrospinning, crystal leaching, gas foaming and lyophilization, have been investigated to prepare highly porous scaffolds, which allow easy diffusion of nutrients, waste and cell-secreted signaling cues.[25] However, these scaffolds are often not good enough because of the inability to effective delivery of cells and precisely control scaffold structure.[26] For instance, microporous scaffolds were able to

encapsulate cells easily but the pore size of scaffold (-100 μm) was much larger than the average diameter of cells (~10 μm); therefore, the efficiency of encapsulation was not satisfied to the purpose. Similarly, biomimetic nanofibrous scaffolds fabricated by fibrillary ECM-derived proteins can encapsulate cells during the self-assembly procedure; however, the mechanical properties of this scaffolds are not satisfactory for applications.[27] These limitations are not applicable to hydrogels, which process several advantages in structure and mechanical properties similar to the native cellular environment.[28]

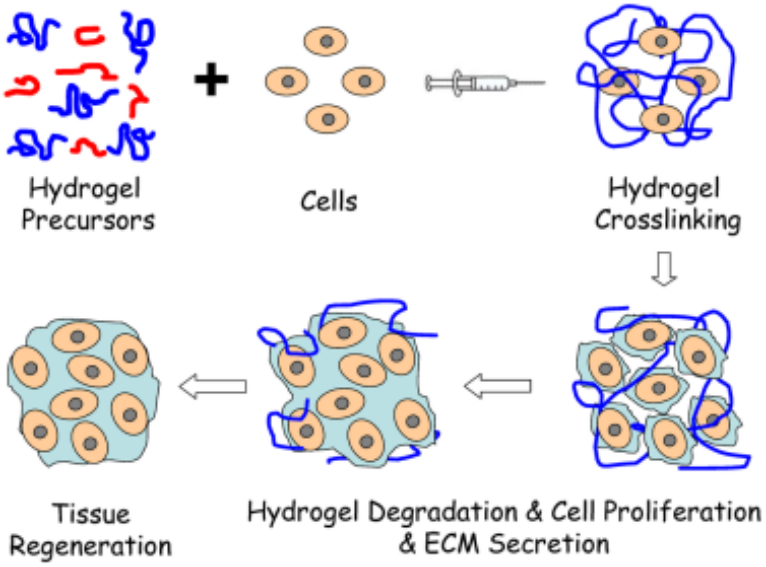

Figure 2.5 Illustration of cell encapsulation steps and the regeneration of new tissue. Cells are cultured, expanded in cell culture flasks, and mixed with hydrogel precursors, which are subsequently injected into the injured tissue. Hydrogels provide structural support and maintain cells in the injured tissue for cell proliferation and regeneration of tissue. The hydrogel will degrade after the cells synthesis their own ECM. This method allows a facile approach to transplant cell encapsulated hydrogel in a minimally invasive way. [29]

In contrary to pre-fabrication methods, *in situ* formed hydrogel presents several advantages: it can be used as an injectable platform to the target injured tissue sites in a minimally invasive method; therapeutic cells can be encapsulated into hydrogel and homogeneously embedded within the real 3-D microenvironment. The procedure of cell encapsulation into hydrogels typically contains three steps (Figure 2.5): 1) trypsinize cells

and suspend them in the hydrogel precursor solution, 2) injecting the mixture to injury tissue, and iii) crosslinking precursor solution to form 3-D hydrogel in situ. The delivery of cells by this method has several advantages. First, the cell mixed hydrogel precursor solution can be injected to the tissue defects directly, allowing formation of the hydrogel *in situ* and fully filling in the cavities of injured tissue. This fabrication method also increases the adhesion of hydrogels to the defect without adding glues. Second, fast crosslinking methods (such as photo-polymerization, physical conjugation) will lead to a homogenous distribution of cells. Third, a hydrogel offers a highly swollen 3-D microenvironment that is similar to natural tissue, while the size and shape of hydrogels can be easily adjusted according to the application. Therefore, hydrogels have been intensively investigated and widely explored as tissue engineering scaffolds.[5]

2.2 Hydrogels for cell encapsulation

Hydrogels are crosslinked 3-D networks that possess high water contents and demonstrated to be idea scaffolds as matrix for 3-D cell culture. Hydrogels can swell and absorb water but do not disappear in water.[30] Owing to their highly hydrated structure, hydrogels can mimic natural 3-D tissue better than any other kind of polymer based scaffolds.[30] Encapsulating cells into hydrogels also possesses several attractive advantages for tissue engineering, including biomimetic microenvironment for cell survival and growth, and the ability to form hydrogel in situ and deliver cells with it. However, the gelation procedure was done with the existing cells, which might harm them. Several important considerations for designing hydrogels for cell encapsulation should be carefully made in order to provide a suitable and effective scaffold.[31] The gelation procedure of hydrogel must be mild and cell compatible.

There are two main types of hydrogels: 1) natural hydrogels, such as alginate, collagen, fibrin, where all the compositions are with a bio-origin based; 2) synthetic hydrogels including synthetic polymers (crosslinking agents and monomers), biosynthetic hydrogels (incorporating biological cues into synthetic hydrogels).

2.2.1 Hydrogel design considerations for cell encapsulation

The relations between the hydrogel fabrication, structure, properties and application determine the rational design for scaffolds. Fabricating biomimetic 3-D hydrogels for cell encapsulation is still a challenge, requiring consideration of several crucial aspects properties (shown in Figure 2.6), such as cell adhesion, degradation, bioactivity, transport, mechanical properties and mesh size.

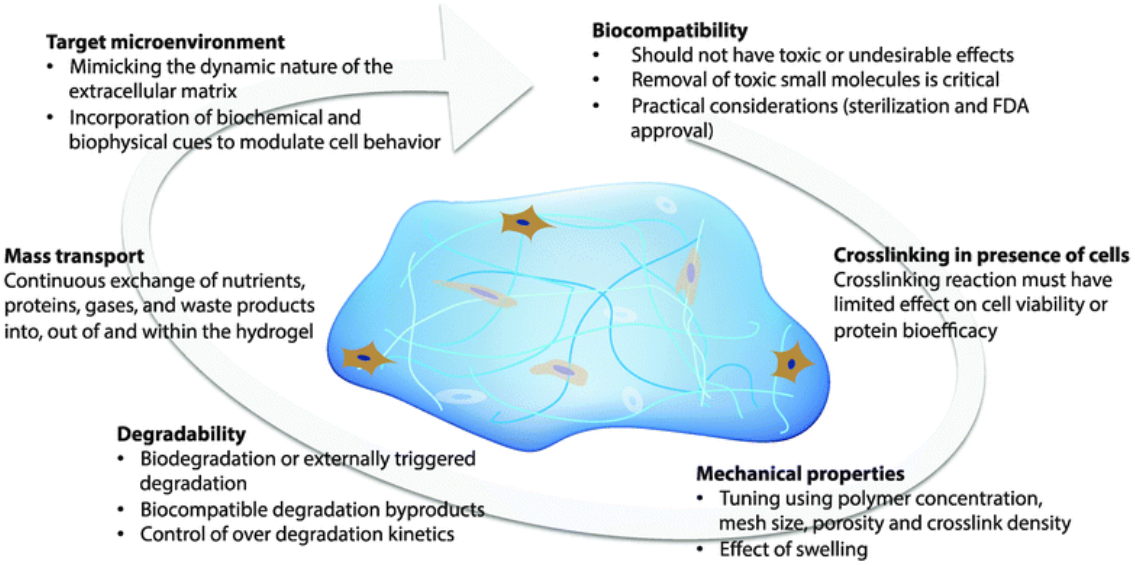

Figure 2.6 Design considerations of hydrogels for cell encapsulation.[32]

Cell adhesion, an important phenomenon that allows cells to attach to hydrogels has enabled their use to repair or regeneration of injured tissue. Some natural hydrogels such as collagen, fibrinogen or fibrin innately contain cell adhesive motifs, while common synthetic and polysaccharide hydrogels do not. As mentioned before, cell adhesion and spreading are crucial for the survival of ADCs. Cells encapsulated into 3-D hydrogel are constrained to a round-shape, no matter which cell types or what native morphology, because of a unique encapsulation mechanism.[5] The bulk of synthetic hydrogels typically exhibit a bio-inert microenvironment,[33] in which the cells (~10 μm) are encapsulated and surrounded in highly aqueous networks with nano-size pores. Without strong biological cues, the encapsulated cells are restricted from attachment to scaffold

and spreading inside. Cell adhesion and spreading are necessary and compulsory to rescue cells from apoptosis and death.[34] Consequently, cells attachment to 3-D hydrogel becomes the first challenge impeding the application of hydrogels for cell therapy. Incorporating cell-adhesion cues to hydrogels have been proved effective to promote the cell attachment in 3-D microenvironment.[21, 31, 33, 35]

Degradation of hydrogels is crucial and essential process for tissue engineering that requires controlled reuptake in vivo and/or in situ. There are several mechanisms of hydrogel degradation, including proteolysis (enzyme), hydrolysis, pH-based, temperature-based and UV triggered. The other major limitation of synthetic hydrogels as scaffolds for tissue engineering is that they have no biodegradation cues. If degradation is faster than the cell growth speed, the encapsulated cell will lose their anchorage sites; on the other hand, if the degradation rate is too slow, the scaffold will be a barrier for cell growth. This will not only influence the regeneration of new tissue, but also affect the cell activities. The degradation of scaffolds can be controlled by changing the structure and constitution of scaffold. For instance, ester linkages related to lactic acid degrade much faster than ester linkages of caprolactone;[36] and the gels with higher crosslinking density led to longer degradation times.[37] The encapsulated cells also can affect the degradation rate of the hydrogels as Hunt et al proved that encapsulation of fibroblasts into alginate hydrogel lead to accelerated degradation.[38] During the design of hydrogel for tissue engineering, there are several factors that should be considered about the degradation, such as polymer length, linkage and crosslinking density. These factors can directly affect the structure of the cell encapsulated hydrogel, which finally influence the cell growth and regeneration of tissue.[31]

The mechanical properties of a hydrogel are affected by polymer chemistry structure, crosslinker properties, swelling, polymer length, and crosslinking density, which influence the cell behavior (growth, migration, spreading, contractility, differentiation) and tissue homeostasis.[39] The network properties of a hydrogel are responsible for maintaining cells *in situ*, as a temporary scaffold, while also offering pathways for diffusion of biological cues, nutrients, oxygen and waste. Once the cell encapsulated hydrogel is fabricated in situ or *in vitro*, regeneration of tissues with desirable functions relies on mechanical properties of hydrogels.[40] Higher crosslinking density in

hydrogels offer benefits such as longer gel life, but also difficulty for nutrients to diffuse to the cells for their survival. Moreover, the smaller porosity of hydrogel can impede the cell growth and tissue regeneration. Previous studies have shown that ADCs can only survive after cell-cleavable domains get rid of the spatial constraints. This is because cell behavior such as migration and cell interactions are important for guiding differentiation and fate; while all of these are restricted when the cells are encapsulated in highly crosslinked hydrogels. It is unrealistic to expect that degradation will solve this issue (provide more space for cell), since the spontaneous degradation of hydrogel is quite slow. Thus, over the recent years, a number of studies have explored how to provide adequate mechanical properties for encapsulated cells.[5]

Bioactivity is one of the basic functions of hydrogels that can innately modulate specific biological events in the tissue including cell growth, morphogenesis, proliferation and differentiation. Many of these cellular events can be triggered by chemical, biological, and physical approaches, while they can help to encourage secretion of appropriate proteins/ polysaccharides to rebuild new ECM and finally lead to tissue regeneration.[41] However, common synthetic hydrogels does not inherently have biological cues and thus cause poor cell behavior. For example, gelatin methacrylamide PEG hydrogel[42] and gelatin-PEG diacrylate hydrogel[43, 44] have shown delayed cell attachment (with mostly rounded cells) and proliferation; other studies have demonstrated that round-shape cells underwent apoptosis and subsequently died in a few weeks[34]. For those cells that did survive well in the above mentioned hydrogels, their spreading, migration, proliferation, phenotype, differentiation and the interactions of cell and matrix were barely controllable: the reason for this is primarily that an artificial hydrogel utilizing just one protein or peptide sequence does not mimic natural ECM well enough due to limited instructive cues. Consequently, this led to unsatisfactory cell behavior and compromised the effect and efficiency of delivered cells.[45] Therefore, rather than providing general biological cues specificity should be considered in the fabrication of hydrogels since every tissue type has its own set of mechanical, chemical gradients, structure, and function.[46]

The proper design and control the network structure of hydrogels are important for the survival of cells, hydrogel biodegradation, diffusion of bioactive molecules and cell

migration *via* the network.[30] Network mesh size is one of the key components in governing mass diffusion and modulating cellular activities, including proliferation, phenotype.[47] In order to study hydrogel network structure, it is necessary to measure certain parameters of the hydrogel network. Four important swelling parameters have been employed to study hydrogel network structure, including:

• The swelling ratio (Q): the mass swelling ratio (Q_m) and the volume swelling ratio (Q_v)

• The polymer volume fraction in the swollen state ($\upsilon_{2,s}$)

• The number average molecular weight of the polymer chain between two adjacent cross-links (M_c)

• The network mesh size (ξ) [48]

The mesh size, or the correlation distance between two neighboring crosslinks, defines an estimation of the space available between the macromolecular chains. Values for $\upsilon_{2,s}$, Mc and ξ can be determined using the equilibrium swelling theory.[49] Above four parameters are important in measuring the hydrogel network structure. Currently, a variety of methods have been used to calculate PEGDA hydrogel mesh, including correlations linking measurable quantities, such as equilibrium hydrogel swelling, to mesh size.[47, 50] Although these calculations appear to give reasonable mesh size estimates for PEGDA hydrogels,[50] the proper hydrogel mesh size for cell attachment have not been explored yet. Thus, in this study, proper hydrogel mesh size for cell attachment was characterized *via* varying the crosslinking density of hydrogel.

2.2.2 Natural hydrogel used for cell encapsulation

Natural polymers have been fabricated into hydrogels for tissue engineering because of their excellent biological instructive cues, biocompatibility, and biodegradability. There are four categories of natural hydrogels, including: DNA-based hydrogels, protein-based hydrogels, polysaccharides hydrogels, and protein / polysaccharide hybrid hydrogels.

DNA-based hydrogels have been widely investigated for biomedical application due to its biodegradability and biocompatibility. DNA-based hydrogels were synthesized from multiple branched DNA macromers by self-assembly or ligase-mediated reactions, while new covalent linkages were formed at the ends of the branches and finally lead a

conjugated hydrogel.[51, 52] The mechanical properties of DNA-based hydrogels were tunable by adjusting the concentrations of DNA, the degree of branching of the DNA or the type of DNA monomers.[30] Scientists successfully encapsulated Chinese hamster ovary cells into these DNA-based hydrogels.[51]

Various Protein-based hydrogels have been designed and fabricated into bioactive scaffolds for tissue engineering because of their inherent instructive cues, biocompatibility, and biodegradability. Collagen is the most abundant protein in mammals and one of the most widely explored proteins for biomedical applications. Although naturally protein-based hydrogels, such as collagen and fibrin based scaffolds, hold several advantages, they are often restricted due to relatively poor mechanical properties, potential immune infections and are not easily modified.[22, 53, 54] Gelatin, the product of collagen denaturation, has emerged as an alternative choice because of retaining some benefits of collagen like RGD sequence, easily tailoring with other components and less immune reactions. Synthetic peptides derived from the natural proteins possessed several biological advantages and have been used to fabricate bioactive hydrogels.[55] For example, an amphiphilic peptide based hydrogel has been fabricated by self-assembly; peptide solution mixed with cells and cell culture medium can form a crosslinked hydrogel through the self-assembly of hydrophobic regions of the peptides. However, one of the main drawbacks of these hydrogels is their poor mechanical properties.[56]

Several polysaccharides have been investigated to fabricate hydrogels for cell encapsulating, such as alginate, hyaluronic acid (HA), chitosan, and chondroitin sulfate. HA possessing a non-sulfated GAG structure is one of the ECM components and widely distributed in all connective tissues. HA plays an important role in many biological activities such as wound healing, angiogenesis, and cell differentiation. Several crosslinkable groups, such as methacrylates[57] and thiols[58], have been conjugated to HA for cell encapsulation. Cell encapsulated HA hydrogels fabricated by photo-polymerization showed enhanced cell proliferation and elastin synthesis.[59] Alginate is able to form hydrogel in the presence of certain cations via ionic crosslinking, but it does not possess cell adhesion cues. Therefore, RGD or gelatin has been conjugated into alginate hydrogel to improve the adhesion of cells, after which cell encapsulations was

successfully achieved.[60] Chitosan is a deacetylate chitin, which is a natural polysaccharide. Chitosan soluble in water and shows positive charge at pH<6, while it shows neutral charge and hydrophobic character at neutral pH and leads to formation of physically crosslinked hydrogel.[31] In order to better control the mechanical properties and structure of chitosan hydrogel, several methods have been explored by the covalent crosslinking approach. Hong et al. conjugated methacrylic acid to chitosan to prepare a macromer while lactic acid was also conjugated to improve its hydrophilic property at neutral pH.[61] In a separate study, cardiomyocytes were successfully encapsulated into azidobenzoic acid conjugated chitosan hydrogel, while RGD was also conjugated to improve the cell attachment. [62, 63] Chondroitin sulfate, a main structural proteoglycan, is found in many tissues, such as tendons, skin, cartilage. Methacrylates have been conjugated with chondroitin sulfate to fabricate photo-polymerization crosslinked hydrogels.[64] Chondrocytes were encapsulated into methacrylate-chitosan hydrogels however the cells did not secret any GAG or collagen after 6 weeks; the addition of PEG to methacrylate-chitosan hydrogels promoted the deposition of ECM.[65]

2.2.3 Synthetic Hydrogel used for cell encapsulation

In contrast to natural hydrogels, synthetic hydrogels possess controllable and predictable physical and chemical properties, which is important for the encapsulated cells and tissue regeneration. Synthetic hydrogels have been used for cell encapsulation because they can be modified according to the application by changing their constitution, molecular weight, crosslinking density, special linkage for biodegradation or conjugating biological cues.[30] Examples for synthetic hydrogels discussed here can be classified into three types, including biodegradable, non-biodegradable synthetic hydrogels and bioactive synthetic hydrogels.

2.2.3.1 Non-biodegradable synthetic hydrogels

For non-biodegradable hydrogel, it is important to maintain appropriate physical and mechanical integrity of hydrogel for tissue engineering, while the mechanical properties

of hydrogels can be tunable by controlling the degree of crosslinking or the length of crosslinker.[66] While higher crosslinking density hydrogels offer several benefits, especially better mechanical property and longer gel life, it is difficult for nutrient to diffuse to the cells for enabling their normal function, such as to secrete and rebuild self-produced ECM.[5, 22] Therefore, it is necessary and important to choose a non-biodegradable hydrogels with appropriate mechanical properties as tissue-engineering scaffolds.

Non-biodegradable synthetic hydrogels can be fabricated from the polymerization of several double bond-containing monomers or macromers including methacrylate (MA) and its derivate, N-isopropylacrylamide (NIPAm), acrylic acid (AAc), acrylamide (AAm), and linear or multi-arm PEG-acrylate and its derivate.[22, 67, 68] Another approach to fabricate non-biodegradable hydrogels is to incorporate non-biodegradable polymers including poly (ethyleneoxide) (PEO), poly (propylene oxide) (PPO), copolymer of PEO and PPO, covalently modified PVA, and crosslinking of linear or multi-arm PEG. Non-biodegradable hydrogels have been extensively explored for bone and cartilage engineering,[3, 5] but are limited in fabricating vascular engineering due to their non-biodegradability.

Poly NIPAm (PNIPAm) has been studied as thermosensitive hydrogels obtained by free radical polymerization of NIPAm. PNIPAm hydrogels can swell in water when the temperature is below its lower critical solution temperature (~32 ℃). Swelling is due to hydrogen bonds between amide groups of PNIPAm and water molecules. On the contrary, when the temperature is above 32 ℃, phase separation and deswelling of the hydrogels can occur due to the hydrophobic interaction between the isopropyl groups of PNIPAm chains.[69] This special property of temperature-dependent swelling/deswelling is useful in detaching cell layers for regeneration of special tissues like cornea or cell sheets.[70]

PEG has been an important and extensively studied hydrophilic polymer used to fabricate hydrogels because of several advantages, such as excellent biocompatibility, non-immunogenity, and nontoxicity.[22, 71] Moreover, the end groups of PEG molecules can be converted into various functional groups, such as vinyl sulfone, azide carboxyl, sulfhydryl groups and acrylate, or conjugated with other molecules or bioactive cues.[72, 73] PEG hydrogels can be fabricated by photo or radical polymerization of PEG

macromers. PVA hydrogels are another synthetic hydrogels studied for tissue-engineering applications. PVA hydrogels can be fabricated by physically or chemically crosslinking methods, such as conjugation with acrylate groups, crosslinking by glutaraldehyde, or repeated freezing/ thawing. [74]

2.2.3.2 Biodegradable synthetic hydrogels

Biodegradability is one of the most critical and essential properties of scaffolds for tissue engineering as introduced before. It is meaningful and important to make sure that the degradation rate matches with the regeneration of new tissue. Many nature derived polymers are biodegradable, including collagen, ECM proteins and chitin, but they are limited in fabricating hydrogel with controllable mechanical and biodegradability properties.[75] Synthetic biodegradable hydrogels have been widely investigated in the past. Polyesters, such as poly (glycolic acid) (PGA), poly (lactic acid) (PLA), poly (ε-caprolactone) (PCL) and their copolymers, have been extensively explored as biodegradable hydrogels.[76] In addition they have been modified in order to possess acrylate bonds or amphiphilic property for fabricating hydrogels by chemical or physical conjugation.[71, 77-80] For instance, the end groups of PEG–PLA–PEG and PLA–PEG–PLA were modified with acrylate groups to form PLA-modified PEG diacrylate, while these acrylated macromers were able to undergo photo-crosslinking to fabricate hydrolytically degradable hydrogels.[81, 82] In addition, several functional groups, such as ester bonds, ketal and disulfides, can be introduced to fabricate biodegradable PEG hydrogels.[83-85]

Michael-addition reactions have been explored to enhance biodegradation rate of PEG hydrogels. For example, PEGDA or multi-arm PEG-acrylated macromers are able to react with sulfhydryl groups containing substances, such as dithiothreitol or cysteine-containing peptide sequences through Michael-addition reaction to form a hydrogel network with thioester bonds next to the ester bond of acrylates.[86-88] The introduced thioester bonds carry a positive charge on the carbonyl carbon of the acrylate ester group, which can enhance its efficiency to react with nucleophilic hydroxyl anions in the hydrolysis of ester bond. Another approach to fabricate biodegradable PEG hydrogels is

to introduce disulfide bonds into PEGDA chain to form disulfide contained PEGDA, while the disulfide bonds can react with sulfhydryl groups containing substances, such as cysteine and glutathione.[79] Therefore, the thiolated hydrogels can be degraded by sulfhydryl groups containing peptides or proteins, which provides an easy and controllable approach to satisfy the application.

Synthetic peptide hydrogels formed by self-assembly have emerged as promising hydrogels due to their excellent biodegradability and cytocompatibility, controllable structure.[89, 90] Peptide amphiphiles are designed with the amphiphilic properties as they contain both hydrophobic and hydrophilic peptides, which allow them self-assembly into nanofibers. Research results proved that these peptide nanofibrous hydrogels fabricated by self-assembly can form biodegradable hydrogels for encapsulating cells and other biomedical applications. [27, 91-93]

2.3 Fabrication methods of cell-responsive PEG hydrogel

Free radical polymerization (FRP) has been extensively investigated to fabrication PEG hydrogels from PEGDA macromers with the addition of photo-initiators. However, pure PEG hydrogel shows poor cell adhesion due to lack of biological cues to interact with cell-surface motifs, while another problem of using PEG hydrogel for tissue engineering is not naturally degradable. Thus, several chemical conjugations have been explored to fabricate a cell-responsive and cell compatible PEG hydrogel (shown in Figure 2.7),[94] while cells can be encapsulated in to the hydrogel simultaneously. Photo-polymerization is one of the most common and easy approach to fabricate PEG hydrogels, which triggers the polymerization of liquid PEG monomer (normally acrylate) solutions to form solid hydrogels by UV at physiological temperature and pH.

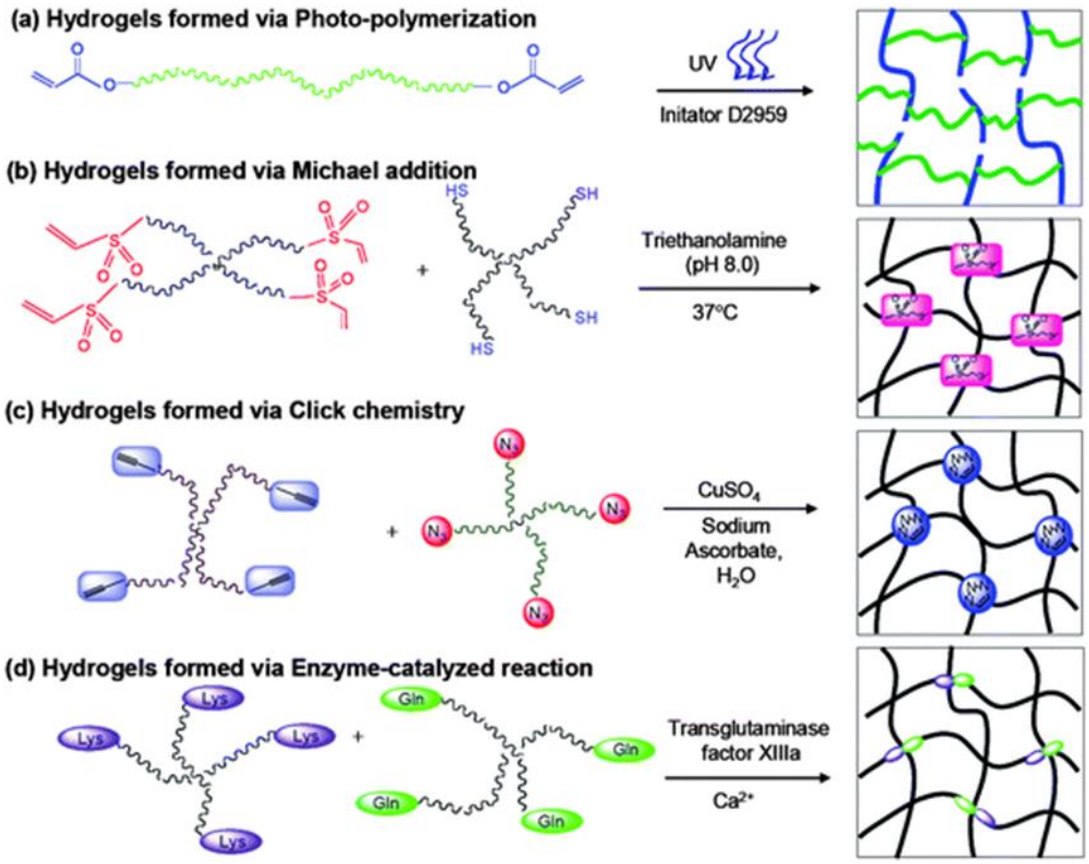

Figure 2.7 Reaction scheme for fabrication of PEG hydrogels by (a) FRP; (b) Michael-addition reaction; (c) click chemistry; (d) enzymatic reaction. [94]

2.3.1 Free radical polymerization FRP

Macromers with two or more vinyl groups are able to be polymerized through a FRP mechanism in the presence of initiator (radical producer) and other triggering conditions.[31] To incorporate biological cues into PEG hydrogel, free radical polymerization based methods has been widely investigated and present an important approach to fabricate cell-responsive PEG hydrogels. Examples for polymerization of biological cues into hydrogels can be classified into three types, including copolymerization with peptide monoacrylates, copolymerization with peptide diacrylates, and thiol-acrylate based photo-polymerization.

Cells culturing in a 3D hydrogel microenvironment needs to provide bioactive peptides in the bulk hydrogel in order to enhance the survival of encapsulated cells. Conjugation of

cell-adhesive peptides to one acrylate of PEGDA has been the major strategy to fabricate bulk cell-adhesive hydrogels. For example, Hern et al. performed synthesis of monoacrylamidoyl RGD (RGD-MA) and RGD-PEG monoacrylate (RGDPEGMA), respectively.[95] RGD-MA or RGD-PEGMA monomers were polymerized with PEGDA via photo-polymerization to fabricate cell-adhesive hydrogels, while these modified PEG hydrogels with different amount of RGD were able to improve the spreading of human foreskin fibroblasts over 24 h.[22] This approach for conjugating cell-adhesive peptides into PEG hydrogels has been extensively investigated with several other cell-adhesive peptides, such as KQAGDV, YIGSR, REDV, VAPG and IKVAV (shown in Table 2.1).[22] Several cell lines have been encapsulated into modified PEG hydrogels, such as fibroblasts, neural cells, vascular endothelial cells, osteoblasts, and stem cells.[31, 96]

Table 2.1 Cell-adhesive peptides that have been studied for the modification of PEG hydrogels.

CAP	Origin	Cell receptor	Monomer type
RGD	FN*, LN**, Collagen	Integrins	Monoacrylate, Diacrylate, Monothiol, Monoazide, Diazide, Monomaleimide
KQAGDV	FN	Integrin	Monoacrylate
REDV	FN	Integrin $\alpha_4\beta_1$	Monoacrylate
PHSRN	FN	Integrin $\alpha_5\beta_1$	Monoacrylate, Monothiol
IKVAV	LNα1	110kDa protein	Monoacrylate, Monothiol
YIGSR	LN	67kDa protein	Monoacrylate, Monothiol
PDGSR	LN	Integrin	Monoacrylate
LRGDN	LN	Integrin	Monoacrylate
LRE	LN	Integrin	Monoacrylate
IKLLI	LN	Heparin	Monoacrylate
GFOGER	Collagen-1	Integrin $\alpha_2\beta_1$	Monoacrylate
VAPG	Elastin	67kDa protein	Monoacrylate

* FN: fibronectin ** LN: laminin

Copolymerization with peptide diacrylates has been another important approach to incorporate biological cues into PEG hydrogel as it is easily controlling the distribution of peptides in bulk hydrogels and not eliminating the mechanical properties of hydrogel. On the contrary, copolymerization of peptide monoacrylate into PEGDA has some drawbacks, such as random distribution of peptides and affects the mechanical properties of hydrogel. For example, RGD-PEGDA and MMP sensitive peptides-PEGDA have been photo-polymerized to fabricate cell-adhesive hydrogels, which have shown the ability to facilitate cell behavior and finally form extensive vascularization.[97]

Copolymerization of acrylated peptide sequences has been a major strategy to incorporate bioactive peptides in PEG hydrogels. This method is very useful to conjugate peptides into hydrogels directly, but this approach has to conjugate peptide sequences with PEG acrylates first. Thiol-acrylate based photo-polymerization has been developed to fabricate cell-responsive PEG hydrogels as thiolated peptides that can be used as chain transfer reagents in FRP of PEGDA.[98, 99] For example, Anseth et al. synthesized thiol-ended RGD peptide like CRGDS and CGRGDSG, which can be photo-polymerized with PEGDA. They proved that about 95% of the peptides were conjugated into PEG hydrogel after 10 min reaction with 5 mW/cm^2 of UV (365 nm). This method is able to encapsulate cells with easy incorporation of peptide sequences, controllable reaction ratio and time, cost-efficient, and cytocompatible reaction for rebuilding new ECM.[98, 100]

2.3.2 Michael-addition reaction

Sulfhydryl groups can react quickly and efficiently with α, β-unsaturated carbonyls through a Michael-addition reaction to form stable thioether bonds (Figure 2.7 b). This reaction occurs at room temperature without any catalysts, initiators, or by-products.[101] For example, linear or multiarm PEG with acrylate-end or vinyl sulfone groups can react with macromers containing thiols. Hubbell et al synthesized multiarm PEG vinyl sulfone and SH-containing RGD peptide for fabricating cell encapsulated PEG hydrogels, while the natural ECM mimicking PEG hydrogel could modulate cell activity by changing its' composition.[102] Sulfhydryl groups in proteins and other peptides can also react with acrylated PEG and derived, thus provides a facile method of conjugating biological cues

into the PEG hydrogels. However, this approach also has several disadvantages, such as longer polymerization time, high pH environment (above 7.4) the dissolution of biological cues after hydrogel degradation and swelling, and the lack of spatial and temporal control over network structure.[103]

2.3.3 Click chemistry

Click chemistry is a class of reactions that are fast, with high efficiency, occur under mild reaction conditions, without by-products or adverse reactions (Figure 2.7 c). For instance, Hedrick et al. synthesized cell encapsulated PEG hydrogels *via* the click reaction, with higher swelling ratios and mechanical properties compared to photo-crosslinking PEG hydrogels.[84] Click reactions are able to achieve structure-tunable hydrogel by changing the ratio of thiols and azide, while the gelation time is also adjustable by increasing temperature and catalyst amount.[104] The biggest drawback with conventional click reactions is the catalyst (cytotoxic copper ions), which have to be removed using chelators before cell culturing. However, DeForest et al. recently improved the click reaction by exploring a copper-free click reaction (with strained cyclic alkynes replacing linear ones), which was able to encapsulate cells *in situ*.[105]

2.3.4 Enzymatic reaction

Enzymatic reactions have been employed to fabricate hydrogels for tissue engineering.[94] Most enzymatic reactions proceed under mild conditions including at room temperature and neutral pH, and in cytocompatible buffer.[106] For example, Hubbell et al. explored an enzymatic reaction that is based on the crosslinking of lysine and glutamine residues mediated by the transglutaminase factor XIIIa (Figure 2.7 d).[94] This reaction combines fibrin molecules together in the final step of the blood clotting procedure *in vivo*. Conjugating transglutaminase into multi-arm PEG precursor can trigger a rapid gelation with enzyme and Ca^{2+} ions.[106] The enzymatic reactions are versatile to fabricate biological cues modified hydrogels, but are unfortunately limited in use due to diffusion limitations and expensive cost of enzymes.[107]

2.4 ECM-derived proteins based synthetic hydrogels

2.4.1 Gelatin-Based Hydrogels for Cell Encapsulation

Gelatin is water soluble, denaturation product of collagen, and widely investigated in applications food industry, medicine, tissue engineering and pharmaceutical processing.[108] Gelatin attracted increasing interest in the above fields because of its various desirable advantages, such as biodegradability, low cost, biocompatibility, and ease of manipulation. Compared to collagen, gelatin has limited antigenicity because of heat denaturation.[109] Moreover, the bioactivity of collagen for cell adhesion [e.g. (RGD) peptides] and MMP-sensitive degradation sequences are reserved in the backbone of gelatin [20]. Gelatin is able to form thermo-dependent hydrogel by physical interactions but this temperature-reversible hydrogel becomes aqueous solution at body temperature. Gelatin has been extensively modified to satisfy the requirements of biomedical applications. Especially in tissue engineering, gelatin is an excellent biological cue for cell adhesion and biodegradability.[110] Gelatin can be incorporated either without modification or following prior conjugation with other polymer. Unmodified gelatin can be covalently crosslinked in two methods to fabricate a hydrogel network, covalently or enzymatic reaction. A prior modification forming a gelatin-polymer precursor can be accomplished by synthesizing macromers with functional groups, such as gelatin-MA, gelatin-SH, gelatin-PEG-acrylate, after which gelatin based hydrogel can be formed by photo-polymerization precursor solution containing suspended cells.[22, 109]

Table 2.2 Modifications of Gelatin, functional groups and Crosslinking Methods for Cell Encapsulation. [108]

Functional group	Crosslinking parameters	Cell response after encapsulation
Acrylamide	Irgacure 2959 (UV-A, 365 nm)	>90% viability after 1 day (HepG2)
Ferulic acid	Laccase+O_2	>91% viability(fibroblasts, ECFCs), angiogenesis
Furfurylamine	Rose Bengal (VIS)	87% viability after 1 day (MSCs), osteochondral tissue formation

Methacryloyl	APS/TEMED	>80% viability after 1 day (chondrocytes)
	Irgacure 2959 (UV-A, 365 nm)	70% to >90% viability depending on crosslinking conditions, cell type, macromer concentration; various differentiations studied
	VA-086 (UV-A, 365 nm)	MSC/HUVEC co-culture, vascularization; >97% viability after extrusion printing (HepG2)
	LAP (VIS430–490 nm)	>96% viability after 1 day (MSCs); cell proliferation increase of 23% over 2 weeks; adipocyte culture
	G2CK or P2CK (near-infrared femtosecond laser 800 nm)	26% viability (MG63 cells) after phot-polymerization
Methacryloyl and acetylation	Irgacure 2959 (UV)	Encapsulation of chondrocyte for inkjet printing
Methacryloyl galactosylation	Irgacure 2959	90% viability (HepG2), functional analysis of hepatocytes
Norborene	DTT or LAP (UV 365 nm)	>91% viability (MSCs)
Phenolation	HRP+H_2O_2	>94% viability; neurogenesis, osteogenesis and vascularization
Styrenation	Camphor-quinone (VIS 400–520 nm)	26% viability (chondrocytes)
Sulfhydryl groups	Irgacure 2959 (UV-A, 365 nm)	>90% viability(fibroblasts, MSCs), skin tissue engineering (MSC)

(UV: ultra violet, VIS: visible light, APS: ammonium persulfate, DTT: dithiothreitol, TEMED: tetramethylethylenediamine, ECFC: endothelial colony-forming cell; G2CK and P2CK: benzyliden ecycloketone-based photo-initiators, HepG2: human hepatocellular carcinoma cell line, HUVEC: human umbilical vein endothelial cells, HRP: horseradish peroxidase, LAP: lithium acylpho-sphinate, MG63: human osteosarcoma cell line, MSC: mesenchymal stromal cells, VA-086: 2,2'-azobis[2-methyl-N-(2-hydroxyethyl) propionamide).

Modification of functional groups of gelatin molecules can be a useful tool to control the structure and properties of hydrogel compared to direct crosslinking methods. Although several crosslinking methods and functional groups can be used to fabricate hydrogels,

only a few of them are suitable for fabricating hydrogel and cell encapsulation at the same time (shown in Table 2.2).[111] Photo-based radical polymerization crosslinking of hydrogels is one of the most promising and attractive method due to uniform and controllable bulk structure, clinically acceptable curing times, encapsulation cells *in situ*, and mild crosslinking environment.[22] For this, both ultraviolet light (UV) and visible light (VIS) have been frequently used for photo-polymerization, thus various functional groups have been widely studied for cell encapsulation (Table 2.2).[22, 112, 113] Most of the reported studies use gelatin-MA with the photo-initiator Irgacure 2959,[108] which is water soluble and has a relatively low cytotoxicity compared to other photo initiators.[111] Gelatin-MA was synthesized through covalently conjugated gelatin with methacrylate, which can be crosslinked into hydrogels by photo-polymerization under mild conditions and encapsulate cell *in situ* with high viability.[114]

2.4.2 Elastin-based hydrogels

Elastin is an important structure protein of natural ECM in elastic tissues, such as vascular, skin and lungs.[115] *In vivo*, water-soluble tropoelastin monomers (elastin precursors) are able to form insoluble elastin fibers after crosslinking, thus elastin fibers are the dominant component of elastic tissue (above 40%). It is well known that elastin and its derivatives, such as tropoelastin and soluble elastin, support the activities of many cells including endothelial cells, fibroblasts and smooth muscle cells. The most well characterized interactions between cells and elastin are related with several cell-surface receptors such as elastin-binding protein (EBP), GAGs and integrins.[116] For example, EBP, expressed by various cells, is a β-galatosidase and binds to the motif like GXXPG, while VGVAPG is one of the well-studied GXXPG peptides and can modulate cell behavior, such as the migration of human keratinocytes, maintain the contractile phenotype of smooth muscle cells(SMCs), the proliferation of human fibroblast.[115, 116] Elastin is highly crosslinked to form a stable and persistent structure that processes the ability to bestow recoil. However, as a potential source of biomaterials, the high insolubility of elastin largely hinders its use. [117] Therefore, soluble bovine elastin, as a relatively easily sourced starting material, has been used to develop elastin-based

biomaterials. Proteolytic enzymes and chemical methods were successfully used to produce solubilized forms of elastin, such as α-elastin (hydrolysis by acid) or κ-elastin (hydrolysis by alkaline). All the methods are based on hydrolysis of the peptide bonds in elastin fibers. Recombinant elastin DNA in *E. coli* systems has been another important method to achieve elastin-like peptides or polymers.[116, 117]

Elastin-based hydrogels have been fabricated from various kinds of elastin including recombinant elastin-like proteins/polymers, soluble bovine elastin, elastin fibers and recombinant human tropoelastin.[115] The designing of elastin-like proteins or polymers for hydrogel can be easily accomplished through a modular strategy. Elastin peptides and specific cell-responsive peptides can be continuous or interspersed designed according to the purpose. For example, lysine residues containing elastin peptides have been designed to be the reaction sites, while sequences based on one of the typical repeating hydrophobic elastin sequences, VPGVG, provide elasticity, self-assembly and stimuli responsive properties in these hydrogels.[118] Their biomedical applications have been widely explored, such as biomimetic elastin based hybrid hydrogels for the fabrication of elastomeric scaffolds,[119] silk/elastin like polymers for controlled DNA delivery[120] and elastin-like polypeptides for injectable hydrogels.[121]

Soluble elastin from bovine neck ligament or tendon, as a relatively easily achieved material, has been studied to fabricate porous elastin hydrogels.[116] High pressure CO_2 was explored to form highly porous structure in elastin based hydrogels.[122] This highly porous structure allowed the proliferation of fibroblasts and also the infiltration into elastin hydrogel. Recombinant human tropoelastin has been investigated to fabricate natural elastin-mimicking hydrogels.[123] The frequently used crosslinkers for fabricating elastin-based hydrogels are chemical reagents such as glutaraldehyde, hexamethylene diisocyanate and bis (sulfosuccinimidyl) suberate, which are not cell compatible and cannot be used for cell encapsulation.[115] Nasim et al. reported methacrylated tropoelastin hydrogel for cell encapsulation. Although 90% of the cells were viable more than one week, they had round shape and were not able to attach and spread.[124] The reason may be explained from the adhesive peptides in methacrylated tropoelastin hydrogel as tropoelastin does not contain any RGD like peptides sequences.[115] Similarly, it has been recently reported that only 80% of encapsulated

cells remained viable in an elastin based thermo-responsive hydrogel fabricated by crosslinking alpha-elastin, Poly (N-isopropylacrylamide), Polylactide, 2-Hydroxyethyl methacrylate and oligo (ethylene glycol); the morphology, differentiation and the remolding of new ECM of cells have not yet been studied.[125] Thus, the effects of elastin on cell encapsulated hydrogels have yet to be elucidated for tissue engineering particularly in a 3-D microenvironment.

References

[1] A. Shekaran, A. J. Garcia. Biochimica et Biophysica Acta (BBA) - General Subjects. 2011, 1810, 350-360.

[2] J. S. Temenoff, A. G. Mikos. Biomaterials. 2000, 21, 2405-2412.

[3] A. N. Buxton, J. Zhu, R. Marchant, J. L. West, J. U. Yoo, B. Johnstone. Tissue engineering. 2007, 13, 2549-2560.

[4] M. S. Hahn, M. K. McHale, E. Wang, R. H. Schmedlen, J. L. West. Annals of biomedical engineering. 2007, 35, 190-200.

[5] C. Wang, R. R. Varshney, D.-A. Wang. Advanced drug delivery reviews. 2010, 62, 699-710.

[6] R. Lanza, R. Langer, J. P. Vacanti. Principles of tissue engineering, Academic press, 2011.

[7] N. Jaiswal, S. E. Haynesworth, A. I. Caplan, S. P. Bruder. Journal of cellular biochemistry. 1997, 64, 295-312.

[8] H. W. Schnaper, D. S. Grant, W. G. Stetler‐Stevenson, R. Fridman, G. D'Orazi, A. N. Murphy, R. E. Bird, M. Hoythya, T. R. Fuerst, D. L. French. Journal of cellular physiology. 1993, 156, 235-246.

[9] A. J. Engler, S. Sen, H. L. Sweeney, D. E. Discher. Cell. 2006, 126, 677-689.

[10] A. J. Engler, F. Rehfeldt, S. Sen, D. E. Discher. Methods in cell biology. 2007, 83, 521-545.

[11] R. S. Gieni, M. J. Hendzel. Journal of cellular biochemistry. 2008, 104, 1964-1987.

[12] K. L. Schmeichel, M. J. Bissell. Journal of cell science. 2003, 116, 2377-2388.

[13] O. W. Petersen, L. Rønnov-Jessen, A. R. Howlett, M. J. Bissell. Proceedings of the National Academy of Sciences. 1992, 89, 9064-9068.

[14] B. Weigelt, C. M. Ghajar, M. J. Bissell. Advanced drug delivery reviews. 2014, 69, 42-51.

[15] X. Fang, S. Sittadjody, K. Gyabaah, E. C. Opara, K. C. Balaji. PloS one. 2013, 8, e75187.

[16] O. Chaudhuri, S. T. Koshy, C. B. da Cunha, J.-W. Shin, C. S. Verbeke, K. H. Allison, D. J. Mooney. Nature materials. 2014, 13, 970-978.

[17] S. C. Wei, L. Fattet, J. H. Tsai, Y. Guo, V. H. Pai, H. E. Majeski, A. C. Chen, R. L. Sah, S. S. Taylor, A. J. Engler, J. Yang. Nat Cell Biol. 2015, 17, 678-688.

[18] Y. Imamura, T. Mukohara, Y. Shimono, Y. Funakoshi, N. Chayahara, M. Toyoda, N. Kiyota, S. Takao, S. Kono, T. Nakatsura. Oncology reports. 2015, 33, 1837-1843.

[19] H. Tanaka, C. L. Murphy, C. Murphy, M. Kimura, S. Kawai, J. M. Polak. Journal of cellular biochemistry. 2004, 93, 454-462.

[20] A. Birgersdotter, R. Sandberg, I. Ernberg. Seminars in Cancer Biology. 2005, 15, 405-412.

[21] M. W. Tibbitt, K. S. Anseth. Biotechnology and bioengineering. 2009, 103, 655-663.

[22] J. Zhu. Biomaterials. 2010, 31, 4639-4656.

[23] B. Brodsky, J. A. Ramshaw. Matrix Biology. 1997, 15, 545-554.

[24] J. E. Scott. Journal of anatomy. 1995, 187, 259.

[25] A. Atala, F. K. Kasper, A. G. Mikos. Science translational medicine. 2012, 4, 160rv112-160rv112.

[26] E. K. Yim, K. W. Leong. Journal of Biomaterials Science, Polymer Edition. 2005, 16, 1193-1217.

[27] G. A. Silva, C. Czeisler, K. L. Niece, E. Beniash, D. A. Harrington, J. A. Kessler, S. I. Stupp. Science. 2004, 303, 1352-1355.

[28] D. Seliktar. Science. 2012, 336, 1124-1128.

[29] H. Tan, K. G. Marra. Materials. 2010, 3, 1746-1767.

[30] J. Zhu, R. E. Marchant. Expert review of medical devices. 2011, 8, 607-626.

[31] G. D. Nicodemus, S. J. Bryant. Tissue Engineering Part B: Reviews. 2008, 14, 149-165.

[32] P. M. Kharkar, K. L. Kiick, A. M. Kloxin. Chemical Society Reviews. 2013, 42, 7335-7372.

[33] C. R. Nuttelman, M. C. Tripodi, K. S. Anseth. Matrix biology. 2005, 24, 208-218.

[34] C. S. Chen, M. Mrksich, S. Huang, G. M. Whitesides, D. E. Ingber. Science. 1997, 276, 1425-1428.

[35] D. Dikovsky, H. Bianco-Peled, D. Seliktar. Biomaterials. 2006, 27, 1496-1506.

[36] A. S. Sawhney, C. P. Pathak, J. A. Hubbell. Macromolecules. 1993, 26, 581-587.

[37] A. T. Metters, K. S. Anseth, C. N. Bowman. The Journal of Physical Chemistry B. 2001, 105, 8069-8076.

[38] N. Hunt, A. M. Smith, U. Gbureck, R. Shelton, L. Grover. Acta biomaterialia. 2010, 6, 3649-3656.

[39] K. S. Anseth, C. N. Bowman, L. Brannon-Peppas. Biomaterials. 1996, 17, 1647-1657.

[40] J. L. Drury, D. J. Mooney. Biomaterials. 2003, 24, 4337-4351.

[41] K. H. Nakayama, L. Hou, N. F. Huang. Advanced Healthcare Materials. 2014, 3, 628-641.

[42] M. A. Daniele, A. A. Adams, J. Naciri, S. H. North, F. S. Ligler. Biomaterials. 2014, 35, 1845-1856.

[43] K. Xu, Y. Fu, W. Chung, X. Zheng, Y. Cui, I. C. Hsu, W. J. Kao. Acta Biomaterialia. 2012, 8, 2504-2516.

[44] Y. Fu, K. Xu, X. Zheng, A. J. Giacomin, A. W. Mix, W. J. Kao. Biomaterials. 2012, 33, 48-58.

[45] J. A. Burdick, K. S. Anseth. Biomaterials. 2002, 23, 4315-4323.

[46] D. E. Ingber, V. C. Mow, D. Butler, L. Niklason, J. Huard, J. Mao, I. Yannas, D. Kaplan, G. Vunjak-Novakovic. Tissue engineering. 2006, 12, 3265-3283.

[47] S. Lin, N. Sangaj, T. Razafiarison, C. Zhang, S. Varghese. Pharmaceutical Research. 2011, 28, 1422-1430.

[48] T. Canal, N. A. Peppas. Journal of biomedical materials research. 1989, 23, 1183-1193.

[49] P. J. Flory. Polymer. 1979, 20, 1317-1320.

[50] H. Liao, D. Munoz-Pinto, X. Qu, Y. Hou, M. A. Grunlan, M. S. Hahn. Acta Biomaterialia. 2008, 4, 1161-1171.

[51] S. H. Um, J. B. Lee, N. Park, S. Y. Kwon, C. C. Umbach, D. Luo. Nature materials. 2006, 5, 797-801.

[52] Y. Xing, E. Cheng, Y. Yang, P. Chen, T. Zhang, Y. Sun, Z. Yang, D. Liu. Advanced Materials. 2011, 23, 1117-1121.

[53] N. Ma, L. Zhang, D. Ying, P. He, M.-g. Jin, H. Liu, C.-y. Chen, in Frontier and Future Development of Information Technology in Medicine and Education, Springer, 2014, 2443-2452.

[54] J. Glowacki, S. Mizuno. Biopolymers. 2008, 89, 338-344.

[55] J. Kisiday, M. Jin, B. Kurz, H. Hung, C. Semino, S. Zhang, A. Grodzinsky. Proceedings of the National Academy of Sciences. 2002, 99, 9996-10001.

[56] L. Haines-Butterick, K. Rajagopal, M. Branco, D. Salick, R. Rughani, M. Pilarz, M. S. Lamm, D. J. Pochan, J. P. Schneider. Proceedings of the National Academy of Sciences. 2007, 104, 7791-7796.

[57] K. A. Smeds, M. W. Grinstaff. Journal of biomedical materials research. 2001, 54, 115-121.

[58] X. Z. Shu, Y. Liu, F. S. Palumbo, Y. Luo, G. D. Prestwich. Biomaterials. 2004, 25, 1339-1348.

[59] K. S. Masters, D. N. Shah, L. A. Leinwand, K. S. Anseth. Biomaterials. 2005, 26, 2517-2525.

[60] A. M. Smith, J. J. Harris, R. M. Shelton, Y. Perrie. Journal of controlled release. 2007, 119, 94-101.

[61] Y. Hong, H. Song, Y. Gong, Z. Mao, C. Gao, J. Shen. Acta biomaterialia. 2007, 3, 23-31.

[62] Y. Yeo, W. Geng, T. Ito, D. S. Kohane, J. A. Burdick, M. Radisic. Journal of Biomedical Materials Research Part B: Applied Biomaterials. 2007, 81, 312-322.

[63] Y. Yeo, J. A. Burdick, C. B. Highley, R. Marini, R. Langer, D. S. Kohane. Journal of Biomedical Materials Research Part A. 2006, 78, 668-675.

[64] Q. Li, C. G. Williams, D. D. Sun, J. Wang, K. Leong, J. H. Elisseeff. Journal of biomedical materials research Part A. 2004, 68, 28-33.

[65] S. J. Bryant, J. A. Arthur, K. S. Anseth. Acta biomaterialia. 2005, 1, 243-252.

[66] C.-C. Lin, A. T. Metters. Advanced drug delivery reviews. 2006, 58, 1379-1408.

[67] A. Hejčl, J. Šedý, M. Kapcalová, D. A. Toro, T. Amemori, P. Lesný, K. Likavčanová-Mašínová, E. Krumbholcová, M. Přádný, J. Michálek. Stem cells and development. 2010, 19, 1535-1546.

[68] J. A. Beamish, J. Zhu, K. Kottke‐Marchant, R. E. Marchant. Journal of Biomedical Materials Research Part A. 2010, 92, 441-450.

[69] M. Burek, M. Kowalczyk, Z. P. Czuba, W. Krol, R. Pilawka, S. Waskiewicz. Polymer Degradation and Stability. 2016.

[70] A. Higuchi, N. Aoki, T. Yamamoto, T. Miyazaki, H. Fukushima, T. M. Tak, S. Jyujyoji, S. Egashira, Y. Matsuoka, S. H. Natori. Journal of Biomedical Materials Research Part A. 2006, 79, 380-392.

[71] S. P. Zustiak, S. Pubill, A. Ribeiro, J. B. Leach. Biotechnology progress. 2013, 29, 1255-1264.

[72] N. A. Peppas, K. B. Keys, M. Torres-Lugo, A. M. Lowman. Journal of controlled release. 1999, 62, 81-87.

[73] C. Echalier, C. Pinese, X. Garric, H. Van Den Berghe, E. Jumas Bilak, J. Martinez, A. Mehdi, G. Subra. Chemistry of Materials. 2016, 28, 1261-1265.

[74] D. A. Ossipov, K. Brännvall, K. Forsberg‐Nilsson, J. Hilborn. Journal of applied polymer science. 2007, 106, 60-70.

[75] J. F. Mano, G. A. Silva, H. S. Azevedo, P. B. Malafaya, R. A. Sousa, S. S. Silva, L. F. Boesel, J. M. Oliveira, T. C. Santos, A. P. Marques, N. M. Neves, R. L. Reis. Journal of The Royal Society Interface. 2007, 4, 999-1030.

[76] J. Lee, M. J. Cuddihy, N. A. Kotov. Tissue Engineering Part B: Reviews. 2008, 14, 61-86.

[77] N. Sanabria-DeLong, S. K. Agrawal, S. R. Bhatia, G. N. Tew. Macromolecules. 2007, 40, 7864-7873.

[78] J. Zhang, A. Skardal, G. D. Prestwich. Biomaterials. 2008, 29, 4521-4531.

[79] M. Deshmukh, Y. Singh, S. Gunaseelan, D. Gao, S. Stein, P. J. Sinko. Biomaterials. 2010, 31, 6675-6684.

[80] S. P. Zustiak, J. B. Leach. Biomacromolecules. 2010, 11, 1348-1357.

[81] J. D. Clapper, J. M. Skeie, R. F. Mullins, C. A. Guymon. Polymer. 2007, 48, 6554-6564.

[82] Z. Jiang, J. Hao, Y. You, Y. Liu, Z. Wang, X. Deng. Journal of Biomedical Materials Research Part A. 2008, 87, 45-51.

[83] S. Kaihara, S. Matsumura, J. P. Fisher. European Journal of Pharmaceutics and Biopharmaceutics. 2008, 68, 67-73.

[84] M. Malkoch, R. Vestberg, N. Gupta, L. Mespouille, P. Dubois, A. F. Mason, J. L. Hedrick, Q. Liao, C. W. Frank, K. Kingsbury. Chemical Communications. 2006, 2774-2776.

[85] K. S. Anseth, H.-A. Klok. Biomacromolecules. 2016, 17, 1-3.

[86] T. O. Machado, C. Sayer, P. H. Araujo. European Polymer Journal. 2016.

[87] P. M. Kharkar, M. Rehmann, K. M. Skeens, E. Maverakis, A. Kloxin. ACS Biomaterials Science & Engineering. 2016.

[88] G. A. Hudalla, T. S. Eng, W. L. Murphy. Biomacromolecules. 2008, 9, 842-849.

[89] C. A. Hauser, S. Zhang. Chemical Society Reviews. 2010, 39, 2780-2790.

[90] K. M. French, I. Somasuntharam, M. E. Davis. Advanced drug delivery reviews. 2016, 96, 40-53.

[91] M. A. Daniele, D. A. Boyd, A. A. Adams, F. S. Ligler. Advanced Healthcare Materials. 2015, 4, 11-28.

[92] M. Goktas, G. Cinar, I. Orujalipoor, S. İde, A. B. Tekinay, M. O. Guler. Biomacromolecules. 2015.

[93] K. M. Galler, L. Aulisa, K. R. Regan, R. N. D'Souza, J. D. Hartgerink. Journal of the American Chemical Society. 2010, 132, 3217-3223.

[94] S. Q. Liu, R. Tay, M. Khan, P. L. R. Ee, J. L. Hedrick, Y. Y. Yang. Soft Matter. 2010, 6, 67-81.

[95] D. L. Hern, J. A. Hubbell. Journal of biomedical materials research. 1998, 39, 266-276.

[96] C. R. Nuttelman, M. A. Rice, A. E. Rydholm, C. N. Salinas, D. N. Shah, K. S. Anseth. Progress in polymer science. 2008, 33, 167-179.

[97] J. J. Moon, J. E. Saik, R. A. Poche, J. E. Leslie-Barbick, S.-H. Lee, A. A. Smith, M. E. Dickinson, J. L. West. Biomaterials. 2010, 31, 3840-3847.

[98] C. N. Salinas, K. S. Anseth. Macromolecules. 2008, 41, 6019-6026.

[99] M. Herten, R. E. Jung, D. Ferrari, D. Rothamel, V. Golubovic, A. Molenberg, C. H. Hämmerle, J. Becker, F. Schwarz. Clinical Oral Implants Research. 2009, 20, 116-125.

[100] K. A. Kyburz, K. S. Anseth. Acta Biomaterialia. 2013, 9, 6381-6392.

[101] D. L. Elbert, A. B. Pratt, M. P. Lutolf, S. Halstenberg, J. A. Hubbell. Journal of Controlled Release. 2001, 76, 11-25.

[102] Y. Park, M. P. Lutolf, J. A. Hubbell, E. B. Hunziker, M. Wong. Tissue engineering. 2004, 10, 515-522.

[103] C.-C. Lin, K. S. Anseth. Pharmaceutical research. 2009, 26, 631-643.

[104] D. A. Ossipov, J. Hilborn. Macromolecules. 2006, 39, 1709-1718.

[105] C. A. DeForest, B. D. Polizzotti, K. S. Anseth. Nature materials. 2009, 8, 659-664.

[106] M. Ehrbar, S. C. Rizzi, R. G. Schoenmakers, B. San Miguel, J. A. Hubbell, F. E. Weber, M. P. Lutolf. Biomacromolecules. 2007, 8, 3000-3007.

[107] R. V. Ulijn. Journal of Materials Chemistry. 2006, 16, 2217-2225.

[108] B. J. Klotz, D. Gawlitta, A. J. Rosenberg, J. Malda, F. P. Melchels. Trends in biotechnology. 2016, 34, 394-407.

[109] S. Gorgieva, V. Kokol. Collagen-vs. gelatine-based biomaterials and their biocompatibility: review and perspectives, INTECH open access publisher, 2011.

[110] D. Loessner, C. Meinert, E. Kaemmerer, L. C. Martine, K. Yue, P. A. Levett, T. J. Klein, F. P. Melchels, A. Khademhosseini, D. W. Hutmacher. Nature protocols. 2016, 11, 727-746.

[111] I. Mironi-Harpaz, D. Y. Wang, S. Venkatraman, D. Seliktar. Acta Biomaterialia. 2012, 8, 1838-1848.

[112] W. Schuurman, P. A. Levett, M. W. Pot, P. R. van Weeren, W. J. Dhert, D. W. Hutmacher, F. P. Melchels, T. J. Klein, J. Malda. Macromolecular bioscience. 2013, 13, 551-561.

[113] T. Mazaki, Y. Shiozaki, K. Yamane, A. Yoshida, M. Nakamura, Y. Yoshida, D. Zhou, T. Kitajima, M. Tanaka, Y. Ito. Scientific reports. 2014, 4.

[114] E. Kaemmerer, F. P. W. Melchels, B. M. Holzapfel, T. Meckel, D. W. Hutmacher, D. Loessner. Acta Biomaterialia. 2014, 10, 2551-2562.

[115] J. F. Almine, D. V. Bax, S. M. Mithieux, L. Nivison-Smith, J. Rnjak, A. Waterhouse, S. G. Wise, A. S. Weiss. Chemical Society Reviews. 2010, 39, 3371-3379.

[116] J. Ozsvar, S. M. Mithieux, R. Wang, A. S. Weiss. Biomaterials science. 2015, 3, 800-809.

[117] W. F. Daamen, J. Veerkamp, J. Van Hest, T. Van Kuppevelt. Biomaterials. 2007, 28, 4378-4398.

[118] A. Girotti, J. Reguera, J. C. Rodr ́guez-Cabello, F. J. Arias, M. Alonso, A. M. Testera. Journal of Materials Science: Materials in Medicine. 2004, 15, 479-484.

[119] S. E. Grieshaber, A. J. Farran, S. Lin-Gibson, K. L. Kiick, X. Jia. Macromolecules. 2009, 42, 2532-2541.

[120] D. Hwang, V. Moolchandani, R. Dandu, M. Haider, J. Cappello, H. Ghandehari. International journal of pharmaceutics. 2009, 368, 215-219.

[121] H. Betre, L. A. Setton, D. E. Meyer, A. Chilkoti. Biomacromolecules. 2002, 3, 910-916.

[122] N. Annabi, S. M. Mithieux, A. S. Weiss, F. Dehghani. Biomaterials. 2010, 31, 1655-1665.

[123] S. M. Mithieux, Y. Tu, E. Korkmaz, F. Braet, A. S. Weiss. Biomaterials. 2009, 30, 431-435.

[124] N. Annabi, S. M. Mithieux, P. Zorlutuna, G. Camci-Unal, A. S. Weiss, A. Khademhosseini. Biomaterials. 2013, 34, 5496-5505.

[125] A. Fathi, S. M. Mithieux, H. Wei, W. Chrzanowski, P. Valtchev, A. S. Weiss, F. Dehghani. Biomaterials. 2014, 35, 5425-5435.

Chapter 3

Experimental Methodology

This chapter describes the materials, fabrication methods and characterization methods used in this work and it is classified into five sections, including materials synthesis, hydrogel fabrication, materials characterization, cell culture and evaluation, and statistics analysis. It explains the mechanism, details of experiments and analysis methods used to prove the hypothesis and materials fabrication for this thesis. The first section explains the synthesis mechanism and experiment detail of PEGDA, thiolation of ECM proteins and PEGylation. The second section introduces the fabrication detail of hydrogel, while the third section reveals material characterization. To evaluate cell response after encapsulation, several cell culture studies and the techniques used are described in the fourth section. Statistics analysis method is introduced in the last section.

3.1 Materials synthesis

3.1.1 Synthesis of PEGDA

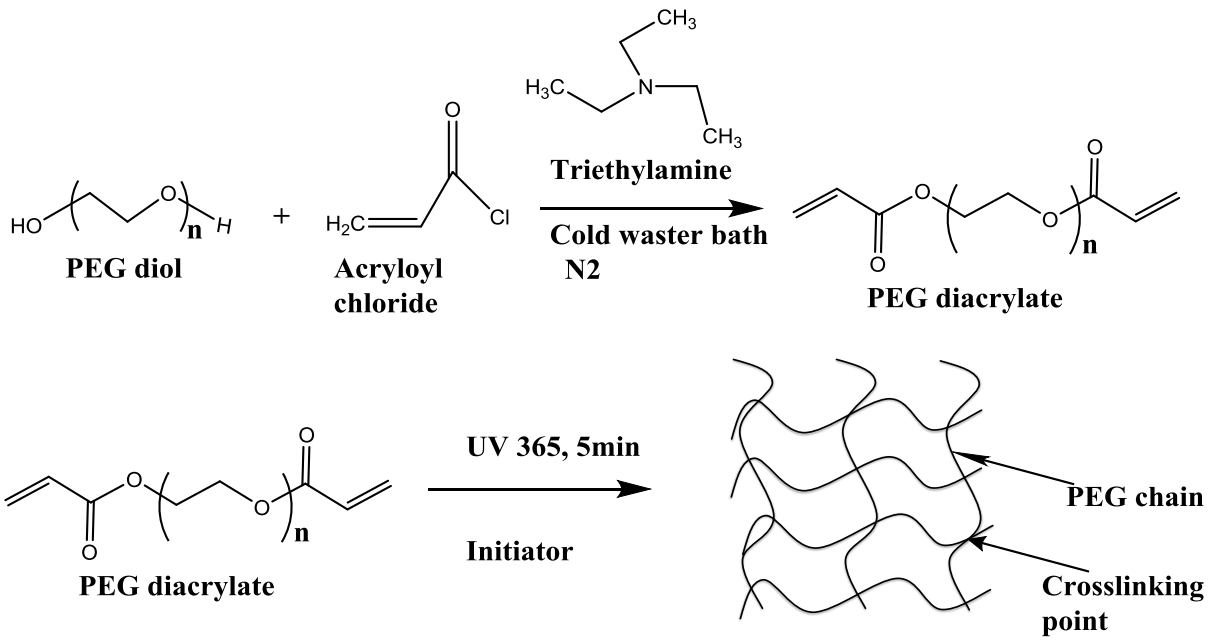

Figure 3.1 The synthesis route of PEGDA and fabrication mechanism of PEG hydrogel.[1]

PEGDA was synthesized based on substitution reaction according to a previous publication (Figure 3.1).[2] PEG-OH(Sigma-Aldrich, USA) was reacted with acryloyl chloride to from acrylate end PEG, while trimethylamine(Sigma-Aldrich, USA) was used to neutralize the byproduct (HCl).[3, 4] PEG-OH powder (MW: 10k or 8k) was dissolved in 100 mL anhydrous toluene (Sigma-Aldrich, USA) and 100 mL dichloromethane (DCM, Sigma-Aldrich, USA). Then two molar equivalent of trimethylamine (for HPLC, Sigma-Aldrich, USA) was added, followed by drop wise addition of four molar of purified acryloyl chloride (Merck, Germany) in excess. The above solution was stirred under argon overnight in ice water bath. The concentrated PEGDA solution was added to cold diethyl ether (Sigma-Aldrich, USA) immediately for precipitation. After filtration, the solid PEGDA was dissolved in DCM and washed with 2 mol/L $KHCO_3$ (Sigma-Aldrich, USA), and separated into aqueous and DCM phases. The solution in aqueous phase was aspirated and discarded. The solution in organic phase was evaporated,

precipitated in diethyl ether and filtered again. Finally, the solid was dried at RT under vacuum overnight. Acylation (90%) was confirmed by proton Nuclear magnetic resonance (^{1}H-NMR). PEGDA was able to form gel under UV light (365nm) with initiator inside (Figure 3.1).

3.1.2 Thiolation of protein

(1-ethyl-3-(3-dimethylaminopropyl) carbodiimide hydrochloride (EDC·HCl, Sigma-Aldrich, USA)) react with carboxyl groups to produce an active O-acylisourea intermediate that is easily substituted by nucleophilic attack from primary amine groups (Figure 3.2(A)). The original carboxyl groups form amide bonds with primary amines, and a soluble EDC by-product was removed after purification.[5] In this study, EDC was employed to modify ECM protein with thiols. Firstly, elastin soluble (ES, American Elastin Product company) and elastin peptides (EP, American Elastin Product company), prepared by treated with hot oxalic acid, were chosen as the biological cues of ECM-mimicking hydrogel. The ES and EP were conjugated to PEGDA by Michael- addition reaction, which was a nucleophilic addition of a nucleophile (sulfhydryl groups) to the molecules containing α, β-unsaturated carbonyl (double bond). However, both the ES and EP do not have the necessary sulfhydryl groups. Therefore, the thiolation to elastin have to be completed before Michael addition reaction, while EDC and N-Hydroxysuccinimide (NHS, Sigma-Aldrich, USA) were used to conjugate thiols *via* amine groups. The primary amine groups on elastin were conjugated with cystamine (Sigma-Aldrich, USA) and followed with cleavage of disulfide bonds by dithiothreitol (DTT, Sigma-Aldrich, USA), as shown in Figure 3.2[6]. DTT is capable of reducing unhidden disulfides and stabilize free sulfhydryl in aqueous environment although oxygen exists. The byproducts of DTT are water-soluble and can be removed by dialysis. The clearage reaction mechanism is illustrated in Figure 3.2 (B). [6] DTT (final concentration of 0.1mol/L) was added to the ES-SS or EP-SS (20mg/mL in PBS), respectively. After two hours reaction, the solution was dialyzed against distill water (pH 5, 4 ℃) for two days.

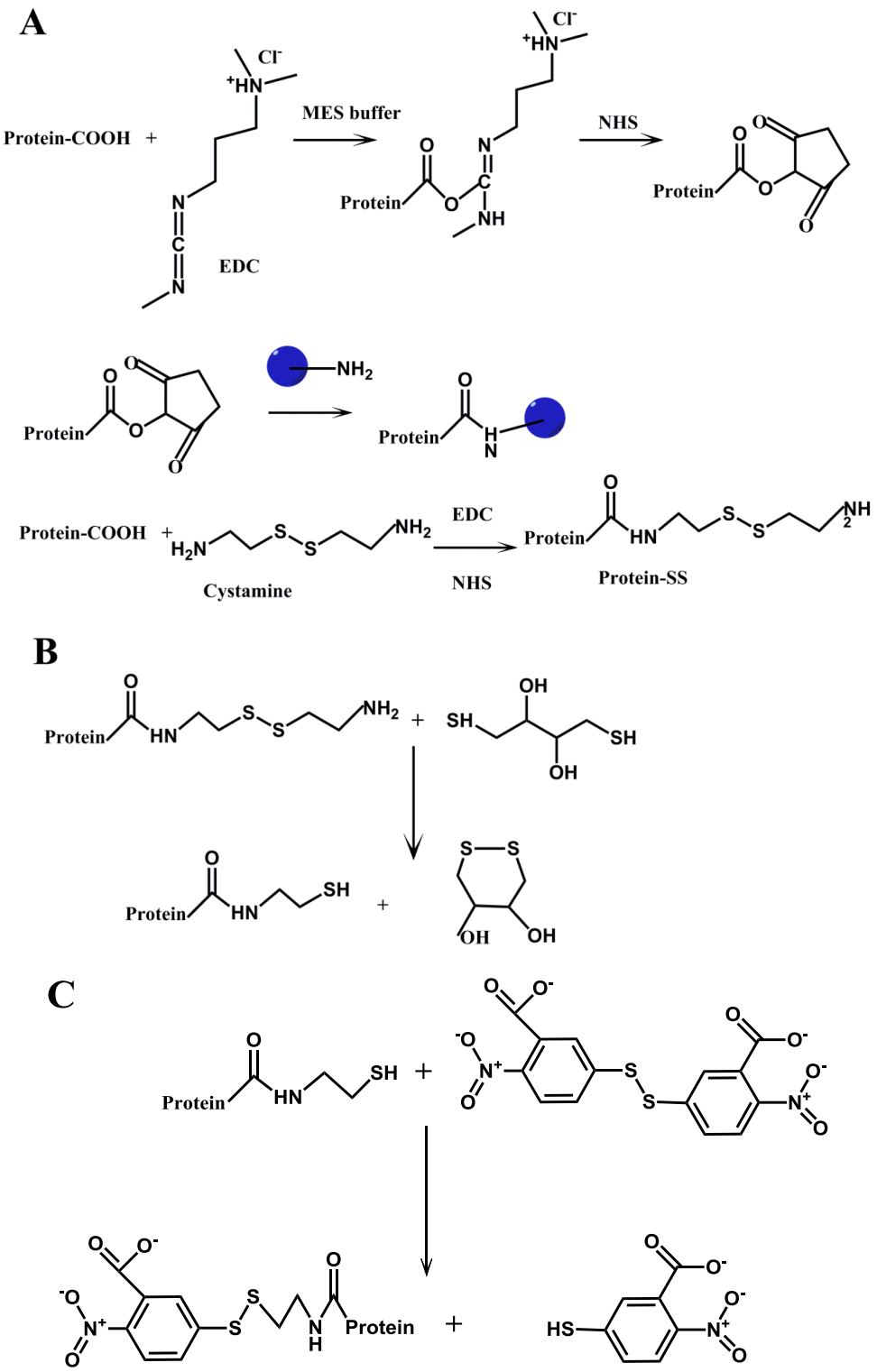

Figure 3.2 (A) EDC and NHS activate carboxyl groups of protein and then react with primary amine groups;(B) The disulfide bonds of protein can be cleaved by DTT, while the byproduct can be removed by dialysis method; (C) Ellman's reagents react with a thiol and then produce the chromogenic TNB anion, which can be measured by its absorbance at 412 nm.

After the dialysis procedure, Ellman's reagent is used to determine the sulfhydryl amount in solution, while Ellman's reagent can react with a free sulfhydryl group to form disulfide and 2-nitro-5-thiobenzoic acid (yellow color product)(shown in Figure 3.2(C))[6] Briefly, Ellman's reagent solution was prepared by dissolving 4mg Ellman's reagent in 1mL of reaction buffer, while reaction buffer was prepared from 0.1mol/L sodium phosphate, pH8.0 with 1mmol/L EDTA. 250μL standards solution (0.25mM~1.5mM cysteine) and sample solution were added into working solution (containing 50μL Ellman's reagent solution and 2.5mL reaction buffer) and incubated at room temperature for 15 mins after mixing. This yellow-colored product can be measured by UV-VIS spectrometer at wavelength 412nm, which has a linear coefficient against its amount. Standard curve can be obtained from plotting the mean absorbance against the standard concentration.

3.1.3 The cleavage of disulfide bond by TCEP

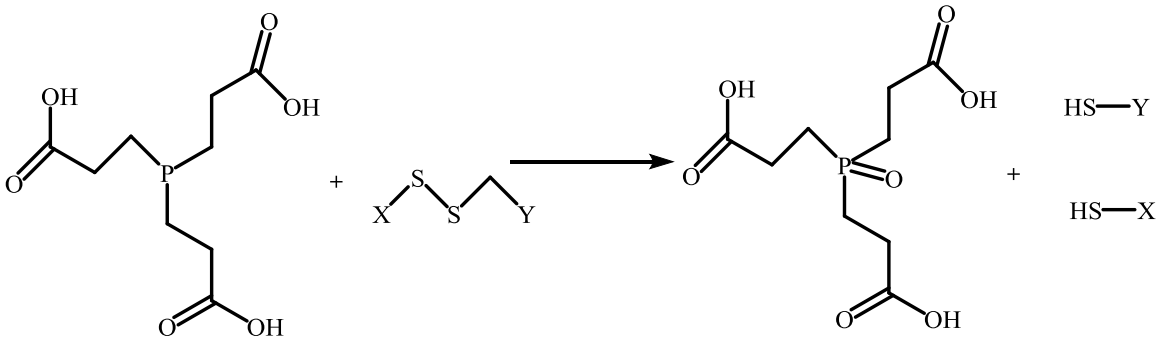

Figure 3.3 The reduction reaction of TCEP and disulfides.

To overcome the instability of sulfhydryl groups, TCEP was introduced in this work. TCEP are able to react with disulfides and results the formation of thiols and oxidation of the phosphine (shown in Figure 3.3).[7] The oxidation product of TCEP is stable and prevents the reversal of disulfides reaction. As this reaction is accomplished without any added free thiol chemicals, the following conjugation reaction can be done without removal of excess TCEP or reaction byproducts.[8] In this work, TCEP was added into

thiolated protein solution immediately after purification, while the amount was calculated from the amount of thiols.

3.1.4 PEGylation

The ES/EP-SH solution was reacted with PEGDA immediately after the dialysis procedure. This reaction was based on the Michael type addition reaction, attack of nucleophilic to a carbanion or a nucleophile.[2, 4, 9-11] ES/EP-SH was reacted with 10k PEGDA at pH 8 for 3 hours at room temperature. The final solution was dialyzed against distill water at room temperature to remove unreacted PEGDA. Finally, the solution after purification was dried by lyophilization.

3.2 Fabrication of hydrogel

Hydrogels were fabricated to covalently crosslinked samples using photo polymerization by adding 0.1 w/v % Irgacure 2959 (Sigma-Aldrich, USA) and exposing to UV light (365nm, 4-5mW/cm^2, Vilber Lourmat, France) for 5 min.[2, 11, 12] Each hydrogel was polymerized from 100 µL of precursor.

3.3 Materials characterization

3.3.1 Proton nuclear magnetic resonance ^{1}H-NMR and Fourier Transform Infrared Spectroscopy (FTIR)

Proton NMR spectra of chemicals are characterized by shift of different H atom in the molecule in the range +14 to -4 ppm, while the value of chemical shit depends on the structure, solvent and applied magnetic field. The integration curve for each peak shows the number of the individual protons. Hydrogen nuclei are highly sensitive to the hybridization of the atom to which the hydrogen atom is combined and to electronic effects at a certain chemical environment. Nuclei will tend to be deshielded by groups which withdraw electron density.[13] Therefore, ^{1}H-NMR can be employed to analyze the structure of molecules. For ^{1}H –NMR sample preparation, 2 ~10 mg samples were dissolved into 0.6-1 mL of Deuterium oxide (Sigma-Aldrich, USA) and then above

solution were transferred into NMR tubes (Sigma-Aldrich, USA). The ^{1}H-NMR spectra were recorded with a 400 MHz spectrum (Bruker, NanoBay 400MHz).

FTIR was used to characterize the chemical composition of the elastin, thiolated elastin and elastin-PEG. For FTIR sample preparation, 1mg of solid sample was mixed with 100mg potassium bromide (Sigma-Aldrich, USA), followed by preparation of pellet and analyzed by FTIR (Perkin Elmer Frontier, USA).

3.3.2 Swelling, degradation and gel fraction

Each hydrogel was polymerized from 100 μL of gelatin-PEG and elastin-PEG precursors, washing for 24 hours in distill water and then lyophilized for 2 days. Swelling studies were performed by immersing the lyophilized hydrogels in 2.0 mL of pH 7.2 PBS and incubating at 37℃ in 24 well plates.[14-16] At predetermined time points, hydrogels were carefully taken out, and weighed. The equilibrium (weight) swelling ratio (Q) is calculated as:

$$Q = \frac{W_2 - W_1}{W_1} \qquad \text{Equation 1}$$

where W_2 is the gel weight at each time point, and W_1 is the original dried weight of hydrogel. Moreover, each hydrogel was immersed into 2.0 mL of fresh medium (PBS) immediately after weighing at each time point.

To determine the possible effect of collagenase on hydrogel degradation, each hydrogel was prepared from 100 μL precursor solution as described above, placed in 24 well plates with 1mL PBS containing 0.1 mg/mL or 0.5 mg/mL collagenase type I A.[15] At each time point the weight of the remaining gel (W_3) was measured and immersed in fresh collagenase solution until the hydrogel was completely degraded. The percentage of weight loss was calculated as (W_4-W_3/W_4) ×100%, where W_4 represents the hydrogel weight after the initial 12 h PBS equilibration.

The gel fraction of the crosslinked hydrogels was determined according to the published paper. [17] Each hydrogel was immersed in 2 mL deionized water at room temperature for 24 h, and lyophilized for 48 h. The residue after extraction was taken as the gel

component. The gel fraction of the crosslinked hydrogels was calculated as (W_5/W_6) ×100%, where W_5 and W_6 are weights of lyophilized hydrogels before and after soaking in deionized water, respectively.

3.3.3 Rheology

The rheological properties of the hydrogels were characterized using Anton Paar Physica MCR 501 rheometer equipped with Peltier plate temperature-controlled systems (P-PTD-200/TG and P-PTD120/GL) and an UV light curing system (Omni Cure S1000). A CP25 cone-plate geometry with 25 mm diameter was used for in situ time-sweep test of cell-free hydrogels and a PP8 parallel-plate with 8 mm was used for cell-laden hydrogels. The testing conditions for all measurements were 1-2% strain amplitude at an oscillation frequency of 0.1 - 1 Hz within the linear viscoelastic regime. Dynamic time-sweep tests were performed by loading 80 µL of cell-free precursor solution and UV irradiation (20 mW/ cm^2) for 5 min to facilitate photo-polymerization.[14, 18, 19]

The damping or loss/dissipation factor of a material: tan δ, the ratio of the loss to the storage modulus of the material, was measured from the rheological measurements:

$$\tan\delta = \frac{G''}{G'} \qquad \text{Equation 2}$$

The average mesh size ξ, defined as the linear distance between two adjacent crosslinks, was calculated from the swelling and rheological data according to the theories summarized by Venkatraman [20, 21] and Peppas [22-24]:

$$G' = 0.5 \times \left(\frac{dRT}{M_c}\right) C_x \qquad \text{Equation 3}$$

$$\left(\overline{r_0}^2\right)^{\frac{1}{2}} = l(2M_c/M_r)^{\frac{1}{2}} C_n{}^{\frac{1}{2}} \qquad \text{Equation 4}$$

$$Q_s = Q = \frac{W_2 - W_1}{W_1} \qquad \text{Equation 5}$$

$$V_{2,s} = \left((Q_s + 1)\,{}^{\rho_2}/_{\rho_1}\right)^{-1} \quad \text{Equation 6}$$

$$\xi = \left(V_{2,s}\right)^{-\frac{1}{3}}\left(\bar{r}_0{}^2\right)^{\frac{1}{2}} \quad \text{Equation 7}$$

where G´is the shear storage modulus of each hydrogel measured after swelling 24 hours, d is the network density (1.21×10^3 kg/m^3 for PEG), R is the molar gas constant, T is the temperature, Mc is the number average molar mass between crosslinks, Mr is the molar mass of the repeating unit (44 g/mol for PEG), l is the C-C bond length (1.54×10^{-10} m), Qs is the mass swelling ratio and calculated from equation 1, ρ_1 is the solvent density, ρ_2 is the polymer density and C_n is the characteristic ratio (4.0 for PEG) [25].

For the in situ rheological property experiments, cell encapsulated Gelatin-PEG hydrogels were taken out from cell culture media at each time point (day 1, day 3 and day 7) and then analyzed immediately. The testing conditions for all measurements were the same as mentioned above.

3.3.4 BCA method

The bicinchoninic acid (BCA) Protein Assay is used for the detection and quantitation of total protein *via* absorbance. This method is based on the biuret reduction reaction of Cu^{+2} to Cu^{+1} by protein in an alkaline medium and the highly sensitive and selective colorimetric detection of the Cu^{+1} *via* BCA (shown in Figure 3.4). The product of above two reactions is purple-colored and generated from the chelation of two molecules of BCA with one Cu^{+1} reaction. This purple-colored product has a strong absorbance at 562nm that shows linear trend with increasing protein concentrations at a wide range of 20-2000μg/mL.[26] Firstly, different concentrations of standard protein and unknown samples were prepared at least a volume of 0.3mL in order to do triplicate tests. 2.0mL working reagent was prepared from mixing 50 parts "A" (sodium carbonate, sodium bicarbonate, bicinchoninic acid and sodium tartrate in 0.1M sodium hydroxide) with 1 part "B" (4% cupric sulfate). 100μL sample was added into 2mL working reagent and

incubated at 37℃ for 30mins. Finally, the absorbance of each standard and protein was measured at 562nm within 10 mins.

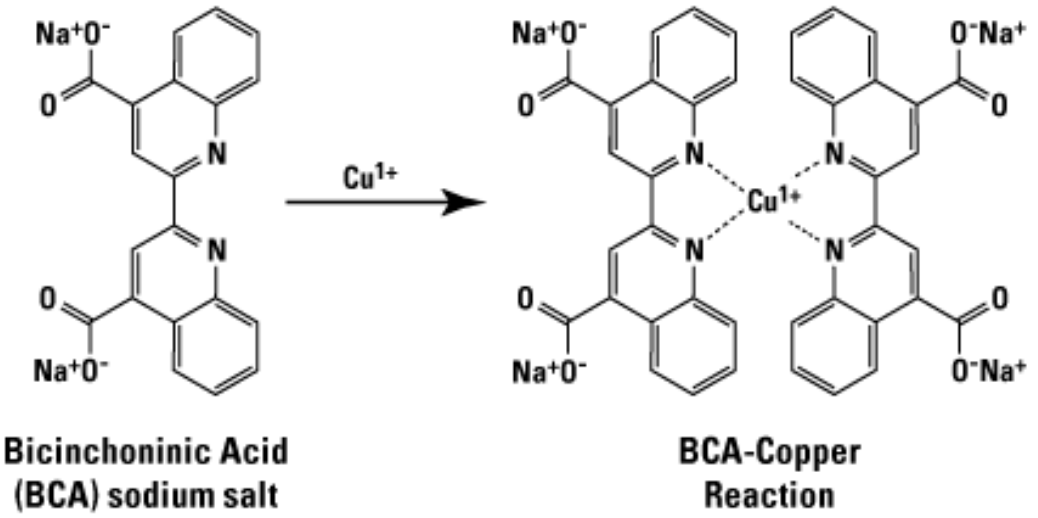

Figure 3.4 Two molecules of BCA react with one copper ion that produced from a protein - mediated biuret reaction.[26]

3.3.5 Sodium dodecyl sulfate polyacrylamide gel electrophoresis (SDS-PAGE)

SDS-PAGE is the most frequently used technique to determine the rough molecular weights of proteins with markers according to the mobility of known proteins on the same gel. Gradient gels have the appropriate pore size in the gel, which can estimate molecular weight more accurate via narrowing down stained protein bands. In this work, SDS-PAGE was used to investigate the molecular weight change after PEGylation.[11] The experiment procedures of SDS-PAGE are as follows:[27]

A) The preparation of gel tank and gel cassette:

1. Put gel into gel running inner tank and add enough volume of Tris-Glycine-SDS running buffer into the inner tank and cover the wells by 5-7mm.
2. Add Tris-Glycine-SDS running buffer to the outer tank to reach the bottom of the sample wells.
3. Using pipette to wash the sample wells with running buffer and remove air bubbles.

B) Sample preparation for SDS

Mix one part sample buffer with four parts of protein sample (e.g., 5μL sample buffer+20μL protein sample), add DTT (final concentration: 10mM), and boil sample for 3-5 minutes to denature proteins. Collect the supernatant after centrifugation at ~1000 g for 3 minutes.

C) Sample loading

Add 5-50μg (total protein) per sample well and make sure the volume adding to each well doesn't exceed the well capacity.

D) Running Conditions

Connect the power supply and set up parameters as follows: 110V, 60mins.

E) Removing a Gel from the Cassette and staining

Remove the gel from the tank after electrophoresis, wash the gel with distill water for 10-15 mins to remove SDS, stained with Pierce Imperial Protein Stain for 1 hour, rinse gel in distill water overnight and image by camera.

3.4 Cell culture and evaluation

3.4.1 2-D cell culture

Neonatal human dermal fibroblasts (NHDFs, passage 1) were obtained from Lonza. NHDFs were cultured in 175 cm^2 tissue culture polystyrene (TCPS) flasks (Corning, USA) with fibroblast basic medium-2 (Lonza, USA) and a FGM-SingleQuot Kit supplements & growth factors at CO_2 incubator (5%, 37℃). When cells grew to 80% confluence, they were subcultured by using 7mL 0.25% trypsin and 1 mmol/L EDTA (Invitrogen, USA) for 5 mins at 37℃. 7mL fetal bovine serum (FBS, Thermo fisher, USA) was added to above solution to neutralize trypsin, while cells were harvested by using centrifuge at 220g for 5min. After removing the supernatant, harvested cells were suspended in 2mL cell culture medium and split into two 175 cm^2 tissue culture flasks with 15mL-20mL cell culture medium. The cells were maintained in fibroblast medium at 37℃ and 5% CO_2.

3.4.2 2-D cell seeding and 3-D cell encapsulation

Hydrogels were photo-polymerized in 96 well plate via UV 5mins and Irgacure 2959(0.1% wt/v) and rinsed twice with PBS before seeding cells. And then cells were trypsinized, suspended in cell culture medium, counted and seeding to each hydrogels at a concentration of 5000 cells/cm^2. After seeding 4 hours, unattached cells were removed by changing cell culture medium. Finally, cells were imaged by microscope at each time point.[2]

Passages 5-7 of NHDFs were used for cell encapsulation. Cell-seeded constructs were made from 100 μL aliquots of the cells in a suspension of precursor (final cell density = 1~2 $\times 10^6$ cells/mL) using a flat-bottom 96-well plate as the mold. After UV photo-polymerization with 0.1 w/v % Irgacure 2959 and exposing to UV light (365nm, 4-5mW/cm^2) for 5 min, the cell-seeded hydrogels were transferred into ultra-low cell attachment 6-well plate (Coring, USA) with cell culture medium. The medium was changed immediately after encapsulation to remove unencapsulated cells.[28]

3.4.3 Cell viability

The viability of NHDFs was measured by Presto Blue cell vitality assay kit (Invitrogen, USA).[15] Cell permeable resazurin is used as a cell viability indicator, and this assay is able to test live-cell viability. When resazurin is added to cells, the reagent is modified by reducing environment of the viable cell and turns red in color, becoming highly fluorescent. This color change can be measured *via* plate reader by measuring fluoresce intensity or absorbance.[29] Each hydrogel with cells was prepared as described above. Cell culture medium (2mL) with 10% Presto Blue was added to each hydrogel on day 7 and 10, followed by incubation for 4h at 37℃ with 5% CO_2. After incubation, the supernatant was transferred to a 96 black plate. The intensity of fluorescence was measured by a microplate reader (excitation: 560nm, emission: 590nm, Tecan Infinite® 200 PRO, Switzerland).

3.4.4 Cell Live/Dead and cell morphology

NHDFs encapsulated in hydrogels were stained with Live/dead stain (calcein-AM/4 μM EthD-1, Life technologies, USA) at each time point and imaged by a florescence microscope (Olympus, CX 51, Japan). Cell encapsulated hydrogels were washed with PBS and incubated in a solution with 2 μM calcein-AM/4 μM EthD-1 in cell culture medium at 37℃ for 2 hours. After incubation, hydrogels were washed with PBS twice before imaging under a fluorescence microscope. In order to further study the morphology of NHDFs in hydrogels, F-actin and nuclei staining were studied by using confocal microscope (CLSM, Leica SP2 inverted microscope, Zurich, Switzerland). Briefly, the cells encapsulated hydrogels were washed three times with PBS (pH 7.4 and then fixed for 20 min by incubating in 3.7% formaldehyde in PBS. Samples were incubated with 0.1% Triton X100 in PBS for 10 min at room temperature and followed by washing with 1% bovine serum albumin (Life technologies, USA) in PBS. Then gels were incubated with 1IU/mL Rhodamine- Phalloidin (Life technologies, USA) for 1h at room temperature. After PBS washing, each hydrogel was finally stained with 300 μL 300nmol/L 4', 6-diamidino-2-phenylindole (DAPI, Life technologies, USA) for 10 min. All the samples were washed with PBS twice before imaging. The images of cytoskeletal F-actin fibers and nucleic acid were acquired by using a confocal laser scanning microscope.

3.4.5 Cell proliferation

As we know, the most accurate method to measure cell proliferation is to directly determine DNA synthesis.[30] However, it is a challenge to measure cell proliferation in 3-D as the cells were encapsulated into 3-D hydrogel and not easily released out from hydrogels. In this thesis, a new analysis method for cell proliferation in3-D was established based on directly measuring DNA synthesis. The proliferation of NHDF was determined by using Click-It 488 EdU flow cytometry assay kit (Life technologies, USA). EdU (5-ethynyl-2’-deoxyuridine) is a nucleoside analog to thymidine and can connect to DNA during new DNA synthesis. This assay is based on a copper catalyzed click reaction between an alkyne and an azide.[31] Firstly, EdU was added to the cell culture

media at the final concentration of 10μM and then incubated with cell encapsulated hydrogels for 24hours. NHDFs in hydrogels were harvested from the gel at day 1, 3, 7 and 9 by degrading each gel in a solution of 2mg/mL collagenase type I A for 2h at 37 ℃. The cells released from gels were collected by centrifugation, washed twice with 3mL 1% BSA in PBS, pelleted the cells and removed the supernatant. After collecting the pellet, 100 μL click-it fixative was added to each tube, and then incubated for 15mins at room temperature. The fixed cells were washed twice with 3mL 1% BSA in PBS. 100 μL saponin-based permeabilization was added to cells and incubated for 15mins. Click-it reaction cocktail reagent was prepared according to the manufacture's protocol. 0.5mL of click-it reaction cocktail reagent was added to each tube and mixed well. The tube was incubated at room temperature for 30mins under dark condition. After labeling step, the cells were washed by 3mL saponin-based permeabilization. After removing supernatant, the cells were resuspended in 100μL saponin-based permeabilization. The percentage of proliferation cells was measured by using a flow cytometer (LSR-II, Becton Dickinson, USA).

3.4.6 Rheological characterization of cell-laden hydrogels

The rheological properties of the cell-laden hydrogels were characterized using an Anton Paar Physica MCR 501 rheometer equipped with Peltier plate temperature-controlled systems (P-PTD-200/TG and P-PTD120/GL). A PP8 parallel-plate with 8 mm was used for cell-laden hydrogels. The testing conditions for all measurements were 1-2% strain amplitude at an oscillation frequency of 0.1 - 1 Hz within the linear viscoelastic regime.[18, 32]

3.4.7 Immunofluorescence staining

Immunofluorescence staining was performed to visualize deposition of ECM proteins produced by NHDFs.[33-37] On days 7 and 10, the hydrogels containing NHDFs were washed three times in PBS and fixed in 3.7% paraformaldehyde (PFA, Sigma-Aldrich, USA) solution in PBS for 30 min. And then the hydrogels were immersed in 0.1% Triton

X-100 (Sigma-Aldrich, USA) in PBS for 30 min at room temperature to permeabilize the cells membrane. For collagen type I and elastin staining, upon fixation, the unspecific binding of antibodies to hydrogels was blocked in 10% goat serum (Abcam, UK) in PBS for 1 h after PFA fixation. To stain for collagen type I, a 1/500 dilution of monoclonal mouse anti-collagen type I antibody (only reacts with collagen type I from human, Abcam, UK) in 10% goat serum was added to the hydrogels and the samples were kept at 4 ℃ for 12 h. The hydrogels were then washed in PBS three times with 10 mins intervals in between the washing steps. After primary antibody staining, the samples were incubated in 1/200 dilution of Alexa Fluor 555 goat anti mouse IgG secondary antibody (Abcam, UK) in 10% goat serum in PBS for 3 h at room temperature. After washing three times in PBS, similar procedure was used to stain elastin with the exception of using monoclonal rabbit anti-elastin antibody as the primary antibody (only reacts with elastin from human, Abcam, UK) and Alexa Fluor 488 conjugated goat anti-rabbit antibody (Abcam, UK) as the secondary antibody. For F-actin cytoskeleton staining, the hydrogels were washed three times by PBS and soaked in a solution with Alexa Fluor 568 phalloidin (5IU/mL, Life technologies, USA) for 90 min incubation at room temperature. DAPI (300nM, Life technologies, USA) was used to stain the nucleic acid of cells in the gel and followed by washing in PBS before for confocal imaging (CLSM, Leica SP2 inverted microscope).

3.5 Statistical Analysis

Student's t-test is most frequently used to determine if two groups of data are significantly different from each other, while the mean of the sample follows a normally distribution and the population standard deviation is unknown.[38] Data are presented as mean ± standard deviation of samples in at least three experiments and analyzed by student-t-test. A value of $p<0.05$ was considered statistically significant between experimental groups.

References

[1] J. Zhu. *Biomaterials*. **2010**, 31, 4639-4656.

[2] M. Gonen-Wadmany, L. Oss-Ronen, D. Seliktar. *Biomaterials*. **2007**, 28, 3876-3886.

[3] M. Parlato, S. Reichert, N. Barney, W. L. Murphy. *Macromolecular bioscience*. **2014**, 14, 687-698.

[4] B. H. Lee, S. P. H. Tin, S. Y. Chaw, Y. Cao, Y. Xia, T. W. Steele, D. Seliktar, H. Bianco-Peled, S. S. Venkatraman. *Journal of Biomaterials Science, Polymer Edition*. **2014**, 25, 394-409.

[5] G. T. Hermanson. *Bioconjugate techniques, Academic press*, **2013**.

[6] G. T. Hermanson. *Bioconjugate techniques, Academic press*, **1996**.

[7] P. Liu, B. W. O'Mara, B. M. Warrack, W. Wu, Y. Huang, Y. Zhang, R. Zhao, M. Lin, M. S. Ackerman, P. K. Hocknell. *Journal of the American Society for Mass Spectrometry*. **2010**, 21, 837-844.

[8] A.-M. Faucher, C. Grand-Ma ître. *Synthetic communications*. **2003**, 33, 3503-3511.

[9] B. D. Mather, K. Viswanathan, K. M. Miller, T. E. Long. *Progress in Polymer Science*. **2006**, 31, 487-531.

[10] L. Almany, D. Seliktar. *Biomaterials*. **2005**, 26, 2467-2477.

[11] L. Oss-Ronen, D. Seliktar. *Acta Biomaterialia*. **2011**, 7, 163-170.

[12] I. Mironi-Harpaz, D. Y. Wang, S. Venkatraman, D. Seliktar. *Acta Biomaterialia*. **2012**, 8, 1838-1848.

[13] M. Balci. *Basic 1H-and 13C-NMR spectroscopy, Elsevier*, **2005**.

[14] I. Frisman, D. Seliktar, H. Bianco-Peled. *Acta Biomaterialia*. **2010**, 6, 2518-2524.

[15] Y. Fu, K. Xu, X. Zheng, A. J. Giacomin, A. W. Mix, W. J. Kao. *Biomaterials*. **2012**, 33, 48-58.

[16] K. Xu, D. A. Cantu, Y. Fu, J. Kim, X. Zheng, P. Hematti, W. J. Kao. *Acta Biomaterialia*. **2013**, 9, 8802-8814.

[17] C. Ghobril, M. Grinstaff. *Chemical Society Reviews*. **2015**, 44, 1820-1835.

[18] M. Gonen-Wadmany, R. Goldshmid, D. Seliktar. *Biomaterials*. **2011**, 32, 6025-6033.

[19] I. Frisman, Y. Shachaf, D. Seliktar, H. Bianco-Peled. *Langmuir*. **2011**, 27, 6977-6986.

[20] S. Venkatraman. *Journal of applied polymer science*. **1993**, 48, 1383-1393.

[21] S. Venkatraman, A. Nixon, A. Highe. *Journal of applied polymer science*. **1994**, 52, 1619-1627.

[22] N. A. Peppas, J. Z. Hilt, A. Khademhosseini, R. Langer. *ADVANCED MATERIALS-DEERFIELD BEACH THEN WEINHEIM-*. **2006**, 18, 1345.

[23] T. Canal, N. A. Peppas. *Journal of biomedical materials research*. **1989**, 23, 1183-1193.

[24] J. Zhu, R. E. Marchant. *Expert review of medical devices*. **2011**, 8, 607-626.

[25] J. S. Temenoff, K. A. Athanasiou, R. G. Lebaron, A. G. Mikos. *Journal of biomedical materials research*. **2002**, 59, 429-437.

[26] P. K. Smith, R. I. Krohn, G. Hermanson, A. Mallia, F. Gartner, M. Provenzano, E. Fujimoto, N. Goeke, B. Olson, D. Klenk. *Analytical biochemistry*. **1985**, 150, 76-85.

[27] H. Schägger. *Nature Protocols*. **2006**, 1, 16-22.

[28] Y. Cao, B. H. Lee, H. B. Peled, S. S. Venkatraman. *Journal of Biomedical Materials Research Part A*. **2016**.

[29] D. Berrington. *International journal of microbiology*. **2013**, 2013.

[30] D. C. Macallan, C. A. Fullerton, R. A. Neese, K. Haddock, S. S. Park, M. K. Hellerstein. *Proceedings of the National Academy of Sciences*. **1998**, 95, 708-713.

[31] S. Diermeier ‐ Daucher, S. T. Clarke, D. Hill, A. Vollmann ‐ Zwerenz, J. A. Bradford, G. Brockhoff. *Cytometry Part A*. **2009**, 75, 535-546.

[32] I. Frisman, D. Seliktar, H. Bianco-Peled. *Biomaterials*. **2011**, 32, 7839-7846.

[33] J. J. Moon, J. E. Saik, R. A. Poche, J. E. Leslie-Barbick, S.-H. Lee, A. A. Smith, M. E. Dickinson, J. L. West. *Biomaterials*. **2010**, 31, 3840-3847.

[34] B. Trappmann, J. E. Gautrot, J. T. Connelly, D. G. Strange, Y. Li, M. L. Oyen, M. A. C. Stuart, H. Boehm, B. Li, V. Vogel. *Nature materials*. **2012**, 11, 642-649.

[35] C. S. Szot, C. F. Buchanan, J. W. Freeman, M. N. Rylander. *Biomaterials*. **2011**, 32, 7905-7912.

[36] C. Wang, Y. Gong, Y. Zhong, Y. Yao, K. Su, D.-A. Wang. *Biomaterials*. **2009**, 30, 2259-2269.

[37] Y. Liu, M. B. Chan-Park. *Biomaterials*. **2010**, 31, 1158-1170.

[38] R. L. Ott, M. T. Longnecker. *An introduction to statistical methods and data analysis*, *Nelson Education*, **2015**.

Chapter 4

Synthesis of elastin-PEG hydrogel for 3-D cell encapsulation

This chapter describes the fabrication method and characterization of the synthesized elastin-PEG hydrogel for 3-D cell encapsulation in this chapter. Elastin, one of the attractive ECM derived proteins, has been conjugated with one double bond of PEGDA via thiolation (EDC/NHS method) and Michael type addition reaction. The relationship between EDC/NHS and grafted thiols has been studied. The conjugation of elastin soluble or elastin peptides has been verified by NMR and FTIR. 2-D cell culture and 3-D cell encapsulation experiments have been accomplished to study the bio-compatibly and cell response. Elastin-PEG-acrylate was found to be biocompatible, and be able to encapsulate cells in situ. This chapter will give a new understanding of elastin –based 3-D hydrogel system and its potential for tissue engineering.

4.1 Introduction

Elastin is the major insoluble protein existing in elastic tissue, contributing to elasticity of the skin and promoting a number of cellular responses including chemotaxis, proliferation, attachment, and differentiation.[1, 2] Elastic fibers are not readily resynthesized after injury due to difficulties in re-expression of tropoelastin and related molecules, thus seriously hampering the quality and speed of new tissue generation and full healing.[1] Therefore, burn survivors still suffer from excessive scarring and skin contractions which substantially compromise their health and quality of life.[1] Despite the need, however, there is a dearth of research on elastin-based dermal substitutes with tunable mechanical property, and elastin is historically under represented in commercial dermal substitutes. Previous studies utilizing elastin have primarily focused on incorporation methods (chemical conjugation or physical blending)[3-5] leading to a 2-D cell study or evaluation *in vivo*.[6, 7] For example, soluble bovine elastin denatured from insoluble elastin has been used to develop highly porous elastic hydrogels using glutaraldehyde and high pressure $CO_{2;}$ however, such hydrogels are still not compatible with cell encapsulation and *in situ* delivery. [8, 9] Solubilized elastin was also used to mediate the attachment and proliferation of dermal fibroblasts and endothelial cells in 2-D.[10] An acellular dermal matrix (70% collagen and 30% elastin) produced by removal of cells from porcine skin was transplanted into animal skin and shown to improve the elasticity and functionality of severe scars by replacing the missing elastic network, yet there were drawbacks such as poor mechanical characterstics and residual cell materials in the scaffold.[1] Similarly, Daamen et al. proved that porous collagen-solubilized elastin scaffolds fabricated by reacting with EDC/NHS and lyophilization, was able to induce cell proliferation and elastin deposition when implanted subcutaneously in rats, compared with collagen-only scaffolds that do not promote elastin synthesis.[6]

A PEG hydrogel that can mimic ECM (gelatin/collagen and elastin) can be an alternative and attractive choice as it can provide biologicals cues and tunable mechanical properties at the same time. Both elastin and gelatin/collagen contribute to different aspects of the mechanical behavior of ECM. For example, it is well-known that in blood vessels, the elastin allows for deformability under blood pressure fluctuations, while the collagen

stiffness prevents uncontrolled deformation. In general over-abundance of collagen makes the ECM too stiff while the reverse is true of elastin.

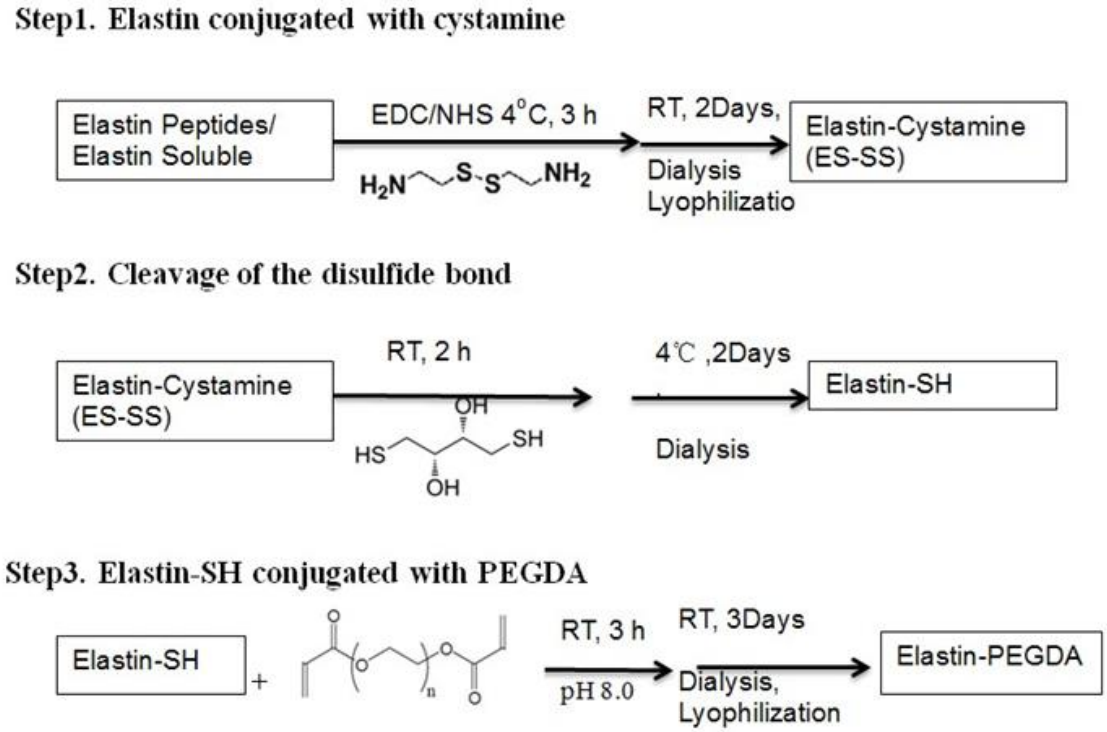

Figure 4.1 The fabrication routine of Elastin-PEG hydrogel.

In this chapter, elastin-PEG acrylate was fabricated first and then photo-polymerized with cells *in situ*. Elastin soluble (ES) and elastin peptides (EP) were first conjugated with PEGDA via Michael type addition reaction. As the ES and EP have no sulfhydryl groups in their structure, they were conjugated with sulfhydryl first in order to couple with the PEGDA (Figure 4.1). More specifically, sulfhydryl groups (-SH) were designed to react with one double bond of PEGDA via Michael type addition reaction, while the other one was remained for photo-polymerization after loading cells in order to form hydrogel with cells *in situ*. However, sulfhydryl groups are not stable in solution and the existence of oxygen, so it was difficult to conjugate sulfhydryl groups to elastin and perform several experiments with good repeatability. To overcome this limitation, cystamine was chosen as the source of thiols as the disulfide bond of cystamine can be cleaved to produce thiols after the conjugation of cystamine to elastin. More specifically, cystamine was

conjugated to the elastin by EDC/NHS method through the reaction between carboxyl and amine. After cleavage of disulfide bond, the thiolated elastin reacted with PEGDA to form elastin-PEG-acrylate precursor for cell encapsulation. The synthesis route is shown in Figure 4.1. Both 2-D and 3-D cell culture were performed to study the cell compatibility. For 3-D cell culture, hydrogels were fabricated as covalently crosslinked cell loaded constructs using photo-polymerization by adding 0.1 w/v % Irgacure 2959 and exposing to UV light for 5 min.

4.2 Experimental Methods

4.2.1 Elastin modified with cystamine

Firstly, ES or EP was dissolved in 2-ethanesulfonic acid (MES, Sigma-Aldrich USA) buffer (0.1mol/L, pH 4.7) at the concentration of 10mg/mL. 10, 20, 30, 40, 50 molar excess of EDC were added to elastin solution, respectively. Next, NHS (2.5 molar folder excess of EDC) was added to the above solution and reacted for 15 minutes at RT. Then pH was increased to 7.5 using sodium hydroxide. A 20 fold molar excess of cystamine compared with elastin was added into the above solution and stirred for 3 h at RT. After the reaction, the byproduct and unreacted cystamine were removed by dialyzed against distilled water. The purified solution freeze dried at -70 ℃ and followed by lyophilized to get a solid sample. ES and EP conjugated with cystamine were labeled as ES-SS or EP-SS.

4.2.2 Cleavage the disulfide to sulfhydryl

The next step was the cleavage the disulfide bond by DTT to reduce disulfides and stabilized free sulfhydryl in aqueous environment although oxygen exists. [11] DTT (final concentration of 0.1mol/L) was added to ES-SS or EP-SS and reacted for two hours. The byproducts of DTT and excess DTT can be removed by dialyzed against distilled water (pH 3.50). After dialysis, Ellman's reagent was used to determine the sulfhydryl amount in solution.

4.2.3 Conjugate Elastin-SH with PEGDA

The purified thiolated elastin solution was reacted with PEGDA immediately after determining the thiol amount by Ellman's reagent since thiols are not stable. This reaction was based on the Michael-addition reaction. Firstly, four molar excess 10k PEGDA (calculated from the sulfhydryl group amount) was dissolved in PBS (pH 7.2). Secondly, the pH of ES/EP-SH solution was adjusted to pH 8.0, which dissociated the proton of sulfhydryl groups. Thirdly, the PEGDA solution was added to the ES/EP-SH solution and reacted for 3 hours at room temperature, respectively. The final solution was dialyzed against distilled water at room temperature to remove unreacted PEGDA. Finally, the solution after dialysis was processed by lyophilization.

4.3 Results

4.3.1 The relationship between thiol amount and EDC

The relationship between EDC and sulfhydryl amount is showed in Figure 4.2. The more EDC was used, the more sulfhydryl were detected in the thiolated elastin. Because EDC can activate more carboxyl group in elastin, more cystamine can be conjugated. Therefore, the concentration of sulfhydryl groups can be adjusted through changing the amount of EDC·HCl.

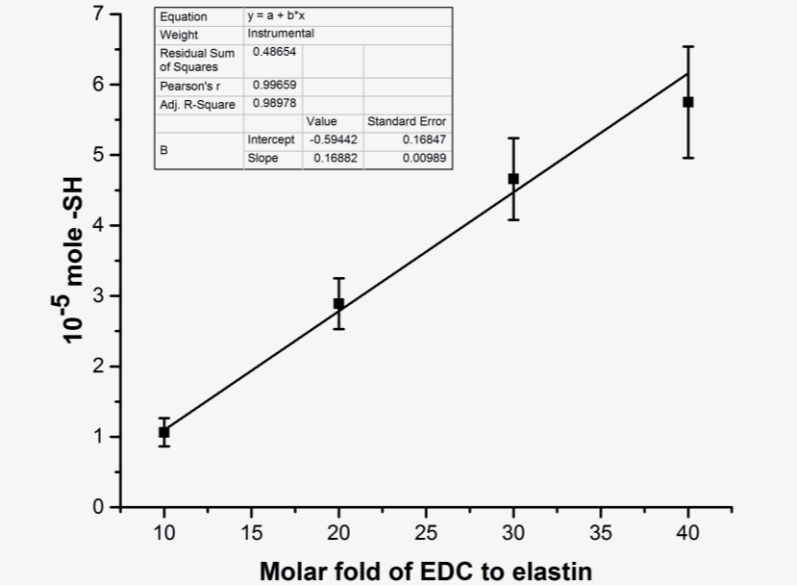

Figure 4.2 The relationship between EDC amount and sulfhydryl group amount. (n=4)

4.3.2 Characterization- FTIR

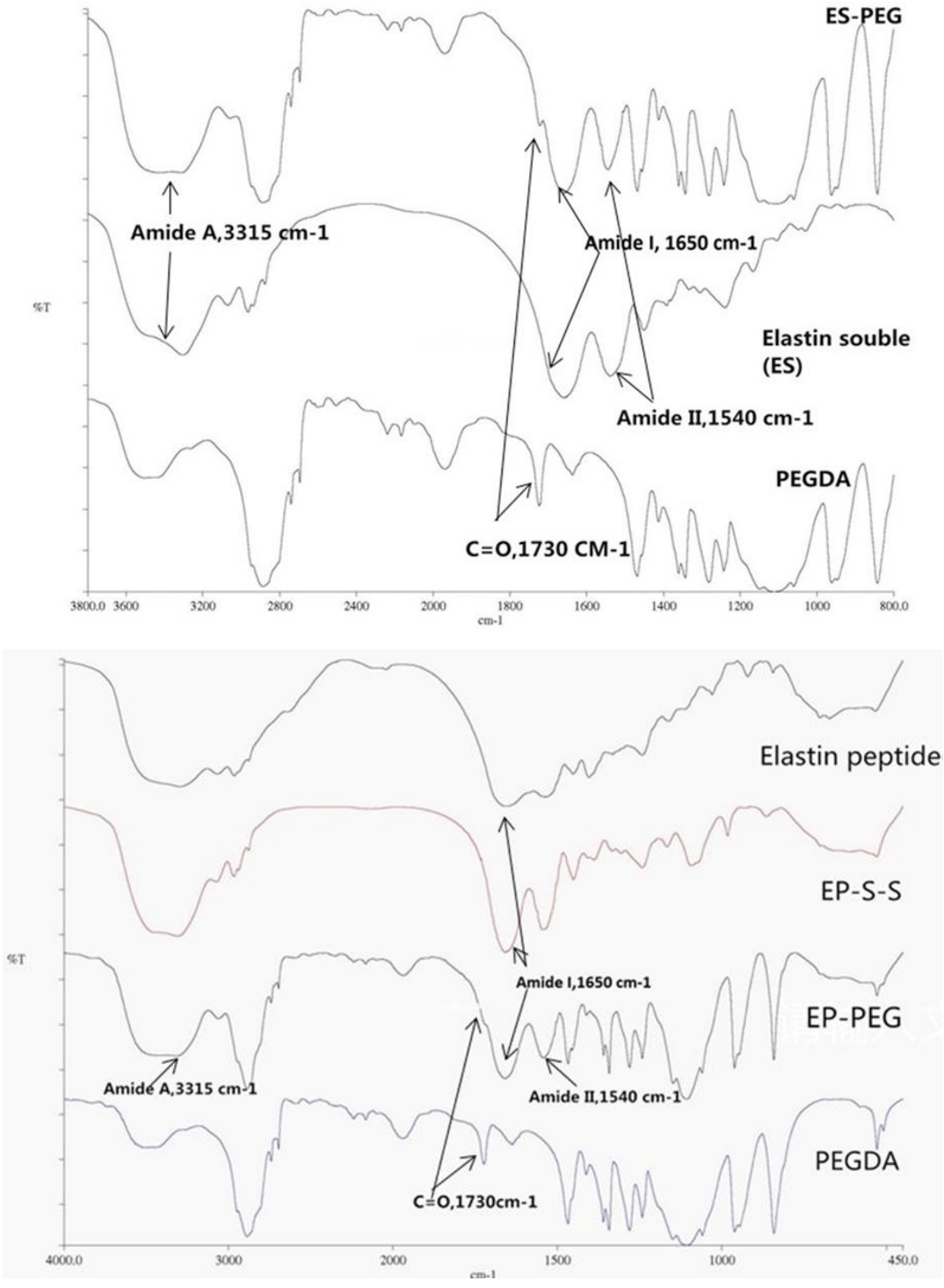

Figure 4.3 FTIR spectra of ES, ES-PEG, EP, EP EP-SS, EP-PEG and PEGDA.

The FTIR spectra of protein and PEGDA were analyzed in KBr pellets. According to the

reference[12], elastin exhibited Amide II, Amide I and Amide A bands at 1540 cm^{-1} , 1650 cm^{-1} and 3315 cm^{-1}, respectively. PEGDA showed C=O of ester band at 1730 cm^{-1}. As the PEGDA does not have amide group, the EP-PEG and ES-PEG showed characteristic bands of elastin and PEGDA, i.e. Amide II at 1540 cm^{-1}, Amide A bands at 3315 cm^{-1} and C=O of ester band at 1730 cm^{-1}(Figure 4.3). After PEGDA conjugation, the FTIR spectrum of EP and ES showed similarity of original protein and PEGDA. So the FTIR spectrums confirm the PEGDA was successfully conjugated to EP and ES, respectively.

4.3.3 Characterization- ^{1}H-NMR

According to the reference[13], PEGDA exhibits two chemical shift peaks (protons in acrylates) at A (6.1 ppm) and B (5.8 and 6.4 ppm) in Figure 4.4, respectively. After PEG conjugation, the spectrum of ES-PEG showed similarity of original ES and PEGDA. So the NMR spectra confirm that the PEGDA was successfully conjugated to ES. ES and EP have several of peptide sequences (including Val-Gly-Val-Ala-Pro-Gly); As seen in Figure 4.4, methyl peaks(6H of valine) at around 1.8 ppm appear, while ethylene peaks (4H of ethylene oxide) at 3.7ppm and 3 protons in acrylates of PEGDA at around 6 ppm are ascribed to PEGDA. After conjugation, Elastin soluble conjugated to PEGDA showed both of characteristic peaks of Elastin and PEGDA in a broad manner in ^{1}H-NMR.

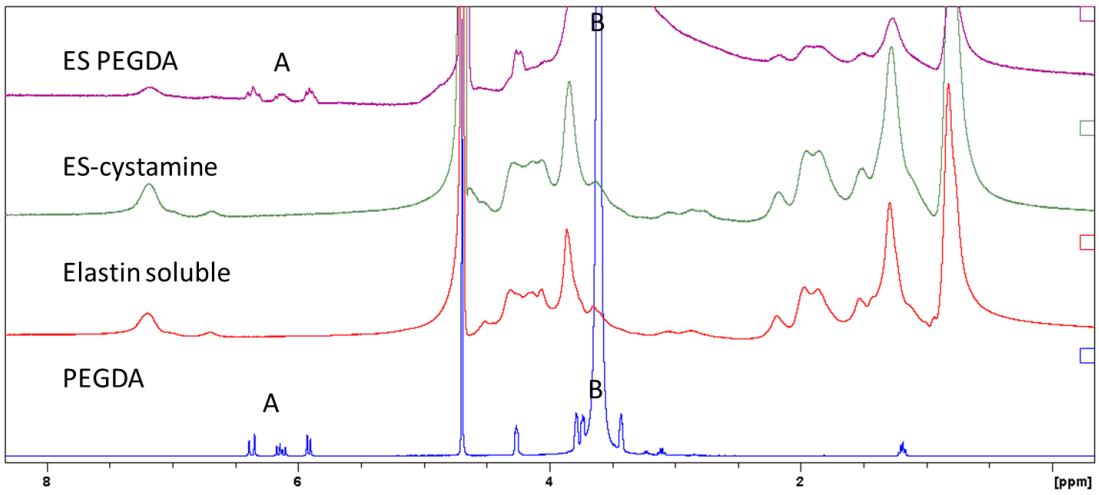

Figure 4.4 ^{1}H-NMR figure: A:6.1 (dd,-CH=CH_2); B:5.8 and 6.4 (dd,-CH=CH_2).

4.3.4 Characterization- Electrophoresis

SDS-PAGE has been a popular strategy to characterize conjugation of PEG to proteins.[13] The conjugation of PEG to the protein can increase the molecular weight of the protein, which causes the higher gel band ladders. Figure 4.5 showed the results of SDS-PAGE for PEGylated-elastin peptide and soluble. The original ES showed a smear band as most of the proteins were around 14k~17k and above 62k, while the ES-SS displayed similar results. The thiolation step did not affect the molecular weight considerably. However, in the ES-PEG a new band between 28k and 38k emerged because the proteins of around 14k were conjugated with at least two PEGDA molecules. The band above 49k showed much deeper color, because there were more proteins shifted after PEGlyation.

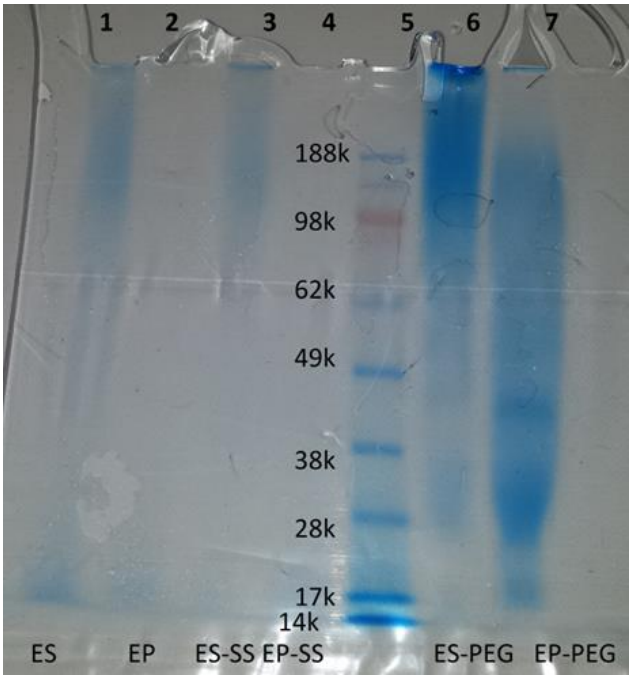

Figure 4.5 The electrophoresis results of elastin and modification elastin. (There were 7 wells. Well 1: ES; well 2: EP; well 3: ES-SS; well 4: EP-SS, well 5: Maker; well 6: ES-PEG; well 7: EP-PEG. The elastin concentration was lower in Elastin-PEG comparing with Elastin or Elastin-SS, so the samples in wells of ES-PEG and EP-PEG were increased about ten times than the others. The protein concentrations would be explained in the BCA part.)

EP-PEG was similar to ES-PEG. But EP and EP-SS were different from ES and ES-SS. Most of the EP and EP-SS may be below 14K according to the electrophoresis image. After PEGlyation, EP-PEG showed a smear band, while there were two main bands around 30k and 40k. Comparing with EP and EP-SS, the molecular weight variation of EP-PEG suggests that EP conjugated with PEGDA. Therefore, PEGDA were successfully grafted to EP and ES according to the molecular weight change shown in bands shift.

4.3.5 Characterization- BCA Protein assay

Table 4.1 The results of BCA protein assay. (n=3)

	Prepared concentration (mg/mL)	Protein concentration (mg/mL)	Elastin percentage in ES-PEG(%)
ES	3.00	0.91 ±0.12	/
EP	3.00	0.64 ±0.10	/
ES purified	3.00	1.19 ±0.18	
EP purified	3.00	1.05 ±0.15	
ES-SS	3.00	1.14 ±0.18	/
EP-SS	3.00	0.99 ±0.15	/
ES-PEG	3.00	0.71 ±0.12	~59.6
EP-PEG	3.00	0.67 ±0.16	~63.8
PEGDA	3.00	0	/

The concentration of elastin in elastin-PEG can be determined by the bicinchoninic acid (BCA) method [14]. The reduction of Cu^{2+} to Cu^{1+} by protein in an alkaline buffer (the biuret reaction) can be determined by BCA kit [97]. Two molecules of BCA can chelate with one Cu^{1+}, which have purple color. The concentration of protein is calculated relative to the original protein. According to the results in table 4.1, the protein concentration in ES and EP was much lower than the original concentration. BSA was used as the standard protein according to the manufactures manual in this experiment. But the determined origin ES and EP concentration were lower than the prepared concentrations because elastin does not have similar structure as BSA. Another reason could be the removal of impurity (salts or low molecular weight molecules) during the

purification step (dialysis). This could be the reason why ES or EP purified have higher amount than original proteins. Therefore, ES or EP was chosen as the standard protein instead of BSA, respectively. At the same time, the protein concentration is low in the elastin-PEG hydrogel, which means the dominant component is PEG-acrylate.

4.3.6 2-D Cell culture and 3-D cell encapsulation

Human adult dermal fibroblast (FBs) and human adult artery smooth muscle cells (SMCs) were seeded into cell culture medium with EP-PEG (100 mg/mL) and ES-PEG (100 mg/mL) (Figure 4.6), where they can attach and grow very well. Those results demonstrate the biocompatibility of ES-PEG and EP-PEG even at very high concentration.

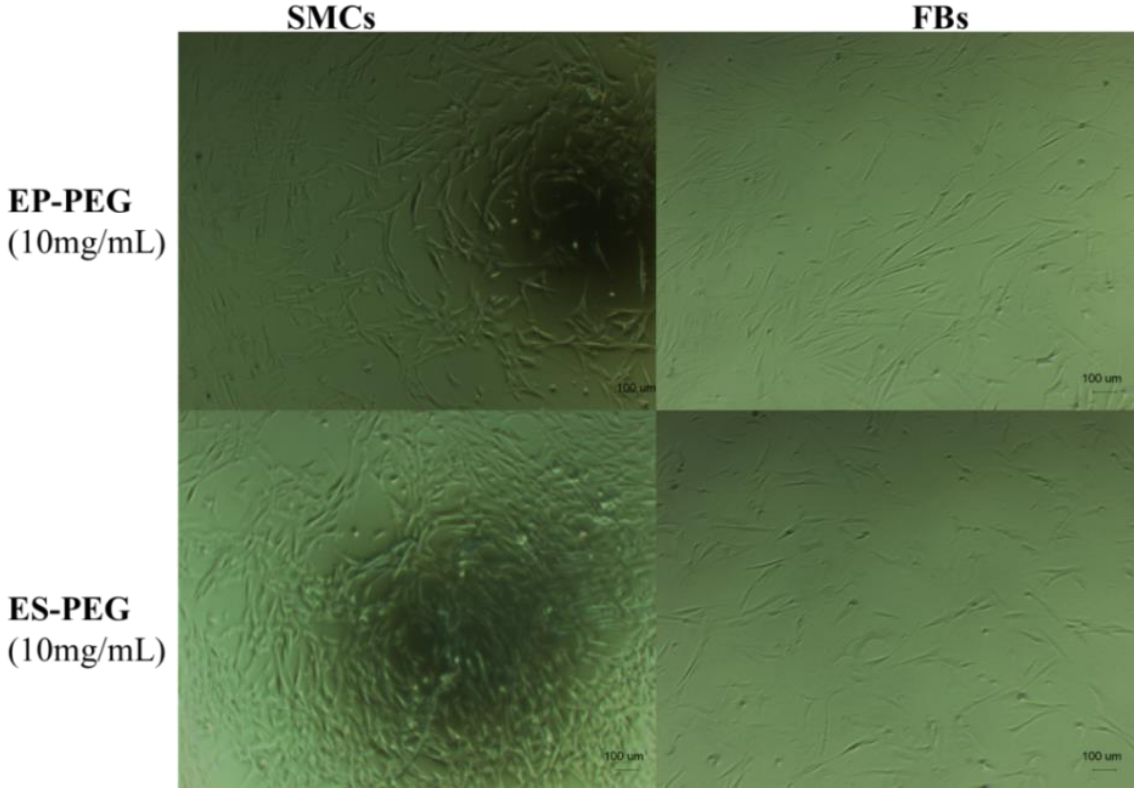

Figure 4.6 FBs and SMCs were seeding into cell culture medium with the existing of ES-PEG (100mg/mL), EP-PEG (100mg/mL), respectively.

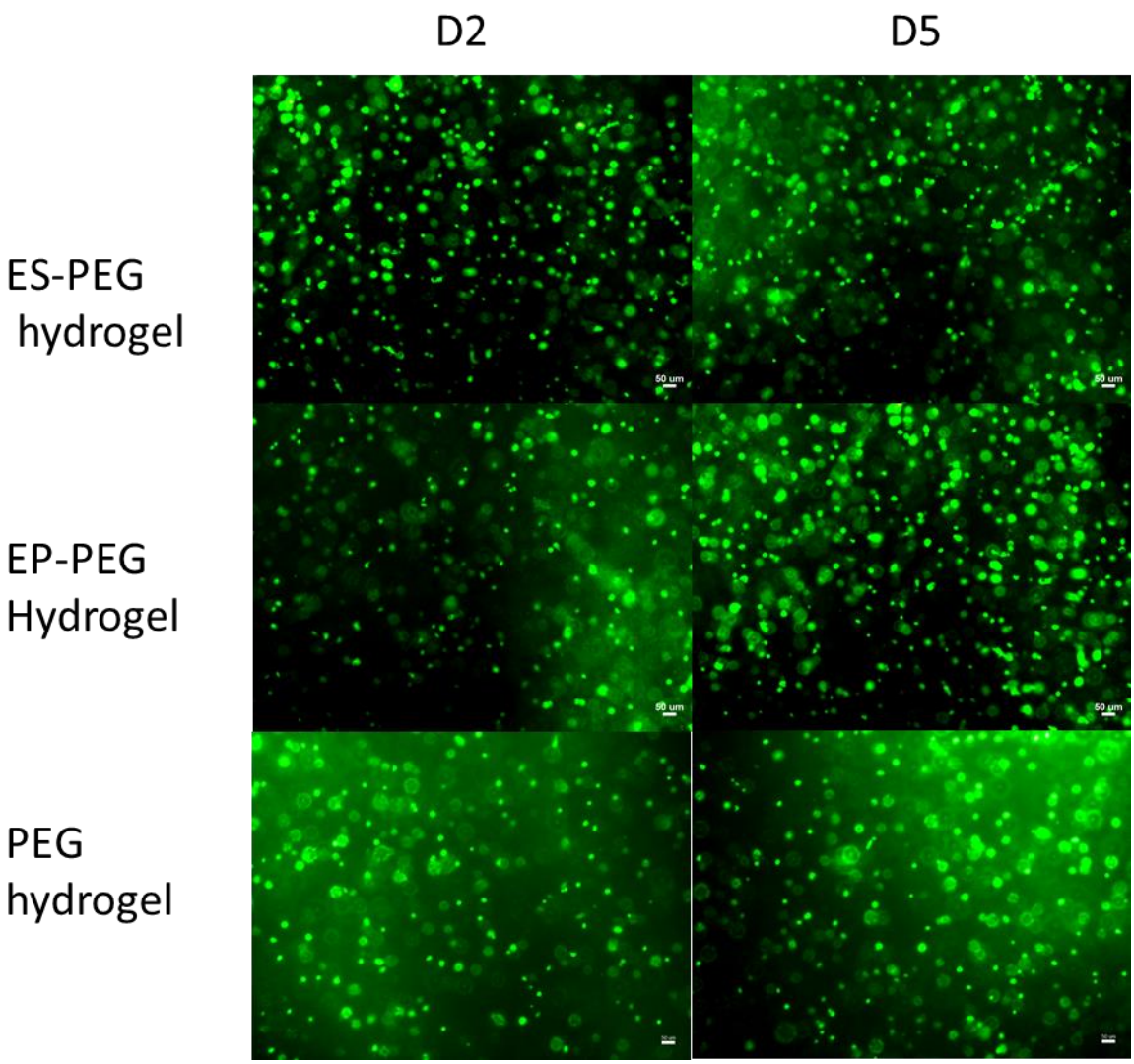

Figure 4.7 Morphology of SMCs encapsulated in ES-PEG, EP-PEG and PEGDA hydrogel.

SMCs were encapsulated into ES-PEG (made from 20 fold EDC, 4.0 wt %), EP-PEG (made from 20 fold EDC, 4.0 wt %) and PEGDA (10k, 4.0wt %) hydrogel, while concentration of cells were 10^6/mL precursor solution. However, the SMCs in hydrogel were not able to attach after five days (Figure 4.7), and maintained the round shape. One possible reason is that elastin has less cell adhesion peptides comparing with gelatin or fibrinogen.[15] It is well known that RGD is the most commonly used cell adhesion peptides, however elastin only has cell adhesive peptides like Val-Ala-Pro-Gly (VAPG) which can promote cell adhesion [16]. As mentioned before, cell adhesion and spreading are crucial for the survival of ADCs (e.g. SMCs, FBs). However, cells do not attach and

spread but maintain a spheroidal shape after encapsulation into 3-D hydrogel network. Cells encapsulated into 3-D hydrogel are constrained to a round-shape, no matter which cell types or what native morphology, because of a unique encapsulation mechanism. Trypsin treated cells were mixed with hydrogel precursor, crosslinked in situ and then surrounded by hydrogel networks.[17] The bulk of synthetic hydrogels, like their surface, typically exhibit a bio-inert microenvironment,[18] while the cells (~10 μm) are encapsulated and surrounded in highly aqueous networks with nano-size pores. Without strong biological cues, the encapsulated cells are restricted from attachment to scaffold and spreading inside. Cell adhesion and spreading are necessary and compulsory to rescue cells from apoptosis and death.[19] Therefore, elastin may not be able to support cell attachment inside a 3-D gel. Anthony Weiss et al. found similar cell behavior in cell laden elastin based hydrogel. In this study, tropoelastin produced by *E coli.* was conjugated with methacrylate to encapsulate cells in 3-D environment. Cells can attach, grow and proliferate in 2-D films, while the encapsulated cells are still round shape after 7 days culture. Therefore, it is necessary to consider that combining other biological cues with elastin to support cell attachment and growth.[20]

4.4 Summary

ES-PEG and EP-PEG have been successfully synthesized via thiolation and Michael addition reaction. Cells were encapsulated into those hydrogels by photo-polymerization. Our results show that the amount of thiol could be controlled by adjusting the amount of EDC and NHS. Accordingly, the constitution of hydrogel precursor was affected by the amount of thiol which determines the amount of PEGDA conjugated with elastin. Finally, the crosslinking density of hydrogel also can be adjusted according to the application. The 2-D cell culture results demonstrated that ES-PEG and EP-PEG are non-toxic and biocompatible. However, SMCs encapsulated into hydrogel were not able to attach and maintain the round shape for five days, presumably due to lack of strong cell adhesion peptides or sequences. Therefore, it is necessary to consider that combining other biological cues with elastin to support ADCs attachment and growth. The major result reported in this chapter is the synthesis of a novel elastin-PEG hydrogel which in

combination with gelatin-PEGDA could yield an ECM scaffold; it is also possible that the new elastin-PEG hydrogel could be used for other applications.

References

[1] J. Rnjak, S. G. Wise, S. M. Mithieux, A. S. Weiss. *Tissue Engineering Part B: Reviews*. **2011**, 17, 81-91.

[2] A. Vasconcelos, A. C. Gomes, A. Cavaco-Paulo. *Acta Biomaterialia*. **2012**, 8, 3049-3060.

[3] L. Buttafoco, P. Engbers‐Buijtenhuijs, A. Poot, P. Dijkstra, W. Daamen, T. Van Kuppevelt, I. Vermes, J. Feijen. *Journal of Biomedical Materials Research Part B: Applied Biomaterials*. **2006**, 77, 357-368.

[4] C. N. Grover, R. E. Cameron, S. M. Best. *Journal of the Mechanical Behavior of Biomedical Materials*. **2012**, 10, 62-74.

[5] A. J. Ryan, F. J. O'Brien. *Biomaterials*. **2015**, 73, 296-307.

[6] W. F. Daamen, S. T. Nillesen, R. G. Wismans, D. P. Reinhardt, T. Hafmans, J. H. Veerkamp, T. H. Van Kuppevelt. *Tissue Engineering Part A*. **2008**, 14, 349-360.

[7] W. Daamen, S. Nillesen, T. Hafmans, J. Veerkamp, M. Van Luyn, T. Van Kuppevelt. *Biomaterials*. **2005**, 26, 81-92.

[8] N. Annabi, S. M. Mithieux, A. S. Weiss, F. Dehghani. *Biomaterials*. **2009**, 30, 1-7.

[9] N. Annabi, S. M. Mithieux, E. A. Boughton, A. J. Ruys, A. S. Weiss, F. Dehghani. *Biomaterials*. **2009**, 30, 4550-4557.

[10] D. V. Bax, U. R. Rodgers, M. M. Bilek, A. S. Weiss. *Journal of biological chemistry*. **2009**, 284, 28616-28623.

[11] G. T. Hermanson. *Bioconjugate techniques, Academic press*, **1996**.

[12] M. C. Popescu, C. Vasile, O. Craciunescu. *Biopolymers*. **2010**, 93, 1072-1084.

[13] D. Dikovsky, H. Bianco-Peled, D. Seliktar. *Biomaterials*. **2006**, 27, 1496-1506.

[14] P. Smith, R. I. Krohn, G. Hermanson, A. Mallia, F. Gartner, M. Provenzano, E. Fujimoto, N. Goeke, B. Olson, D. Klenk. *Analytical biochemistry*. **1985**, 150, 76-85.

[15] J. F. Almine, D. V. Bax, S. M. Mithieux, L. Nivison-Smith, J. Rnjak, A. Waterhouse, S. G. Wise, A. S. Weiss. *Chemical Society Reviews*. **2010**, 39, 3371-3379.

[16] J. Zhu. *Biomaterials*. **2010**, 31, 4639-4656.

[17] C. Wang, R. R. Varshney, D.-A. Wang. *Advanced drug delivery reviews*. **2010**, 62, 699-710.

[18] C. R. Nuttelman, M. C. Tripodi, K. S. Anseth. *Matrix biology*. **2005**, 24, 208-218.

[19] C. S. Chen, M. Mrksich, S. Huang, G. M. Whitesides, D. E. Ingber. *Science*. **1997**, 276, 1425-1428.

[20] N. Annabi, S. M. Mithieux, P. Zorlutuna, G. Camci-Unal, A. S. Weiss, A. Khademhosseini. *Biomaterials*. **2013**, 34, 5496-5505.

Chapter 5

Synthesis of stiffness-tunable and cell-responsive gelatin-PEG hydrogel for 3-D cell encapsulation

This chapter describes the fabrication method and characterization of the synthesized gelatin-PEG hydrogel for 3-D cell encapsulation in this work. Gelatin, one of the attractive ECM derived proteins, has been conjugated with one double bond of PEGDA via thiolation (Traut's reagent method) and Michael type addition reaction. Gelatin-PEG precursor or gelatin-PEG hydrogel have been characterized in this work by ^{1}H-NMR, swelling, degradation, gel fraction and Rheological measurements. Two types of gelatin-PEG acrylate have been prepared via adjusting the amount of Traut's reagent. The conjugation of gelatin molecules was verified by ^{1}H-NMR. 3-D cell encapsulation experiments have been accomplished to study the bio-compatibly and cell response. The relationship between stiffness and cell attachment was also investigated by preparing different types of cell encapsulated gelatin-PEG hydrogels. Gelatin-PEG hydrogel was found to be able to support NHDFs growth, spreading and proliferation in 3-D. This chapter will give a new understanding of gelatin –PEG hydrogel and its potential for tissue engineering.

This section published substantially as Ye Cao, Bae Hoon Lee, Havazelet Bianco Peled, Subbu S Venkatraman. Journal of Biomedical Materials Research Part A, 2016, DOI: 10.1002/jbm.a.35779.

5.1 Introduction

ECM derived natural proteins and peptides such as collagen, fibrin, MMP sequences, gelatin, and RGD sequences [1-4] have been conjugated into natural hydrogels due to excellent cell adhesion and biodegradation advantages. But the use of the ECM proteins based natural hydrogels is often compromised due to the risk of immunogenic response and unsatisfied mechanical properties.[5-7] On contrast to ECM proteins based natural hydrogels, synthetic hydrogels process several benefits such as controllable structure and tunable mechanical properties.[8] However, the main drawback of these synthetic materials for tissue engineering is the absence of biologically cues, which are essential for cell survival in 3-D microenvironment. Thus, several ECM-derived proteins have been incorporated into synthetic hydrogels for creating a 3-D cell responsive scaffold, containing the advantages of both ECM proteins and synthetic hydrogels.[9-11]

Gelatin and PEGDA were designed to synthesize biomimetic hydrogels in this chapter for developing ECM-mimicking synthetic hydrogels. PEG hydrogels have been extensively investigated as tissue engineering scaffolds as they have an aqueous, stiffness-tunable and biocompatible 3D environment and also allow easy diffusion of nutrients and waste.[8, 12, 13] But pure PEG hydrogels cannot support the ADCs activities (e.g. attachment, growth) effectively due to lack of cell binding motifs.[7] Taking advantages from PEG hydrogel, natural ECM proteins such as collagen, fibrin and fibronectin have been incorporated into PEG networks, to enhance cell responsive in these 3-D hydrogels [11]. Gelatin is a well-known natural ECM protein in biomedical application because of excellent cytocompatibility, and possessing cell adhesive motifs and MMP sequences.[14] However, physically crosslinked gelatin hydrogel alone is not suitable for 3-D cell encapsulation because of its poor mechanical properties and dissolution over time.[15] The general approach to these limitations has been to synthesize crosslinked networks of gelatin.

Several researches have accomplished this *via* photo-polymerization or Michael type addition reaction,[13] when fabricating gelatin-based hydrogels for biomedical application.[16-18] An interpenetrating gelatin-MA PEG hydrogel was synthesized by combining gelatin-MA,PEG tetra-thiol and PEG

tetra-alkyne in various macromer weight percentages.[19] But most cells were round and exhibited delayed proliferation due to the improper initial mechanical properties (storage modulus from 10.8 to 327.7 kPa) of the hydrogel and absence of cell adhesion motifs due to gelatin progressive dissolution.[19] Gelatin-PEG diacrylate hydrogel was fabricated by crosslinking the thiols of gelatin-PEG-cysteine with the acrylates of PEGDA. The concentration of gelatin-PEG-cysteine was constant at 10 wt/v %, while the concentration of PEGDA was changed in the range from 10 wt/v % to 20 wt/v %, (50% - 66.7%, dry weight percentage).[17] These hydrogels showed results similar to the gelatin-MA PEG hydrogel mentioned above. Fu Yao et al. encapsulated cells *via* a Michael type addition reaction based polymerization,[18] while gelatin-PEG precursor was finished by a three-step reaction thiolation, followed by lyophilization of the gelatin-SH and then crosslinking with PEGDA and cells at pH 8.5. However, thiols would easily undergo oxidation and formation of disulfide bonds,[20] which would be a challenge for store thiolated gelatin and subsequently affect the consistency and reproducibility of thiolated gelatin and hydrogel. Another shortcoming is that cell encapsulation *in situ* was done at pH 8.5 for 30 mins, while high pH may affect the viability of encapsulated cells.

To overcome these shortcomings, in this chapter an easy and effective modification approach was used to fabricate a biomimetic gelatin-PEG hydrogel for 3-D cell encapsulation. Thiolation of gelatin was finished by conjugating with Traut's reagent in a one-step reaction followed by reacting with PEGDA immediately after purification. This approach was able to achieve constant and repeatable gelatin-PEG-acrylate precursor. For the purpose of encapsulating cells and forming a hydrogel *in situ*, thiolated gelatin was reacted with one double bond of PEGDA *via* thiols based Michael type addition reaction, while the other double bond of PEGDA was photo-polymerized 5 mins after adding cells and initiator. This new approach, in which the first step involves conjugating thiols with PEGDA at pH 8 overnight, is designed to decrease the dissolution of gelatin significantly and provide better cell adhesion sites compared with above two types of gelatin-based hydrogels. Gelatin-PEG hydrogels prepared by this facile and new approach exhibited better cell activities (viability, morphology and F-actin secretion)

compared with gelatin-MA PEG hydrogel and gelatin-PEG-cysteine hydrogel mentioned above.

Among the many cues required for cell attachment, spreading, proliferation and migration, the initial rheological properties of scaffolds appear to be critically important but have not been fully exploited or appreciated. High initial mechanical properties can caused cells maintaining round shape (not attached) until hydrogel soft enough.[21] In fact, Chen et al. reported that round-shaped cells would be prone to apoptosis and consequently die.[22] McBeath et al. demonstrated that human mesenchymal stem cells that adhered, flattened and spread on a micro-patterned polydimethylsiloxane, underwent osteogenesis, while unspread and round shaped cells became adipocytes. [23] Therefore, it is important to provide the proper growth microenvironment for cell attachment, spreading and proliferation, which governs the fate of encapsulated cells in the new 3-D microenvironment. In this work, gelatin-PEG hydrogels prepared by this new approach have been fabricated to investigate the optimum initial rheological properties. Understanding and controlling the mechanical property to guide cell behavior is complex, as several factors in 3-D microenvironment can affect cell behavior. The relationship between cell behavior, such as proliferation, viability and morphology, and the hydrogel properties including mesh size and concentration of binding motifs, was studied by manipulating a tunable PEG hydrogel system.

5.2 Experimental Methods

5.2.1 Synthesis of gelatin-PEG acrylate

The thiolation of gelatin was accomplished *via* a method published by Hermanson et al. with modifications (Figure 5.1).[20] Sulfhydryl groups were conjugated with gelatin (from porcine skin, type A and with the gel strength of 300 bloom, Sigma-Aldrich, USA) by reacting primary amine groups of gelatin with Traut's reagent (Pierce Thermo Fisher, USA) and prepared as a gelatin-PEG acrylate precursor (GP, Figure 5.1 (A)). 0. 60g (6.85×10^{-6} mol) of gelatin was dissolved in 60 mL of pH 8.0 PBS (0.1mol/L) solution and then reacted with 30mg (0.217mmol) or 60mg (0.436 mmol) of Traut's reagent for 1 hour at

37℃, respectively. The unreacted Traut's reagent was removed by Tangential flow filtration (TFF, Pall life sciences, USA) with 30K MWCO capsule at 37℃, while pH 3.5 purification buffer prepared by adding hydrogen chloride to distilled water. The amount of sulfhydryl groups in gelatin was measured by Ellman's reagent (Sigma, USA).[20] TCEP was added into above thiolated gelatin solution for the purpose of cleaving disulfides. The pH of gelatin-SH was adjusted to pH 8 for dissociation the hydrogen of thiol, while dissociated thiols became nucleophilic. A four-fold molar excess PEGDA dissolving in pH 7.4 PBS was added into above solution and was left stirring overnight at 37℃.[24, 25] The final product was purified *via* dialysis (MWCO 50K) at 37℃, filtered by 0.22 μm filter in a biosafety hood and lyophilized. Protein amount in the lyophilized precursor was determined by BCA assay, while the amount of PEG was calculated *via* deducting the gelatin weight from the total weight. Gelatin's standard curve of BCA was Y= 0.0002X+0.2005 (R^2 = 0.999).

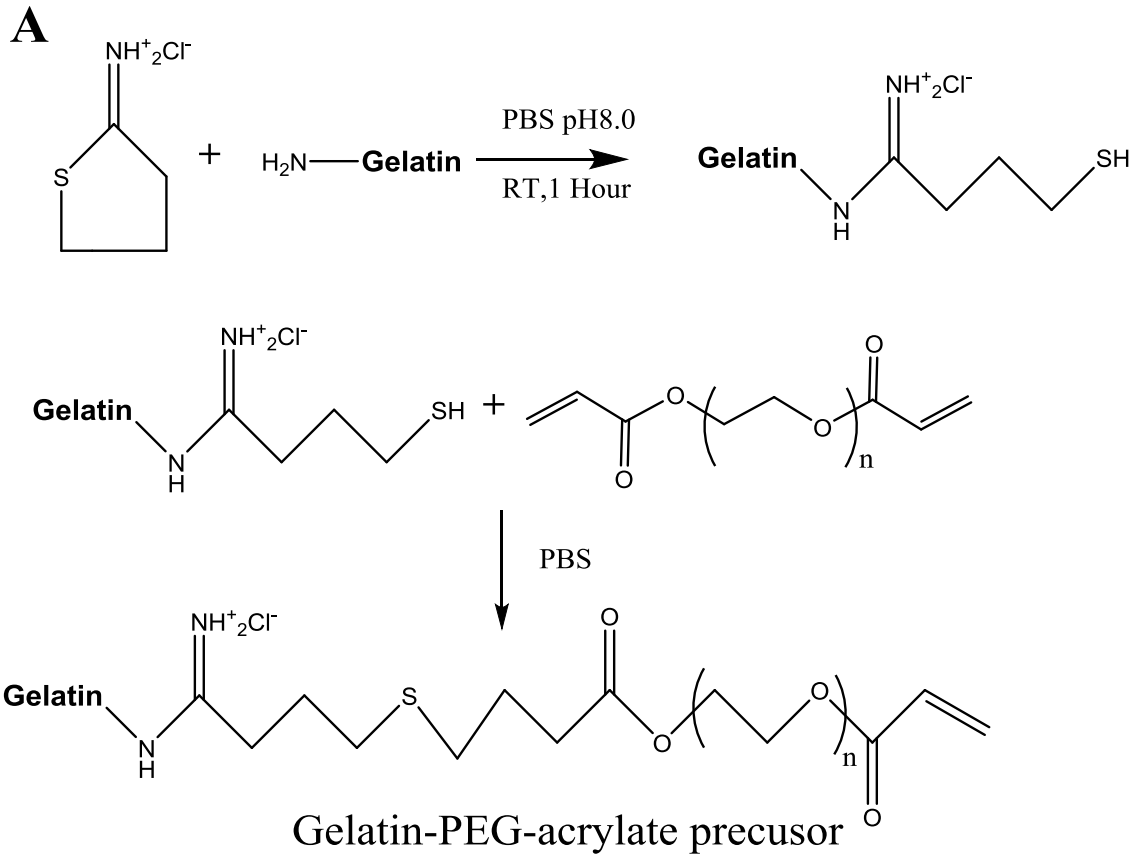

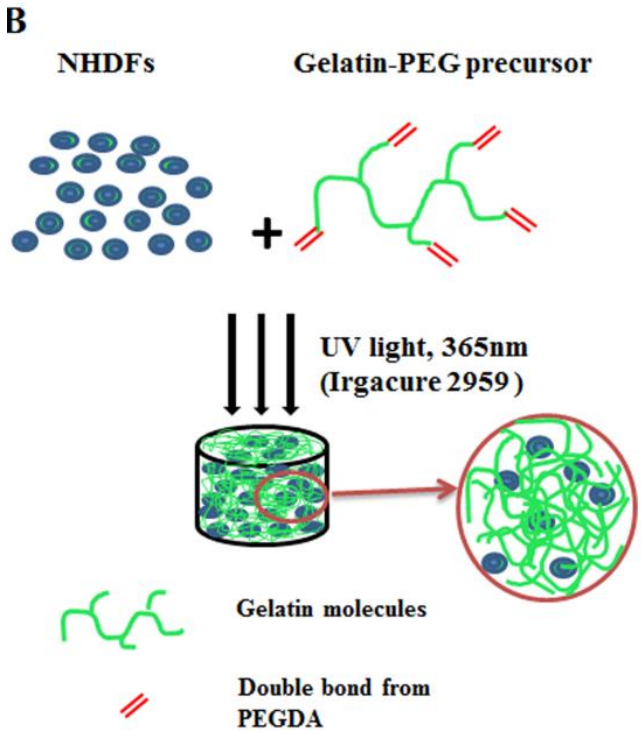

Figure 5.1 (A) The synthesis method of Gelatin-PEG precursor. Sulfhydryl groups were conjugated with the lysine residual of gelatin through reacting with Traut's reagent. (B) Cells were encapsulated into 3-D hydrogel via UV photopolymerization with photo-initiator.

5.2.2 Cell encapsulation in Gelatin-PEG hydrogel

Cell encapsulated gelatin-PEG hydrogels were fabricated as schematically shown in Figure 5.1 (B). Neonatal human dermal fibroblast cells (NHDFs) were purchased from Lonza and cultured up to passage 7 with FGM-2 SingleQuot Kit medium, supplements & growth factors (Lonza, USA) inside. Passages 5-7 of NHDFs were used for encapsulation. Cell laden constructs were fabricated from 100 μL aliquots of the cells in a suspension of gelatin-PEG (final cell density = 1×10^6 cells/mL) using a flat-bottom 96-well plate as the mold. After UV photo-polymerization, the cell encapsulated hydrogels were put into cell culture medium, while the ultra-low cell attachment 6-well plate (Coring, USA) was used in order to inhibit cell attachments to plate. New cell medium was added after washing cell encapsulated hydrogels for removing unencapsulated cells.

5.2.3 Gelatin-PEG hydrogel fabrication

In this work, the name of hydrogel is named in accordance with the precursor used to fabricate the hydrogel, as "GP A-B", where A represents the amount of Traut's reagent added in the gelatin's thiolation step and "B" represents the final concentration of gelatin-PEG precursor. For example, GP30-45 hydrogel is fabricated from a precursor synthesized using 30mg Traut's reagent; the concentration of the precursor used to fabricate hydrogel was 45 mg/ml (4.5 w/v %). Consequently, the GP60-55 precursor is using 60mg Traut's reagent and dissolving the gelatin-PEG at the concentration of 55 mg/ml (5.5 w/v %). In order to have similar rheological property and gelatin concentration as another samples, GP control hydrogel was prepared by crosslinking a solution of 5.0 w/v % PEGDA, 2.5 w/v % gelatin (physically blended) and 0.1 w/v % Irgacure 2959 and irradiating to UV for 5 mins. This control was designed to demonstrate that only chemically connected gelatin could support cells attachment as physically blended gelatin would leak out after hydrogel swelling.

5.3 Results

5.3.1 Hydrogel characterization

Conjugating thiols to gelatin were accomplished in a one-step reaction (Figure 5.1 (A)) *via* Traut's reagent. Two types of gelatin-PEG were fabricated by adjusting the scale of Traut's reagent and gelatin: 30mg (0.217mmol) or 60mg (0.436mmol) reagent vs. 600mg gelatin (6.86 μmol). The control was fabricated with physically blended gelatin since gelatin would be dissolute due to the swelling of hydrogel and change medium. The amount of sulfhydryl group in gelatin was measured by Ellman's reagent (section 3.1.2).[20] The amount of gelatin in the lyophilized power (dissolved at 5mg/mL in PBS) was determined via BCA assay (section 3.3.4), while the amount of PEG was calculated by deducting the gelatin amount from the total weight of lyophilized power. Table 5.1 exhibits the sulfhydryl group amount of gelatin and the constitution of GP30 and GP60 precursors. More thiol could be connected to gelatin by adding Traut's reagent amount from 0.217 mmol to 0.436 mmol.

Thus, more PEGDA can be grafted to gelatin by Michael type addition reaction as present in Table 5.1.

Table 5.1 Sulfhydryl groups amount in gelatin after conjugation with Traut's reagent and the composition of gelatin-PEG precursor. ($p<0.05$)

	-SH amount	
	Molar amount of –SH per 1 molar gelatin (n=3)	Molar percentage of -SH
GP30	1.147 ± 0.219	53.4% ± 10.2%
GP60	2.584 ± 0.200	72.8% ± 5.6%

	Amount of gelatin-PEG precursor			Amount of gelatin-PEG precursor	
	Gelatin amount in final product (w/v %)	PEG amount in final product (w/v %))		Gelatin amount in final product (w/v %))	PEG amount in final product (w/v %)
GP30-40	2.368 ± 0.210	1.632 ± 0.145	GP60-40	1.760 ± 0.194	2.240 ± 0.246
GP30-45	2.664 ± 0.236	1.836 ± 0.163	GP60-45	1.980 ± 0.218	2.520 ± 0.277
GP30-55	3.256 ± 0.289	2.244 ± 0.199	GP60-55	2.420 ± 0.266	3.080 ± 0.339

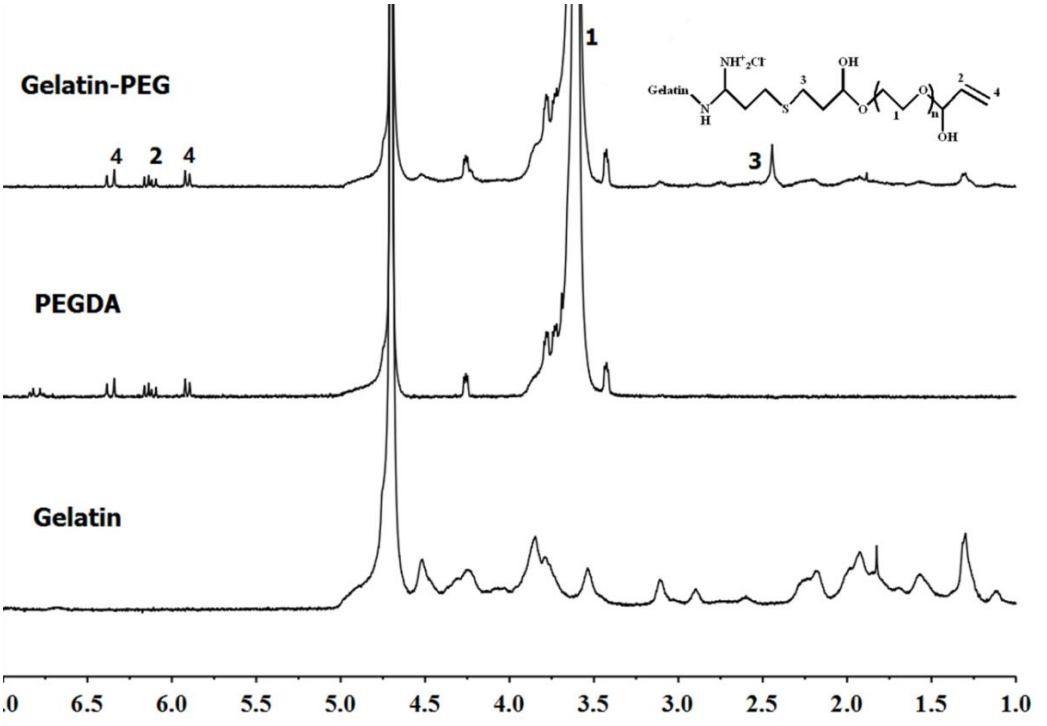

Figure 5.2 ^{1}H NMR spectrums of original gelatin, PEGDA, and gelatin-PEG.

The modification of gelatin to PEG was proved by ^{1}H NMR spectra (Figure

5.2). The PEGDA shows chemical shift peaks (protons in acrylates) at peak 1 (3.6ppm, -OCH_2CH_2-), peak 2 (6.1 ppm, -$CH=CH_2$), and peak 4 (5.8 and 6.4 ppm, -$CH=CH_2$) in Figure 5.2.[26] Gelatin-PEG exhibits a new peak 3 (2.5 ppm) from the methylene protons of Traut's reagent moieties, which demonstrated Traut's reagent was successfully conjugated to gelatin.[27] After PEGylation, the spectra of gelatin-PEG possessed typical peaks of both unmodified gelatin and PEGDA. So the ^{1}H-NMR results proved that the PEGDA was successfully connected to gelatin.

5.3.2 Hydrogel swelling, degradation and rheological properties

Dynamic time-sweep measurements were employed to monitor rheological property change during UV photo-polymerization. The photo-polymerization of gelatin-PEG hydrogel begins once the UV light is turned on: the storage modulus of hydrogel increases and a plateau is reached after polymerization is done. According to Figure 5.3(A), the photo-polymerization reaction of gelatin-PEG acrylates were very fast (less than 3 mins), leading to the formation of an on-going hydrogel network from gelatin-PEG acrylates. The storage modulus of all the hydrogels was much higher than the loss modulus of them in Figure 5.3(A), which demonstrated the gelation procedure after photo-polymerization effectively. The polymerization rate constants (slope, unit: Pa/second) that are calculated from the linear region of the crosslinking profile (Figure 5.3(A)) of all the hydrogels shows a trend as follows: GP30-40(0.48) < GP30-45(1.23) < GP30-55(4.41) < GP60-40(5.52) < GP60-45(7.14) < GP60-55(12.57) < GP control (24.99), which is depending on the amount of acrylate. Therefore, the rheological results (Figure 5.3(A)) proved the formation of hydrogel and showed the change of storage modulus during gelation process., All samples from the "GP-60" series possessed higher storage modulus due to more PEG acrylates (2.584±0.200, Table 5.1) in Figure 5.3, compared with all the "GP30" series (1.147±0.219, Table 5.1). The rheological properties of the gelatin-PEG hydrogels correlated with the amount of precursor and also PEG amount (acrylate). Thus, more thiols in the gelatin (GP60>GP30) led to graft more acrylates and finally a higher storage modulus (GP60-45>GP30-45, GP60-55>GP30-55).

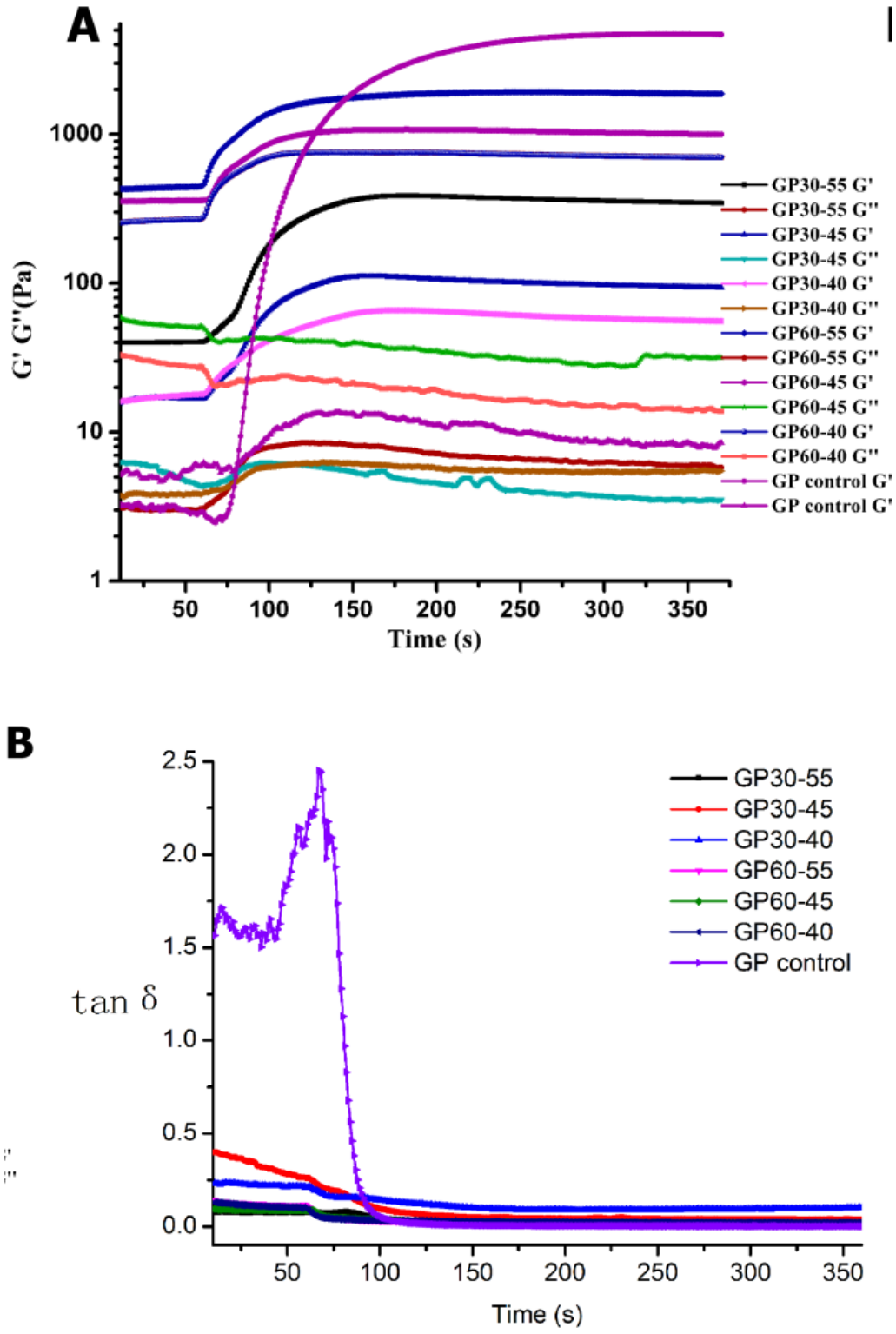

Figure 5.3 Shear storage modulus and loss modulus data (A) and damping factor-tan δ (B) from rheological experiments that were determined during photo-polymerization of all the hydrogels. The UV light was turned on after 60 seconds.

The damping factor (tan δ= G′/G′′) is the ratio of the energy dissipated to the maximum energy deposited in the material during one cycle of oscillation. So, for G′′> G′, the damping factor tan δ > 1, meaning that the material acts as a viscoelastic liquid. While for G′ > G′′, the damping factor tan δ < 1, which means that the sample acts as a viscoelastic solid. As presented in Figure 5.3(B), tan δ of all GP30 and GP60 are initially lower than 1 because of physical aggregation below 40 ℃ or entanglements caused by high molar mass.[28] Tan δ decreases continuously to very low values because of the substantially formation of crosslinks, therefore proving the viscoelastic solid-like property.

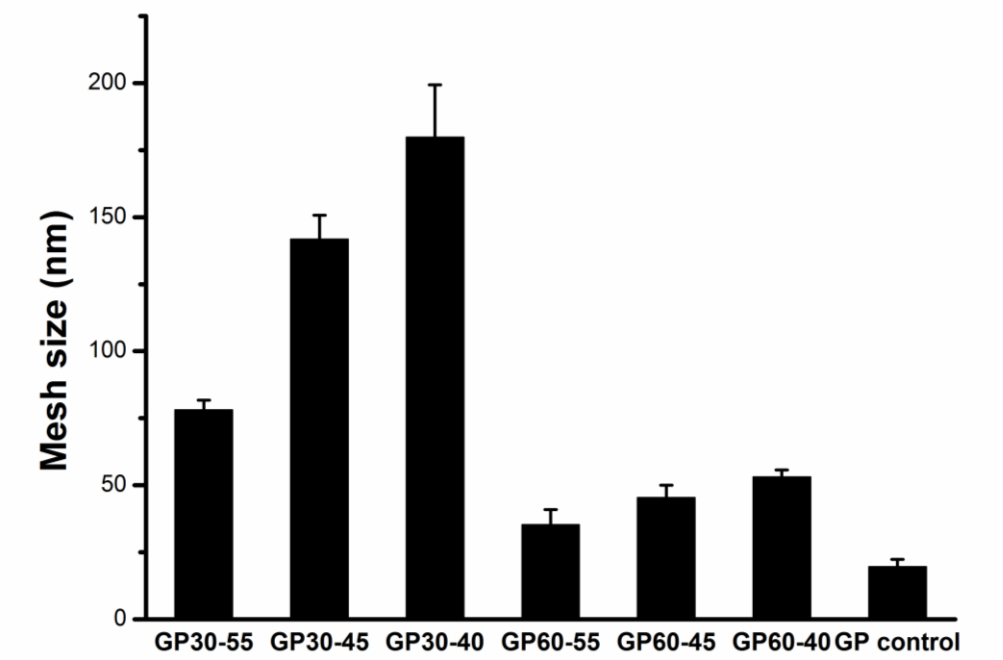

Figure 5.4 Initial mesh sizes of gelatin-PEG hydrogels after UV crosslinking.

The network average mesh size is an effective estimation of its "molecular" porosity which is intuitively relatable to its ability to encapsulate cells, and their ability to grow within the network. However, it should be borne in mind that several parameters that could influence the mesh size such as physical entanglements, and defects (unreacted double bonds and encapsulated cells), which could cause an increased mesh size. In this work, the initial mesh size of each hydrogel was achieved by using equation 1, 3, 4, 5, 6 and 7 (Page 40); however, the Q_s used in the equations is the swelling at the time of crosslinking (not equilibrium). The initial swelling of gelatin-PEG hydrogels was measured

immediately after the crosslinking (dissolving of precursor powder) and presented in Table 5.2. Other researchers found that the initial mesh size decreases as the concentration of PEGDA increases.[29-31] As expected, the "initial" mesh size of gelatin-PEG hydrogels decreased with increase in the concentration of gelatin-PEG precursor according to Figure 5.4 (for example, GP30-55 vs. GP30-45 and GP60-55 vs. GP60-45). In general, GP60 hydrogels containing more acrylates had lower mesh size than GP30 hydrogels due to the higher concentration of crosslinkable groups in the precursor for GP60 which caused higher crosslinking densities (lower M_c).

Table 5.2 Initial swelling ratio of gelatin-PEG hydrogels after photo-polymerization. (n=3)

	GP30-55	GP30-45	GP30-40	GP60-55	GP60-45	GP60-40	GP control
Initial Swelling ratio	18.18 ± 0.22	22.22 ± 0.15	25.00 ± 0.11	18.18 ± 0.22	22.22 ± 0.18	25.00 ± 0.20	20.00 ± 0.18

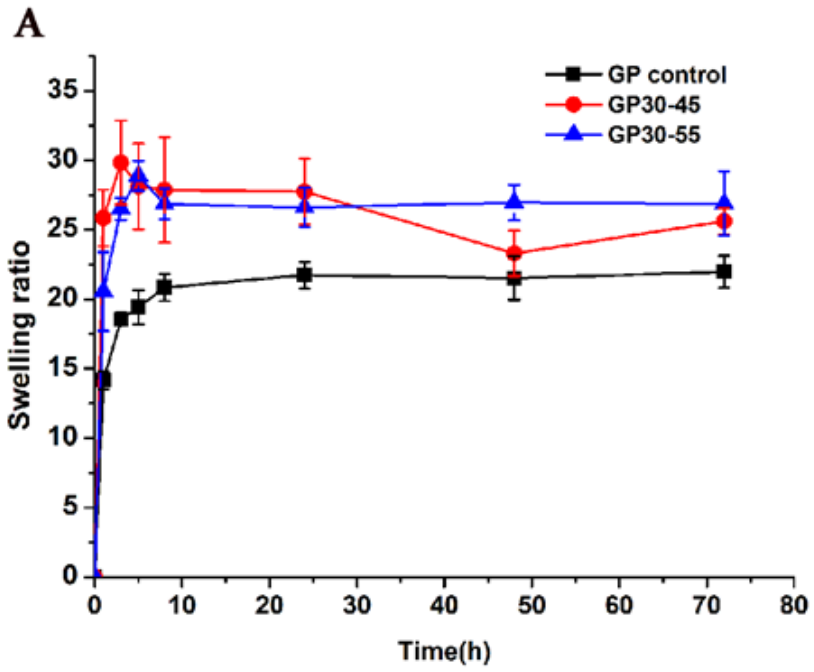

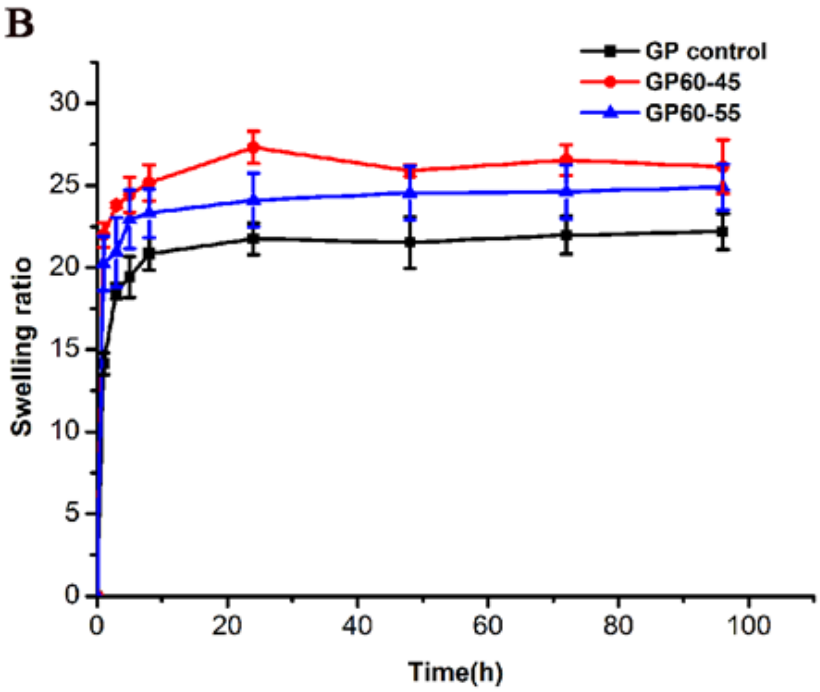

Figure 5.5 Swelling ratio results of gelatin-PEG hydrogel (A: GP 30 hydrogels; B: GP 60 hydrogels) and control PEG hydrogel (n=4).

Figure 5.5 (A) and (B) presented the swelling properties of GP30-45, GP30-55, GP60-45, GP60-55and GP control hydrogels at different time. One of the most important factors that influence the swelling property of hydrogels is the crosslinking density. After PBS immersion the GP30-45 and GP30-55 hydrogels rapidly swelled within 8 h (an increase in swelling ratio of 28 and 30, respectively), while the GP60-45 and GP60-55 hydrogels almost reached fully swollen status within 24 h (an increase swelling ratio of 27.5 and 23, respectively). The swollen hydrogels reached a plateau or "equilibrium swelling", and remained relatively constant afterward. As the concentration of gelatin-PEG precursor GP60 increased from 45mg/mL to 55mg/mL, the equilibrium swelling ratios of GP60-55 decreased compared with GP60-45. This could be easily understood as the GP60-55 precursor contains more acrylates, therefore increasing the crosslinking density, and consequently lower swelling ratio. For the same reason, GP60-55 hydrogel has lower swelling ratios than GP30-55 hydrogel. GP30-55 exhibited a higher equilibrium swelling ratio as expected (measurements of swelling of GP30-45 and GP30-55 both became difficult due to sample disintegration). It should be noted that the control sample had the lowest swelling as the crosslink density of the

PEGDA hydrogel is expected to be quite high, as it crosslinks with itself.

5.3.3 3-D cell encapsulation in Gelatin-PEG hydrogel

The *in situ* storage modulus of cell encapsulated GP30-45 and GP30-55 hydrogel decreased after the swelling and cell growth of hydrogel as shown in Figure 5.6 (A), with corresponding increases in mesh size as shown in Figure 5.6 (B).

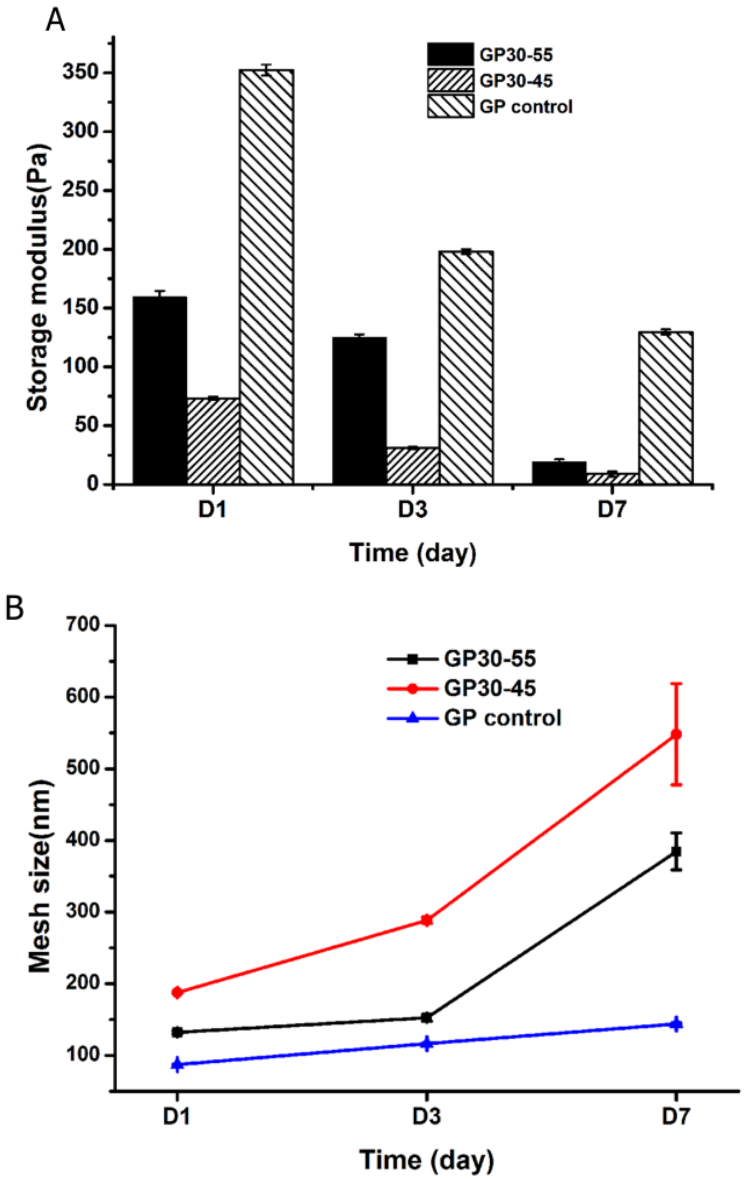

Figure 5.6 The mesh size change (mesh size at each time point divided by initial mesh size) of various cell encapsulated Gelatin-PEG hydrogel at day 1, day 3 and day7 (n=3, $p<0.05$).

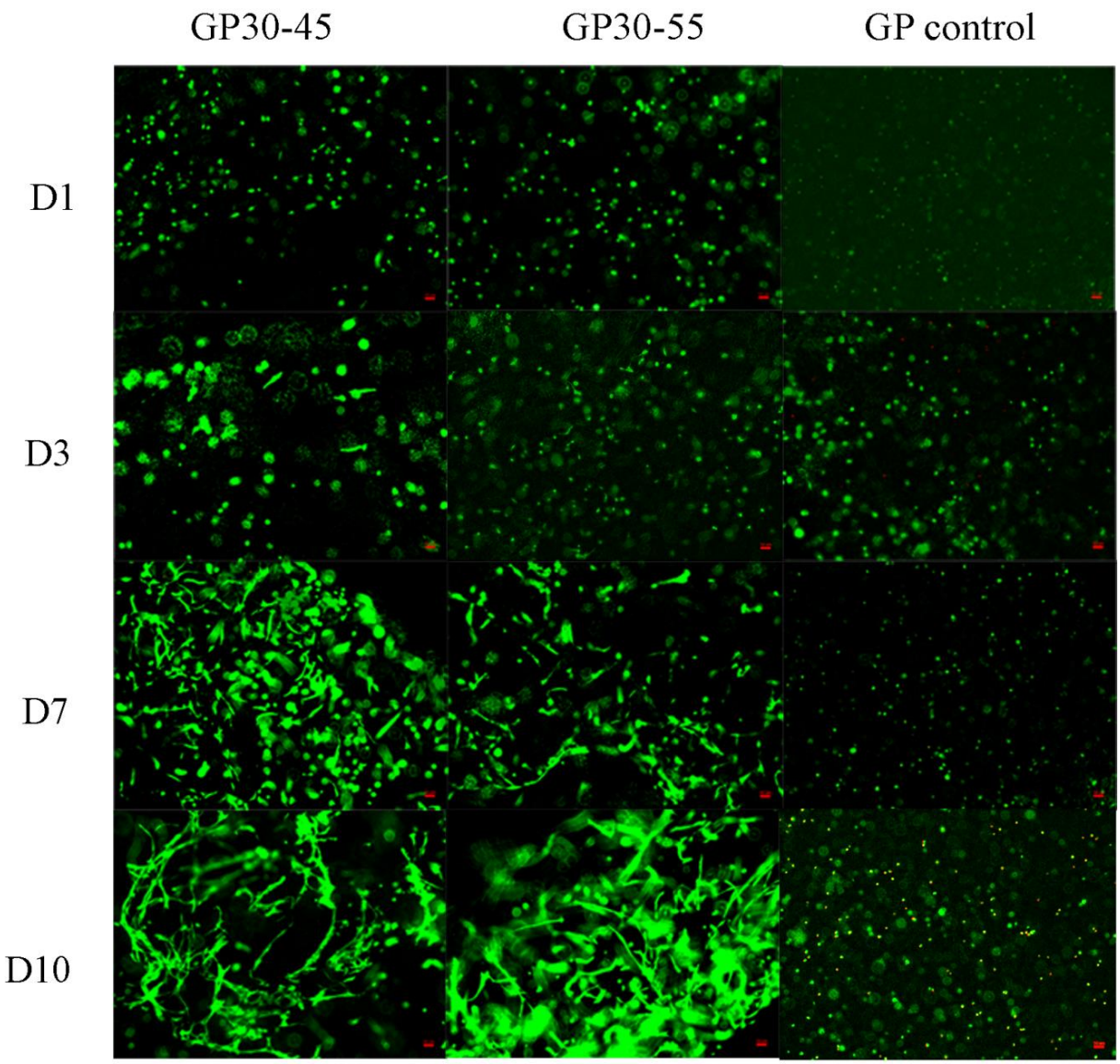

Figure 5.7 3-D cell encapsulation in GP30-45, GP30-55 and control PEG hydrogels. Live/dead staining reveals the situation of cells inside the gel (Live: green/Dead: red). The red scale bar at the bottom right side represents 50μm.

Figure 5.7 reveals the effect of gelatin-PEG composition on cell adhesion and cell morphology. In our study, where GP30 and GP60 samples were studied in the cell encapsulation experiments, it was proved that only GP30 can support cell growth effectively (Figure 5.8). Thus, we systematically followed the cell study of GP30 samples. NHDFs were encapsulated into three types of hydrogels including GP30-45, GP30-55 and control PEG hydrogel. We found that NHDFs in all three hydrogels exhibited high survival rate with few dead cells at day 1 (Figure 5.7), which means that the long wave length UV photo-polymerization is safe for cell encapsulation. Interestingly, NHDFs encapsulated in GP30-45 hydrogels could attach on day 1(Figure 5.7), while those encapsulated in GP30-55 needed more time to achieve a suitable

environment and thus attached only on day 3. Attachment of NHDFs in GP60-55 was not showed until day 16 (Figure 5.8) probably due to unsuitable rheological properties (storage modulus above ~100 Pa). Though the initial storage modulus of GP60-55 was up to 2000 Pa (Figure 5.3 (A)), reduction in stiffness leading to proper microenvironment (larger porosity) for cells could show after several days. The cells in the control PEG hydrogel and GP60-45 hydrogels did not attach probably due to limit binding sites (gelatin concentration <2.3 w/v %), while those in GP60-55 could attach on day 16 because of enough gelatin molecules (Table 5.1, 2.4 w/v %) and proper rheological properties (storage modulus ~ 100 Pa) after day 16. Figure 5.9 is showing (schematically) the interactions between cells and gelatin-PEG hydrogel networks. Cells encapsulated inside gelatin-PEG hydrogels exhibited initially round shape morphology (left of the first row and left of the second row). Figure 5.10 shows the viability of NHDFs in three types of gelatin-PEG hydrogels, while GP30-45 has the highest cell viability because of excellent cell growth compared with another two gels.

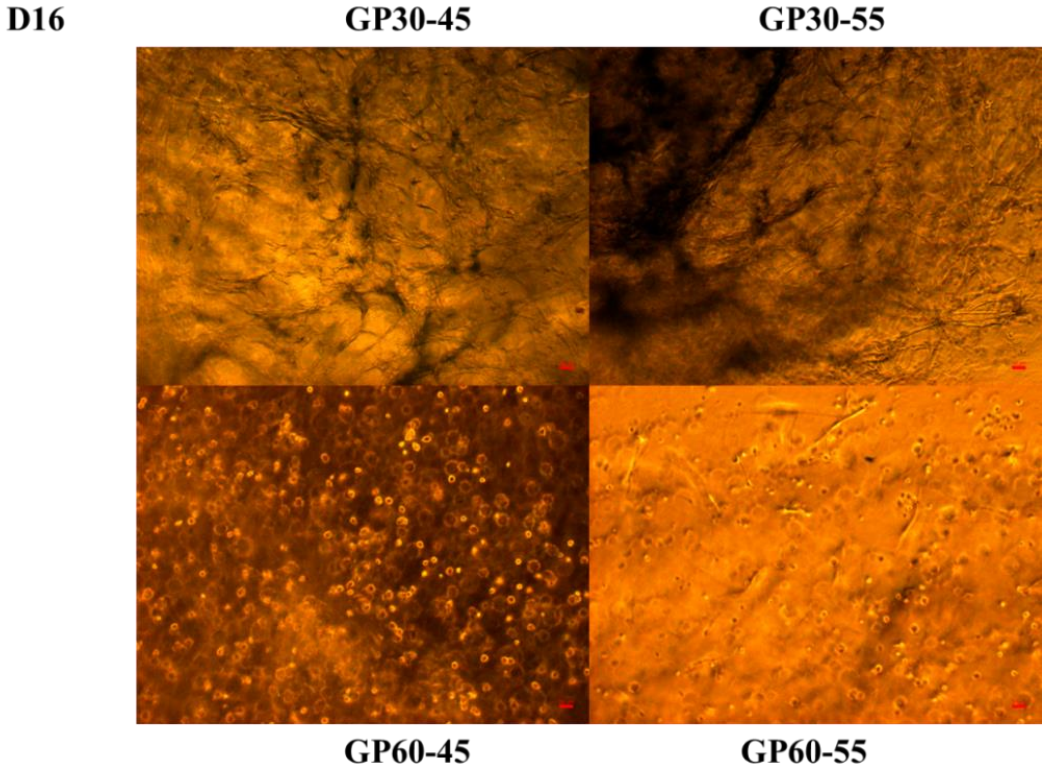

Figure 5.8 Cell morphology of 3-D cell encapsulation in GP30-45, GP30-55, GP60-45 and GP60-55 at day 16. The red scale bar at the bottom right side is 50µm.

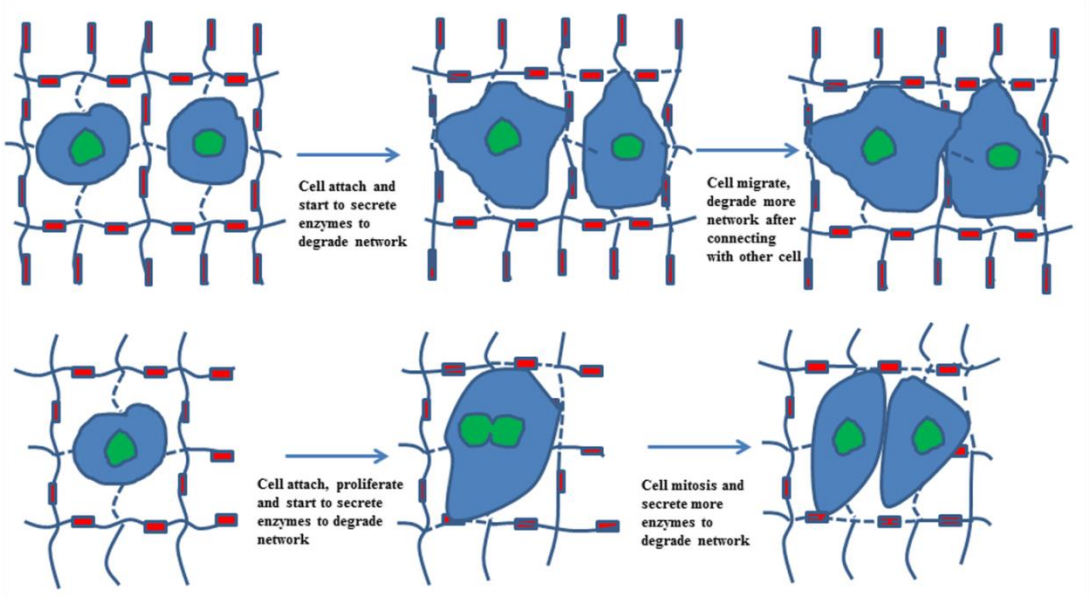

Figure 5.9 Schematic illustrations of interactions between cells and the microenvironment. (The dotted line means the broken network of hydrogel, while the solid line is network of hydrogel. And then the red rectangle means gelatin molecules.)

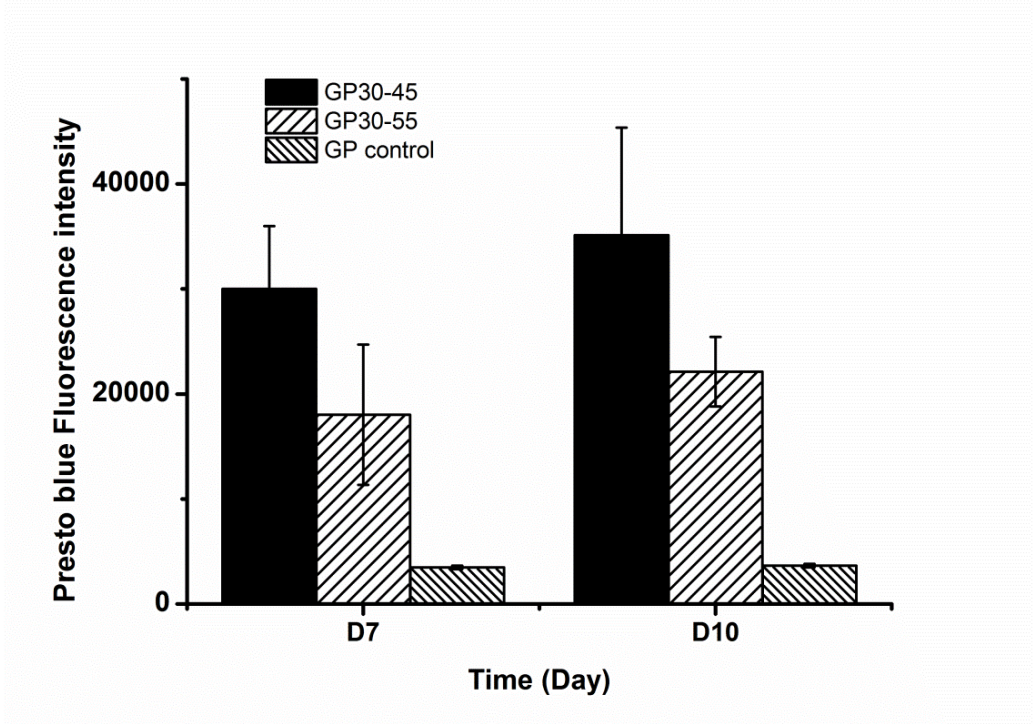

Figure 5.10 NHDFs viability in 3-D Gelatin-PEG hydrogels at day 7 and 10. (n=3)

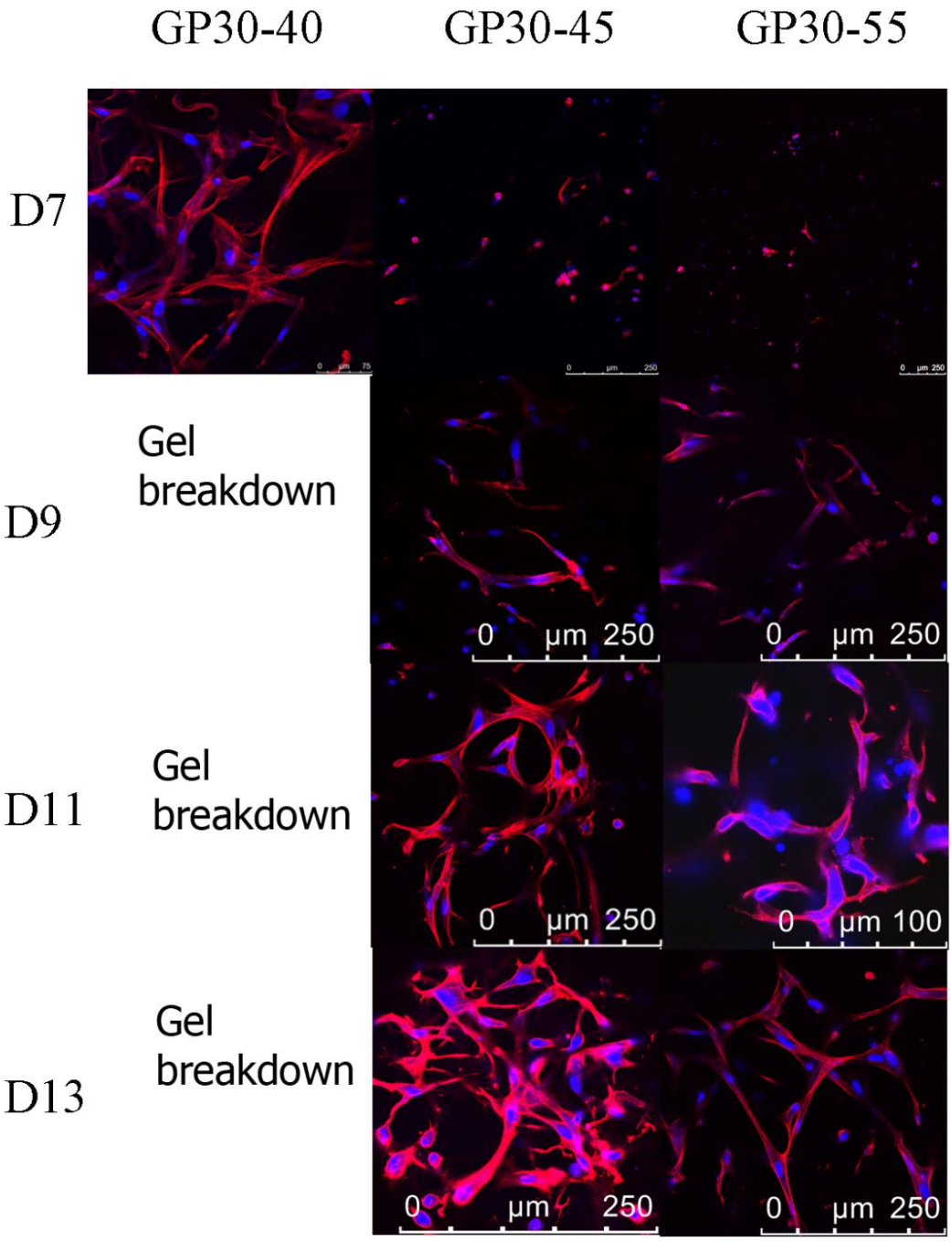

Figure 5.11 Cytoskeletal assembly is modestly influenced by matrix mechanical properties to NHDFs in 3-D gelatin-PEG hydrogels. NHDFs encapsulated into PEG gelatin-hydrogels of different storage modulus were fixed and stained for nucleic acid (Dapi, blue) and F-actin (Rhodamine–Phalloidin, red). The degradation of GP30-40 was fast due to lower crosslinking degree of gelatin-PEG, while it only maintained its structure for 7days.

The actin cytoskeleton has been extensively investigated and proven to play a

important role in cell behaviors, as well as linking the ECM and cell interior through cell attachments.[32] NHDFs encapsulated in GP30-40 gelatin-PEG hydrogel exhibited a high degree of cell adhesion, spreading and formation of interconnected cellular networks at day 7, while the NHDFs in GP30-45 and GP30-55 hydrogels needed more time to form similar F-actin network (Figure 5.11).

5.4 Summary

The remolding of new tissue, as well as the interaction between cells and ECM *in vivo*, occur in 3-D microenvironments. In this work, the results proved an effective and facile approach of fabrication gelatin-PEG hydrogel for 3-D cell encapsulation; these hydrogels can be easily manipulated for initial rheological characteristics. Swelling and rheological properties of gelatin-PEG hydrogels could be changed by adjusting the concentration of gelatin-PEG precursor or the reaction ratio of gelatin and PEG. By preparing gelatin-PEG hydrogels that crosslink *via* photo-polymerization, this work studied how the growth and morphology of NHDFs encapsulated in these gelatin-PEG hydrogels (in 3-D) were affected by the storage modulus or mesh size of the hydrogels. Even with the existing of enough gelatin molecules, this study showed clearly that higher stiffness or smaller mesh size of gelatin-PEG hydrogel could be a barrier for NHDFs in 3-D hydrogels, delaying attachment, spreading and proliferation. Interestingly, our results revealed that “proper” stiffness (storage modulus < ~ 100 Pa) or mesh size (>150 nm) could enhance the viability of cells compared with previous researches. In summary, this study indicates that the physically relevant feature affecting cellular proliferation and spreading is the network mesh size, which of course is measured *via* the crosslinking density of network as determined from the storage modulus.

References

[1] J. G. Hardy, P. Lin, C. E. Schmidt. *Journal of Biomaterials Science, Polymer Edition*. **2015**, 26, 143-161.

[2] D. J. Munoz-Pinto, A. C. Jimenez-Vergara, T. P. Gharat, M. S. Hahn. *Biomaterials*. **2015**, 40, 32-42.

[3] A. Huttenlocher, R. R. Sandborg, A. F. Horwitz. *Current opinion in cell biology*. **1995**, 7, 697-706.

[4] L. T. Jensen, N. B. Høst. *Cardiovascular research*. **1997**, 33, 535-539.

[5] S. Gundy, G. Manning, E. O'Connell, V. Ellä, M. S. Harwoko, Y. Rochev, T. Smith, V. Barron. *Acta biomaterialia*. **2008**, 4, 1734-1744.

[6] R. M. Nerem, D. Seliktar. *Annual review of biomedical engineering*. **2001**, 3, 225-243.

[7] J. Zhu. *Biomaterials*. **2010**, 31, 4639-4656.

[8] J. L. Drury, D. J. Mooney. *Biomaterials*. **2003**, 24, 4337-4351.

[9] A. S. Hoffman. *Advanced drug delivery reviews*. **2012**.

[10] S. B. Anderson, C.-C. Lin, D. V. Kuntzler, K. S. Anseth. *Biomaterials*. **2011**, 32, 3564-3574.

[11] E. A. Phelps, N. Landázuri, P. M. Thulé, W. R. Taylor, A. J. García. *Proceedings of the National Academy of Sciences*. **2010**, 107, 3323-3328.

[12] A. S. Hoffman. *Advanced drug delivery reviews*. **2012**, 64, 18-23.

[13] J. Zhu. *Biomaterials*. **2010**, 31, 4639-4656.

[14] T. Loth, R. Hötzel, C. Kascholke, U. Anderegg, M. Schulz-Siegmund, M. C. Hacker. *Biomacromolecules*. **2014**, 15, 2104-2118.

[15] H. Waldeck, W. Kao. *Journal of Biomaterials Science, Polymer Edition*. **2012**, 23, 1595-1611.

[16] K. Xu, Y. Fu, W. Chung, X. Zheng, Y. Cui, I. C. Hsu, W. J. Kao. *Acta biomaterialia*. **2012**, 8, 2504-2516.

[17] Y. Fu, K. Xu, X. Zheng, A. J. Giacomin, A. W. Mix, W. J. Kao. *Biomaterials*. **2012**, 33, 48-58.

[18] K. Xu, D. A. Cantu, Y. Fu, J. Kim, X. Zheng, P. Hematti, W. J. Kao. *Acta biomaterialia*. **2013**, 9, 8802-8814.

[19] M. A. Daniele, A. A. Adams, J. Naciri, S. H. North, F. S. Ligler. *Biomaterials*. **2014**, 35, 1845-1856.

[20] G. T. Hermanson. *Bioconjugate techniques, Academic press*, **2013**.

[21] Y. Fu, K. Xu, X. Zheng, A. J. Giacomin, A. W. Mix, W. J. Kao. *Biomaterials*. **2012**, 33, 48-58.

[22] C. S. Chen, M. Mrksich, S. Huang, G. M. Whitesides, D. E. Ingber. *Science*. **1997**, 276, 1425-1428.

[23] R. McBeath, D. M. Pirone, C. M. Nelson, K. Bhadriraju, C. S. Chen. *Developmental Cell*. **2004**, 6, 483-495.

[24] D. Dikovsky, H. Bianco-Peled, D. Seliktar. *Biomaterials*. **2006**, 27, 1496-1506.

[25] L. Oss-Ronen, D. Seliktar. *Advanced Engineering Materials*. **2010**, 12, B45-B52.

[26] M. B. Browning, E. Cosgriff-Hernandez. *Biomacromolecules*. **2012**, 13, 779-786.

[27] R. Singh, L. Kats, W. A. Blättler, J. M. Lambert. *Analytical biochemistry*. **1996**, 236, 114-125.

[28] S. B. Ross-Murphy. *Polymer*. **1992**, 33, 2622-2627.

[29] H. Liao, D. Munoz-Pinto, X. Qu, Y. Hou, M. A. Grunlan, M. S. Hahn. *Acta biomaterialia*. **2008**, 4, 1161-1171.

[30] M. B. Mellott, K. Searcy, M. V. Pishko. *Biomaterials*. **2001**, 22, 929-941.

[31] T. Canal, N. A. Peppas. *Journal of biomedical materials research*. **1989**, 23, 1183-1193.

[32] M. Vicente-Manzanares, C. K. Choi, A. R. Horwitz. *Journal of cell science*. **2009**, 122, 199-206.

Chapter 6

Hybrid Crosslinked Gelatin / Elastin Based PEG Hydrogel: A Novel Injectable and Tunable Platform for *In situ* Cell Delivery

This chapter describes the work involved to enhance the ability of guiding cell behavior in gelatin-PEG hydrogel via introducing elastin-PEG. The background and challenges in guiding cell behavior in 3-D microenvironment are introduced in the first section. To overcome these challenges, a gelatin and elastin hybrid PEG hydrogel system is chosen as a potential solution and explained in first section. The synthesis and characterization of gelatin-PEG and elastin-PEG were described in the second section. The third section shows the results of materials characterization and cell evaluation experiments. The last section summarized the findings of gelatin and elastin hybrid PEG hydrogel system. This chapter will give a new understanding of utilizing elastin to innately guide cell behavior in gelatin-PEG hydrogel and its potential for dermal tissue engineering.

6.1 Introduction

A major challenge in tissue engineering is the design and fabrication of bioactive scaffolds with necessary biological instructive cues to innately guide cell behavior, while the scaffolds being required to possess suitable mechanical properties.[1] These advantageous cues can be chemical, biological, and physical and play an important role in mediating cellular attachment, migration, spreading, proliferation and differentiation, while encouraging secretion of appropriate proteins/ polysaccharides to rebuild their own ECM.[2] The natural ECM components play a crucial instructive role in governing cell behavior and functions and thus a biomimetic approach for design and fabrication of biomaterial has a variety of innate advantages.[1, 3, 4]

Biomimetic hybrid hydrogels were developed to combine the benefits of synthetic (tunable mechanical characteristics) and natural ECM proteins (biological cues) hydrogels.[5-10] For example, PEG hydrogels can be tailored with adhesive peptides or ECM proteins that can promote cell attachment, proliferation and ECM deposition.[11-13] In spite of these advantages, substantial challenges remain in the use of hydrogels to precisely control the behavior and fate of delivered therapeutic cells. For example, gelatin methacrylamide PEG hydrogel[14] and gelatin-PEG diacrylate hydrogel[5, 6] have shown delayed cell attachment (with mostly rounded cells) and proliferation; other studies have demonstrated that round-shape cells underwent apoptosis and subsequently died in a few weeks[15]. For those cells that did survived well in the above mentioned hydrogels, their spreading, migration, proliferation, phenotype, differentiation and the interactions of cell and matrix were barely controllable. The reason for this is primarily that an artificial hydrogel utilizing just one protein or peptide sequence does not mimic natural ECM well enough due to limited instructive cues. Consequently, this led to unsatisfactory cell behavior and compromised the effect and efficiency of delivered cells.[16] Therefore, rather than providing general biological cues specificity should be considered in the fabrication of hydrogels since every tissue type has its own set of mechanical, chemical gradients, structure, and function.[1] To overcome those several challenges and finally better control of cell fate, there is a need to develop hybrid hydrogels that can mimic multiple functions of ECM with tunable mechanical properties

and finally provide predictable control over cell fate while allowing facile delivery of the cells to injuried tissue.

In this new approach to such hybrid hydrogels, multiple ECM-proteins PEG hydrogels for soft tissue engineering with tunable mechanical property were explored in this chapter. More specifically, dermal substitutes were designed based on PEG combined with both gelatin and elastin. Gelatin is a extensively studied ECM protein in biomedical application due to the presence of cell adhesive cues and MMP peptides.[17] Elastin is the major insoluble protein existing in elastic tissue, contributing to elasticity of the skin and promoting a number of cellular responses including chemotaxis, proliferation, attachment, and differentiation.[18, 19] Elastic fibers are not readily resynthesized after injury due to difficulties in re-expression of tropoelastin and related molecules, thus seriously hampering the quality and speed of new tissue generation and full healing.[18] Therefore, burn survivors still suffer from excessive scarring and skin contractions which keep compromising their health and quality of life.[18] Despite the need, however, there is a dearth of research on elastin-based dermal substitutes with tunable mechanical properties, while elastin is historically underrepresented in commercial dermal substitutes. Previous studies utilizing elastin have primarily focused on incorporation methods (chemical conjugation or physical blending)[20-22] leading to a 2-D cell study or evaluation in vivo.[23, 24] For example, soluble bovine elastin denatured from insoluble elastin, as a relatively easily sourced starting material, has been used to develop highly porous elastic hydrogels using glutaraldehyde and high pressure CO_2; however, such hydrogels are still not compatible with cell encapsulation and in situ delivery. [25, 26] Solubilized elastin was also used to mediate the attachment and proliferation of dermal fibroblasts and endothelial cells in 2-D.[27] An acellular dermal matrix (70% collagen and 30% elastin) produced by removal of cells from porcine skin was transplanted into animal skin and shown to improve the elasticity and functionality of severe scars by replacing the missing elastic network, yet the drawbacks were poor mechanical property and residual cell materials in the scaffold.[18] Similarly, Daamen et al. proved that porous collagen-solubilized elastin scaffolds fabricated by reacting with EDC/NHS and lyophilization, was able to induce cell proliferation and elastin deposition when implanted subcutaneously in rats, compared with collagen-only scaffolds that do

not promote elastin synthesis.[23] Substantial challenges remain in the incorporation of elastin into scaffolds with high cell viability and controlled behavior in 3-D. For instance, it has been recently reported that only 80% of encapsulated cells remained viable in an elastin based thermo-responsive hydrogel fabricated by crosslinking alpha-elastin, PNIPAMoly, Polylactide, 2-Hydroxyethyl methacrylate and oligo (ethylene glycol); the morphology, differentiation and the remolding of new ECM of cells have not yet been studied.[28] Therefore, the effects of elastin on cell encapsulated hydrogels have yet to be elucidated for tissue engineering particularly in a 3-D microenvironment. We hypothesize that elastin plays a crucial role in skin healing and regeneration, due to its fundamental role in skin structure and function.

In consideration of the above, a novel multiple ECM-proteins/ hybrid PEG hydrogel have been explored to encapsulate NHDFs in 3-D microenvironment. In order to truly mimic the biological microenvironment, gelatin was designed to support cell adhesion as PEG hydrogels are relatively inert to cell adhesion, while elastin was incorporated to guide the behavior of dermal fibroblast and promote remodeling of their own ECM for skin tissue engineering. It was hypothesized that covalent crosslinking of elastin into gelatin-PEG hydrogel would markedly alter the biological response and, from a skin or soft tissue engineering perspective, that its corporation was able to promote cell's spreading, migration and proliferation while rebuilding their own ECM. Combining the results from the characterizations and cell studies, the hypothesis is that the covalent incorporation of gelatin and elastin into PEG hydrogel provides a tunable and cytocompatible biomaterial that promotes the proliferation of NHDFs and remolding of ECM and may be useful in soft tissue engineering such as dermal substitutes.

6.2 Experimental Methods

6.2.1 Gelatin and Elastin PEGylation

The thiolation of gelatin was accomplished by following the protocol showed in Section 5.2.1 (Figure 6.1). Briefly, sulfhydryl groups were conjugated to gelatin by reacting gelatin with Traut's reagent, and thiolated gelatin was used as a precursor to fabricate gelatin-PEG (GP, Figure 6.1). 2.40 g (0.00060 mol) of gelatin was added into 240 mL of

pH 8.0 PBS (0.1mol/L) solution and incubated at 37℃ until dissolved. 120 mg of Traut's reagent were mixed with above solution and reacted for 1 hour at 37℃.The unconjugated Traut's reagents were by TFF with 30K MWCO capsule at 37℃, while distilled water (pH 3.5) was chosen as a purification buffer. The amount of sulfhydryl after thiolation was determined by Ellman's reagent, while one fold molar amount of TCEP was added to the above solutions to improve the subsequent Michael-type addition reaction as TCEP can inhibit the formation of disulfide bond [29]. The pH of solutions was changed to pH 8.0, while a 4-fold molar excess of PEGDA dissolved in pH 7.4 PBS (0.1mol/L) was put into above solutions and stirred overnight at 37℃. Gelatin-PEG was purified and concentrated by MWCO 70K TFF capsule in PBS (for cell culture), filtered by 0.22 μm filter in a biosafety hood and stored in -80℃. Soluble elastin-PEG precursor (Elastin-PEG) was synthesized by the same method and reaction ratio, while the purification was finished by 10K (after thiolation) and 50K (after PEGylation) MWCO TFF capsule, respectively. The final product was lyophilized and stored in 4℃.

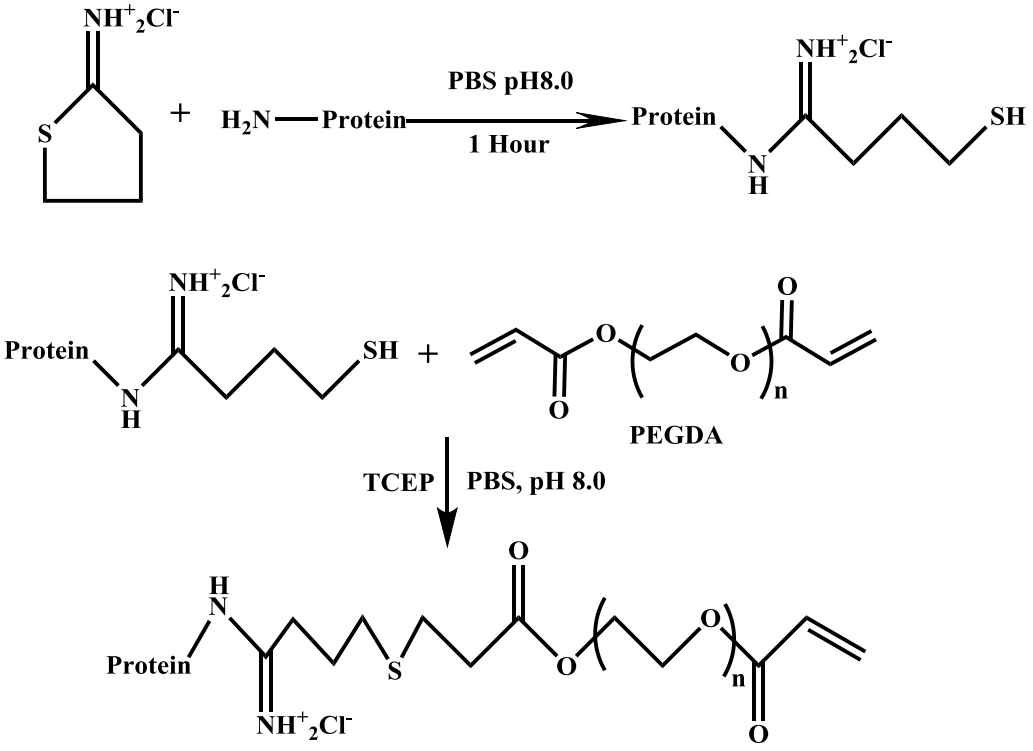

Figure 6.1 Synthesis of Gelatin-PEG and Elastin-PEG precursor. Gelatin and elastin was modified with free sulfhydryl group on the backbone via reacting with Traut's reagent.

The gelatin and elastin amount in the precursor were determined using the BCA kit assay for protein. The amount of gelatin in the concentrated precursor solution (purified by PBS and stored in PBS) was measured by BCA assay, while the amount of PEG was obtained by deducting the gelatin and PBS salts amount from the total weight of lyophilized power. The weight of elastin in the lyophilized power (dissolved at 5mg/mL in PBS) was also measured by BCA assay, while the weight of PEG was achieved by the same method (gelatin-PEG). The BCA standard curve of gelatin was Y= 0.0002X+0.2005 (R^2 = 0.999), while the BCA standard curve of elastin was Y=4.3622X-0.5551(R^2 = 0.998).

6.2.2 Gelatin and Elastin hybrid PEG hydrogel preparation

Gelatin-PEG and Elastin-PEG hybrid hydrogels were crosslinked to form hydrogels *via* UV photo-polymerization with 0.1 w/v % Irgacure 2959, and exposing to UV light (365nm, 4-5mW/cm^2) for 5 min. The hydrogel nomenclature used in this study is defined as ‘‘GEPX’’ or ‘‘GPE control’’ and shown in Table 6.1, where ‘‘GEP’’ represents covalently crosslinked gelatin-PEG and elastin-PEG hybrid hydrogel. ‘‘X’’ is the concentration of Elastin-PEG precursor (wt/v %), while the concentration of Gelatin-PEG is fixed at 48mg/mL (4.80 wt/v %). For example, GEP45 hydrogel was prepared from a mixture of gelatin-PEG and elastin-PEG precursor, with the concentration of elastin-PEG at 45 mg/ml (4.5 w/v %). In this study, the concentration of gelatin-PEG of all three kinds of hydrogels were fixed at 48mg/mL (4.80 wt/v %). Different amounts of elastin-PEG were then intermixed with the same amount of gelatin-PEG in order to investigate how cell behavior could be guided by elastin amount. ‘‘GPE control’’ represents the gel made from gelatin-PEG precursor 48mg/mL (4.80 wt/v %) with 9mg/mL (0.90 wt/v %) PEGDA and 15 mg/mL (1.50 wt/v %) physically-incorporated soluble elastin. The control was designed to explore whether covalently-bound elastin had a different effect on cells as compared to physically-incorporated soluble elastin. The 0.90 wt/v % PEGDA was added to the control in order to obtain comparable mechanical properties as acrylate groups in elastin-PEG (GEP 45 and GEP30) also could increase the mechanical properties.

Table 6.1 The composition of GEP45, GEP30 and GPE control hydrogels. GPE control contains physically incorporated soluble elastin, gelatin-PEG precursor (4.80 wt/v %) and 0.90wt/v % PEGDA. Soluble elastin and PEGDA were covalently conjugated to the elastin-PEG precursor before fabricating GEP45 and GEP30, while PEGDA was adding to GPE control to have similar mechanical properties as GEP45 and GEP30.

	Gelatin-PEG concentration (wt/v %)	Elastin-PEG concentration (wt/v %)	Elastin concentration (wt/v %)	PEGDA concentration (wt/v %)
GEP45	4.80	4.50	0	0
GEP30	4.80	3.00	0	0
GPE control	4.80	0	1.50	0.90

6.2.3 Cell encapsulation in gelatin/elastin hybrid PEG hydrogel

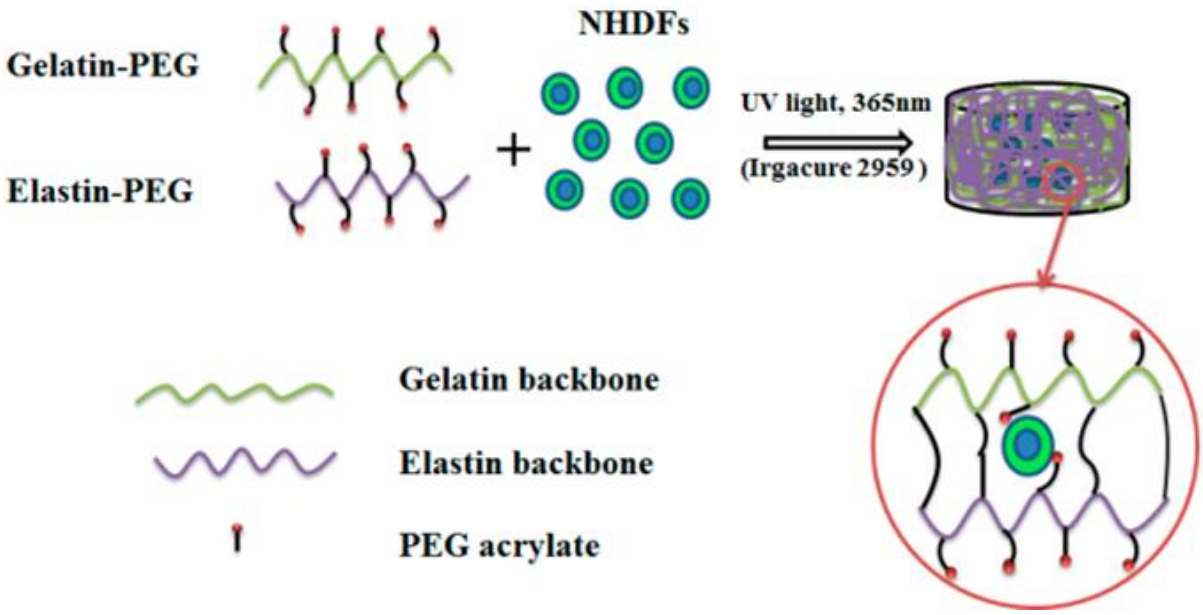

Figure 6.2 Illustration of Cells encapsulation into ECM proteins hybrid PEG-hydrogel using photo-polymerization with photo-initiator.

Cell laden gelatin-PEG and elastin hybrid hydrogels were fabricated as presented in Figure 6.2. NHDFs (Passages 5-8) were used for cell encapsulation. The precursor

solution was made by dissolving elastin-PEG powder into gelatin-PEG solution with 0.1 w/t % Irgacure 2959 at 37℃ as gelatin-PEG precursor was purified and stored in PBS (mentioned in section 2.2) at -80℃. Cell encapsulated hydrogels were fabricated from 100 μL of cells loaded suspension of gelatin-PEG and elastin-PEG (cell concentration = 2×10^6 cells/mL). After photo-polymerization, cell encapsulated hydrogels were washed by PBS and put into cell culture medium.

6.3 Results

6.3.1 Characterization of Gelatin-PEG and Elastin-PEG modification

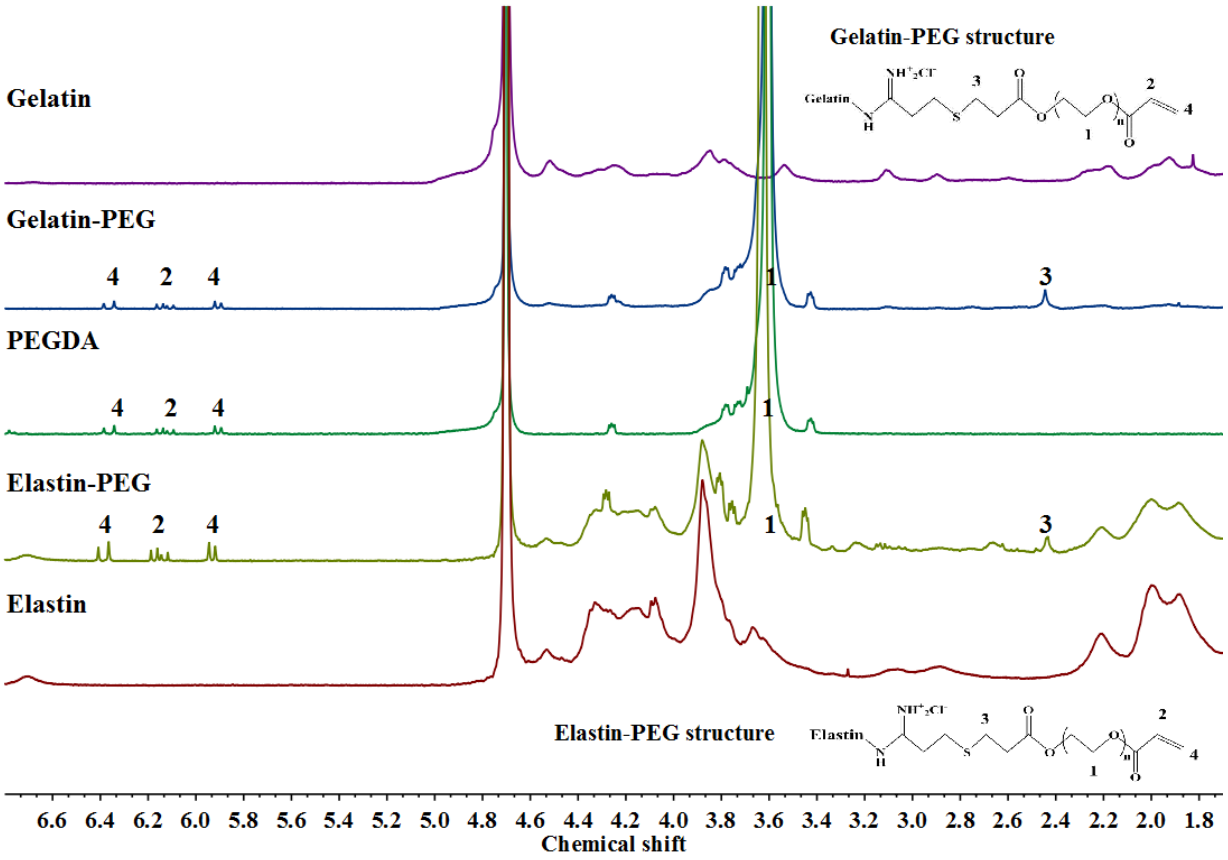

Figure 6.3 ^{1}H-NMR spectra of gelatin, elastin, PEGDA, Gelatin-PEG and Elastin-PEG.

The PEGDA shows three chemical shift peaks (protons of acrylates) at peak 1 (3.6ppm, -OCH_2CH_2-), peak 2 (6.1 ppm, -$CH=CH_2$), and peak 4 (5.8 and 6.4 ppm, -$CH=CH_2$) in

Figure 6.3,[30] while both gelatin-PEG and elastin-PEG have a new peak 3 (2.5 ppm) from the methylene protons of Traut's reagent moieties.[31] The constitution of Gelatin-PEG and Elastin-PEG precursor were shown in Table 6.2 as the protein concentration in precursor was measured by BCA method.

Table 6.2 The composition of gelatin-PEG and Elastin-PEG precursor. The concentration of gelatin and elastin in precursor were measured by BCA method. (Mean±STDEV, n=3, $p<0.05$)

	Protein ratio (%)	**PEG ratio (%)**
Gelatin-PEG	60.2±4.5	39.8±4.5
Elastin-PEG	56.4±5.8	43.6±5.8

6.3.2 Hydrogel swelling, degradation and mechanical properties

The bulk properties of the hydrogel, such as elastic modulus and swelling property, have a direct influence on cell behavior. Further, the structure of the hydrogel is related to pore size and its water amount, both of which influence oxygen and nutrients diffusion. To allow better realization of the role of hydrogel composition and architecture while minimizing the effect of mechanical properties, the three studied hydrogels GEP45, GEP30 and GPE control were selected based on preliminary measurements to give similar storage modulus.

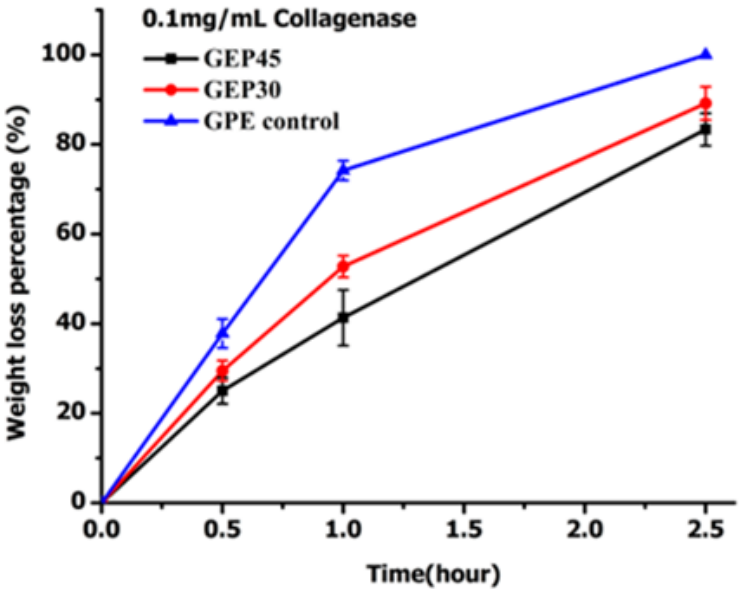

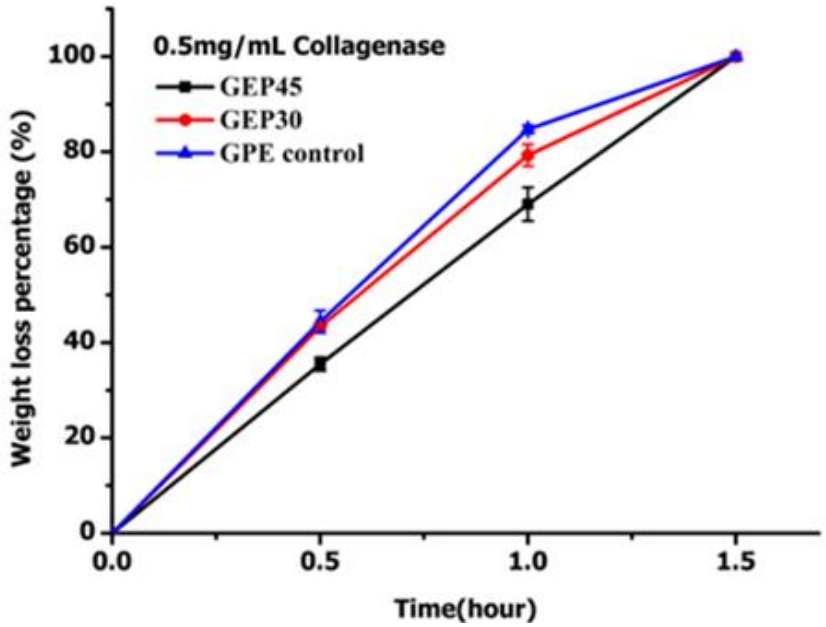

Figure 6.4 Degradation kinetics of GEP45, GEP30 and GPE control in 0.1mg/mL (top) and 0.5mg/mL(below) collagenase solution. (n=3)

The gel fractions of the resultant gelatin and elastin hybrid PEG hydrogels were investigated in order to evaluate the efficiency of the crosslinking process. The gel fractions were 88.2%±1.1%, 91.4%±2.7%, 73.8%±3.4% for GEP45, GEP30 and GPE control, respectively (n=3, $P<0.05$). The results of the gel fraction study indicate on GPE control as the hydrogel with lowest gel fraction because the physically incorporated elastin was leaching out after immersing in distilled water for 24 hours. The gel fraction of GEP 45 and GEP30 were found to be the same within experimental error and around 90%, similar to other UV photo-crosslinked PEG hydrogels. [32]

Proteolytic degradation is a basic feature for a cell-encapsulated scaffold that allows cells to rebuild their surrounding microenvironments *in situ*. Gelatin and elastin-based materials are often applied in tissue engineering based partly on their proteolytic susceptibility and partly on the ease with which the incorporated cells can remodel the ECM. Accordingly, the biodegradation kinetics of GEP45, GEP30 and GPE control in 0.1mg/mL and 0.5mg/mL collagenase type I A solution were studied and shown in Figure 6.4. Collagenase specifically recognizes and hydrolyses the X-Gly peptide bond of the peptide sequence Pro-X-Gly-Pro (X : neutral amino acids), since collagen and gelatin contain this sequence.[33, 34]All hydrogels fully degraded after 3h (0.1mg/mL

collagenase I A) or 1.5h (0.5mg/mL collagenase I A) incubation. The GEP45 and GEP30 hydrogels degraded slower than GPE control because of covalently crosslinking elastin-PEG; the hydrogel with larger elastin-PEG content displays a slower degradation rate (GEP30>GEP45). Hydrogels incubated with 0.5mg/mL collagenase displayed larger mass loss than those immersed in 0.1mg/mL collagenase at the same incubation time. Thus, PEGylation of gelatin and elastin did not obstruct the proteolytic degradation of gelatin and elastin. It should be borne in mind that such high concentrations of collagenase are not realized *in vivo*, and hence it is expected that *in vivo* biodegradation rates would be slower.

The bulk properties depend on the swelling of the hydrogel and the swelling has a direct impact on behaviors of encapsulated cells in the 3-D microenvironment. Because the encapsulation of cells into hydrogel was done during hydrogel formation, the hydrogel is in the non-equilibrium swollen state. Subsequently, when exposed to excess cell culture medium, the hydrogel will swell until equilibrium state is reached. The swelling characteristics of the gelatin and elastin hybrid PEG hydrogels are summarized in Figure 6.5. Both the covalently crosslinked gelatin/elastin hybrid hydrogels and GPE control showed rapid water absorption and swelling to near maximum swelling ratio within 1-2 days (Figure 6.5). GEP45 displayed the lowest mass swelling ratio because of the highest crosslink density due to the larger amount of crosslinked polymer (elastin + gelatin)-PEG. Conversely, the GEP30 hydrogel was expected to have a looser and more permeable polymer network after swelling. GPE control has the highest swelling ratio, as expected, as the number of crosslinked chains per unit volume is low, due to the uncrosslinked elastin part.

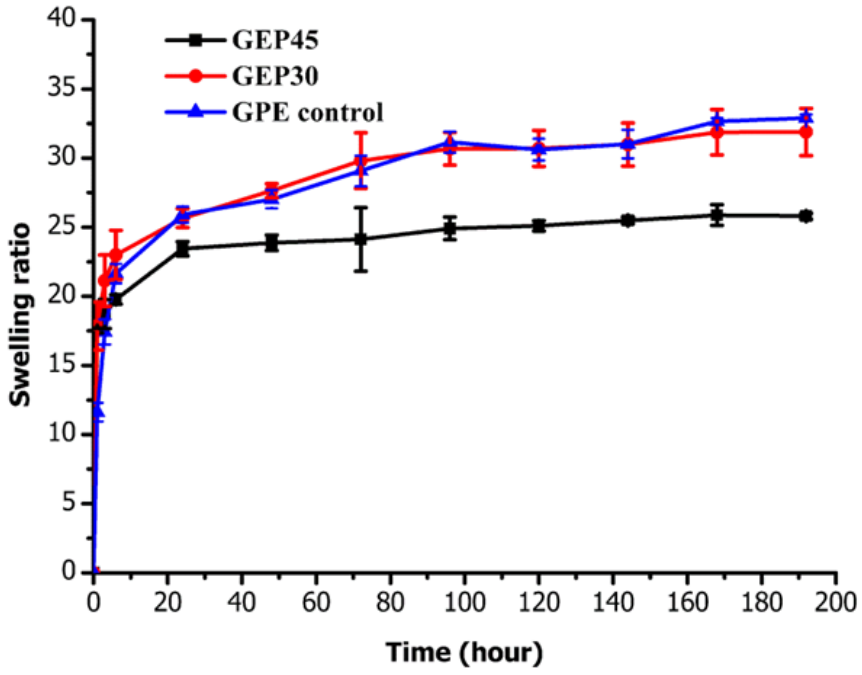

Figure 6.5 Swelling profiles of GEP45, GEP30 and GPE control. (n=3)

In this study, the change of storage modulus (G') during UV induced polymerization (without cells) was measured and shown in Figure 6.6(A). Dynamic time-sweep tests were used to measure the change of G' during UV induced polymerization (shown in Figure 6.6(A)). The polymerization of all the hydrogels started when the UV light was switched on: the G' of hydrogel increased and a plateau was reached when crosslinking was complete. As shown in Figure 6.6(A), the GEP 45 and GEP 30 polymerizations were very fast (about 3 mins), resulting in the formation of a continuous polymer network from the precursors. The initial complex viscosity of GEP45, GEP30, GPE control at 1Hz and GP are 44.0, 22, 0.2 and 0.1 Pa·s. The viscosities of GP, GEP 30, GEP 45 and GPE control precursor were measured at three different shear rates (0.1, 230, 500 s^{-1}) and shown in Table 6.3. The viscosity of GEP 30 and GEP 45 decreased with increasing the shear rates as expected of shear thinning materials, the low viscosities at shear rates >100 sec^{-1} are indicative of injectability using the appropriate needle dimensions that dictate the imposed stress levels of injection.

Porosity available for cells in the hydrogel is another crucial obstacle that hinders cellular growth and tissue regeneration.[35] As we all know, higher the storage modulus (smaller

mesh size) cause less space in the 3-D microenvironments for the cells, and it is more challenge for the cells to possess enough porosity for the attachment and spreading. In this study, the *in situ* shear storage modulus (G') of the three hydrogels (with incorporated cells) were studied as shown in Figure 6.6(B). All the cell encapsulated hydrogels have similar initial storage modulus at day 0 (GEP45, GEP30 and GPE control have moduli of 157.7±14.9 Pa, 131.0±10.0 Pa and 150.0±15.9 Pa, respectively in Figure 6.6(b)). The mechanical properties of the hybrid hydrogels are highly related to the increasing precursor amount (higher acrylate content) and thus G' of GEP45 > G' of GEP30. The storage modulus of GEP45, GEP30 and GPE control hydrogels decreased rapidly after swelling for one day as shown in Figure 6.6(B) and then continuously decreased during the following 7 days.

Table 6.3 The viscosities of GP, GEP 30, GEP 45 and GPE control precursor at different shear rates.

	Viscosity (Pa·s)		
Shear rate (s^{-1})	0.1	230	500
GP	0.0880	0.0109	0.0105
GPE control	0.0506	0.0133	0.0128
GEP 30	648	0.510	0.2620
GEP 45	1080	0.675	0.3450

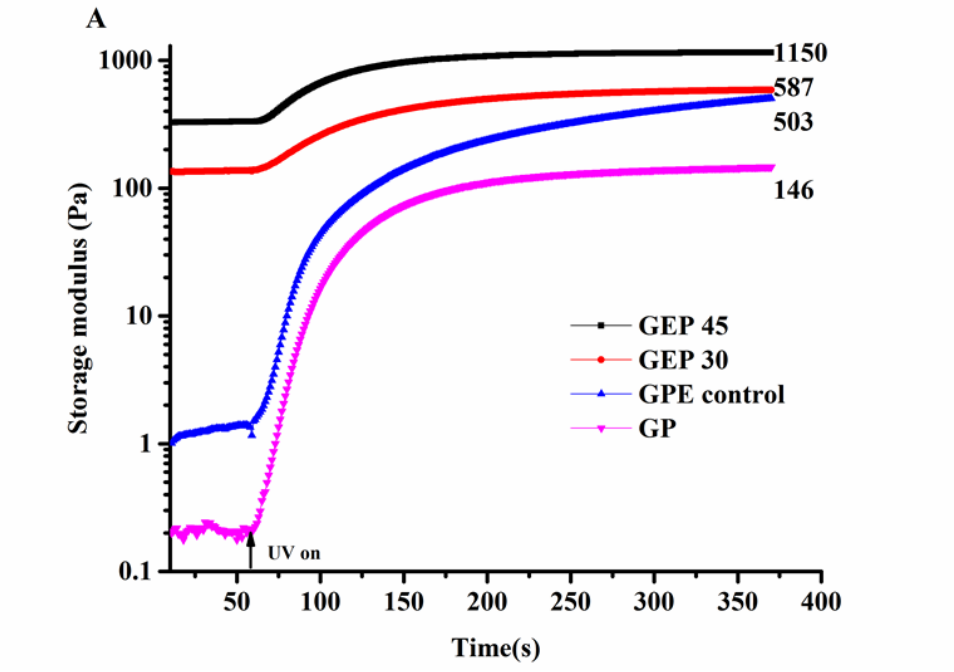

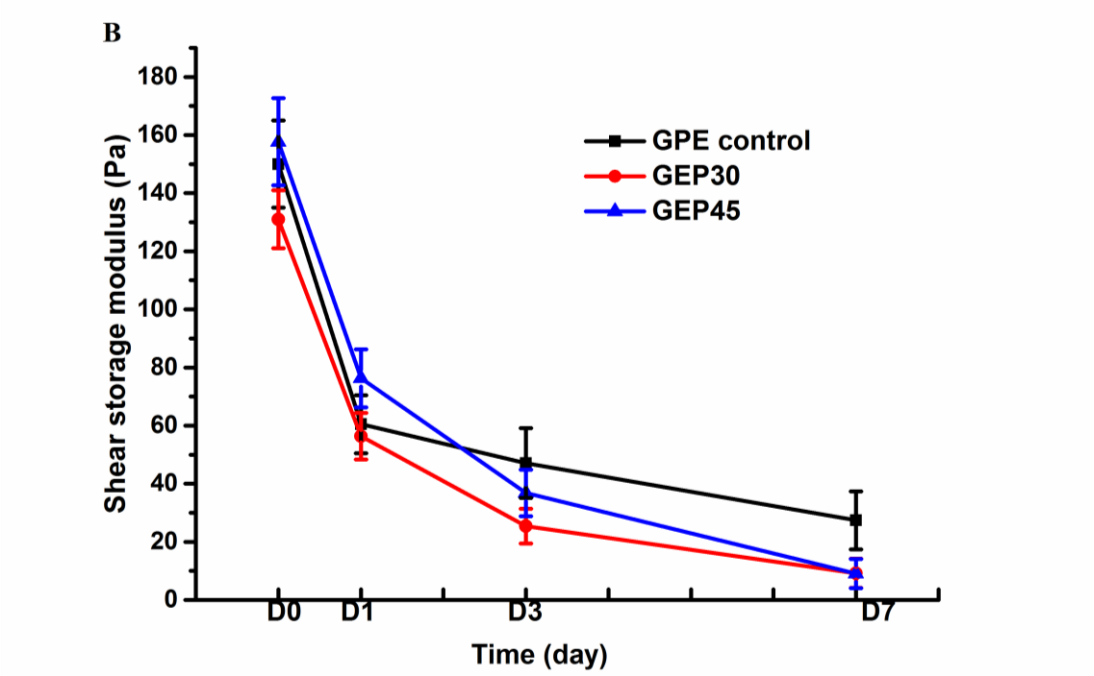

Figure 6.6 (A) Shear storage modulus from dynamic time-sweep tests that were measured during the polymerization of all the hydrogels. The UV light was switched on after 60 seconds. The initial complex viscosity of GEP45, GEP30, GPE control and GP hydrogels were 44, 22, 0.20 and 0.05 Pa·s, respectively; (B)The *in situ* storage modulus change of several cell laden gelatin and elastin hybrid PEG hydrogel at day0, 1, 3 and day7. (n=3, $p<0.05$).

6.3.3 Cell Morphology in 3-D hydrogels

To explore cell-material interaction in 3-D microenvironments, human dermal fibroblasts encapsulated in covalently crosslinked gelatin and elastin hybrid PEG hydrogels (GEP45, GEP30 and GPE control) were studied by staining with Calcein-AM and EthD-1. The interactions between fibroblasts and 3-D microenvironments are initiated by the binding of integrin receptors to the specific motifs in ECM. [35] Gelatin provides cell binding motifs as it contains several cell adhesion sequences, such as RGD. As shown in Figure 6.7, some of NHDFs encapsulated in GEP45 and GEP30 hydrogels were able to attach on day 1, while those incorporated in GPE control hydrogels needed more time to attach (on day 3). More NHDFs in GEP45 and GEP30 hydrogel attached on day 3, while only some of NHDFs attached on day 3 in the control. By day 7, the cells in GEP45 and GEP30 hydrogel started to spread and join with neighboring cells to form intercellular networks,

whereas in the GPE control hydrogel, the cells were dispersed with limited intercellular contacts. In the three hydrogels studied here, significant differences were shown on day 10: NHDFs in gelatin and elastin hybrid PEG hydrogels (GPE45 and GPE30) showed extensive cell spreading and the formation of intercellular networks, whereas NHDFs encapsulated in GPE control with physically incorporated elastin showed limited spreading and intercellular networks. All the cells encapsulated into those three hydrogels showed live cell percentage over 95% from day 1 to day 10.

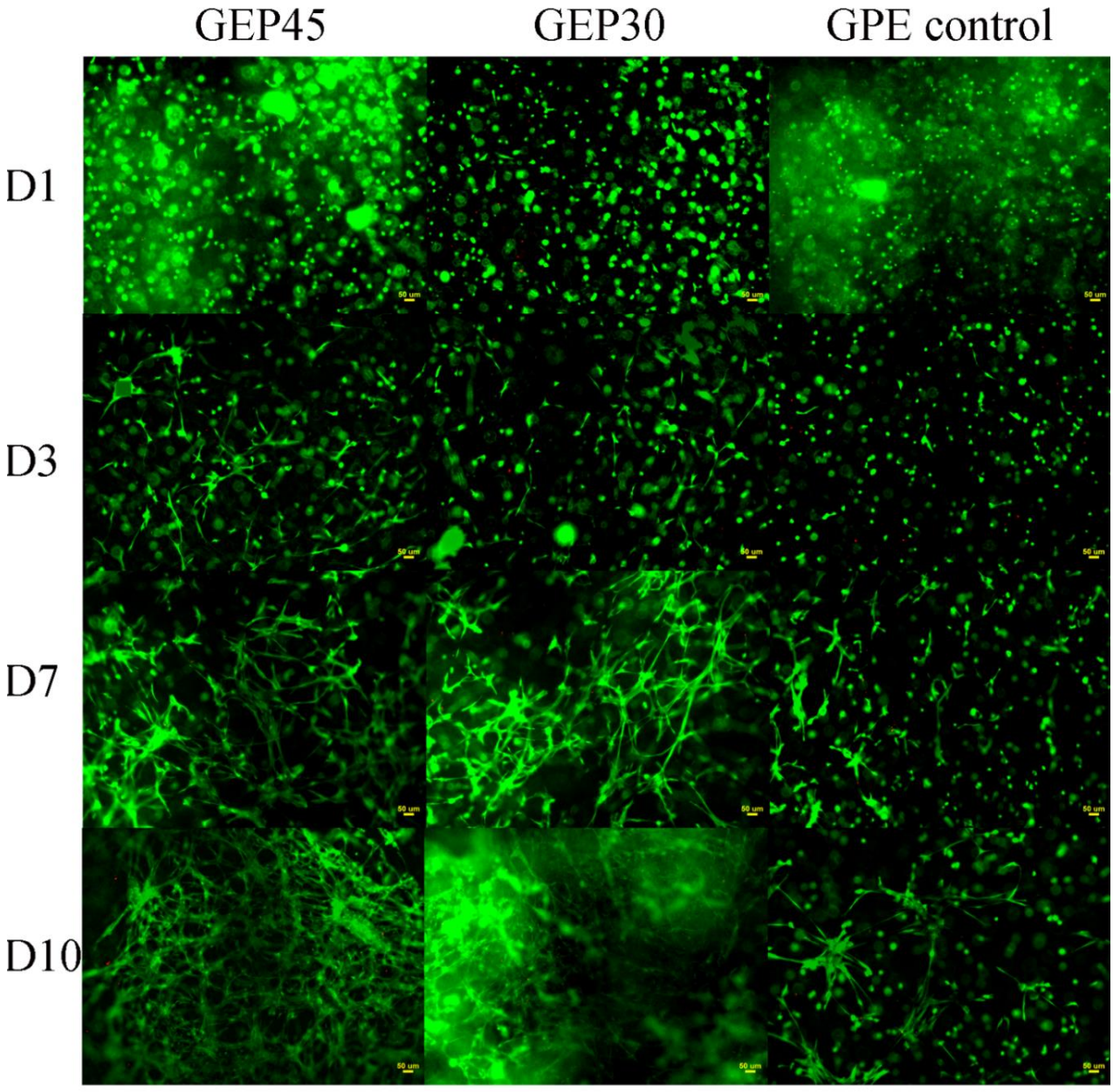

Figure 6.7 3-D cell encapsulation in gelatin and elastin hybrid PEG-hydrogels. Live/dead staining shows the morphology and survival of cells inside the gel (Live: green/Dead: red). The scale bar represents 50μm.

6.3.4 Cell proliferation

To further explore the interaction between cell and material, a cell proliferation study was conducted to investigate cell behavior on these three types of hydrogels. EdU is a nucleoside analog to thymidine and is incorporated into DNA during active DNA synthesis.[36] In this study, EdU was incubated with cell encapsulated hydrogel for 24 hours in order to measure the proliferation of NHDFs in 24 hours. Using flow cytometry to quantify the proliferation of cells, we observed that the percentage of proliferated cells in the gelatin and elastin hybrid PEG hydrogel constructs increased faster than those in Gelatin-PEG hydrogel with physically incorporated elastin (Figure 6.8). The cells in all three hydrogel formulations showed no proliferation on day 1, while the percentage of proliferated cells increased from day 3 after they attached to the ECM protein and the hydrogels swell to the maximum status. Further on, with sufficient degradation and enough space, cells migrate toward one another to form cell-cell junctions, adopt a more elongated morphology (shown in Figure 6.7) and proliferate more in these hybrid hydrogels (illustrated in Figure 6.8). In the case of the GPE control, this benefit is counterbalanced by the leaching out of elastin, as leaching and degradation occur concurrently. Thus we conclude that covalently crosslinking soluble elastin into gelatin-PEG hydrogels facilitates faster proliferation rate compared to the control (gelatin-PEG hydrogel with physically incorporated elastin).

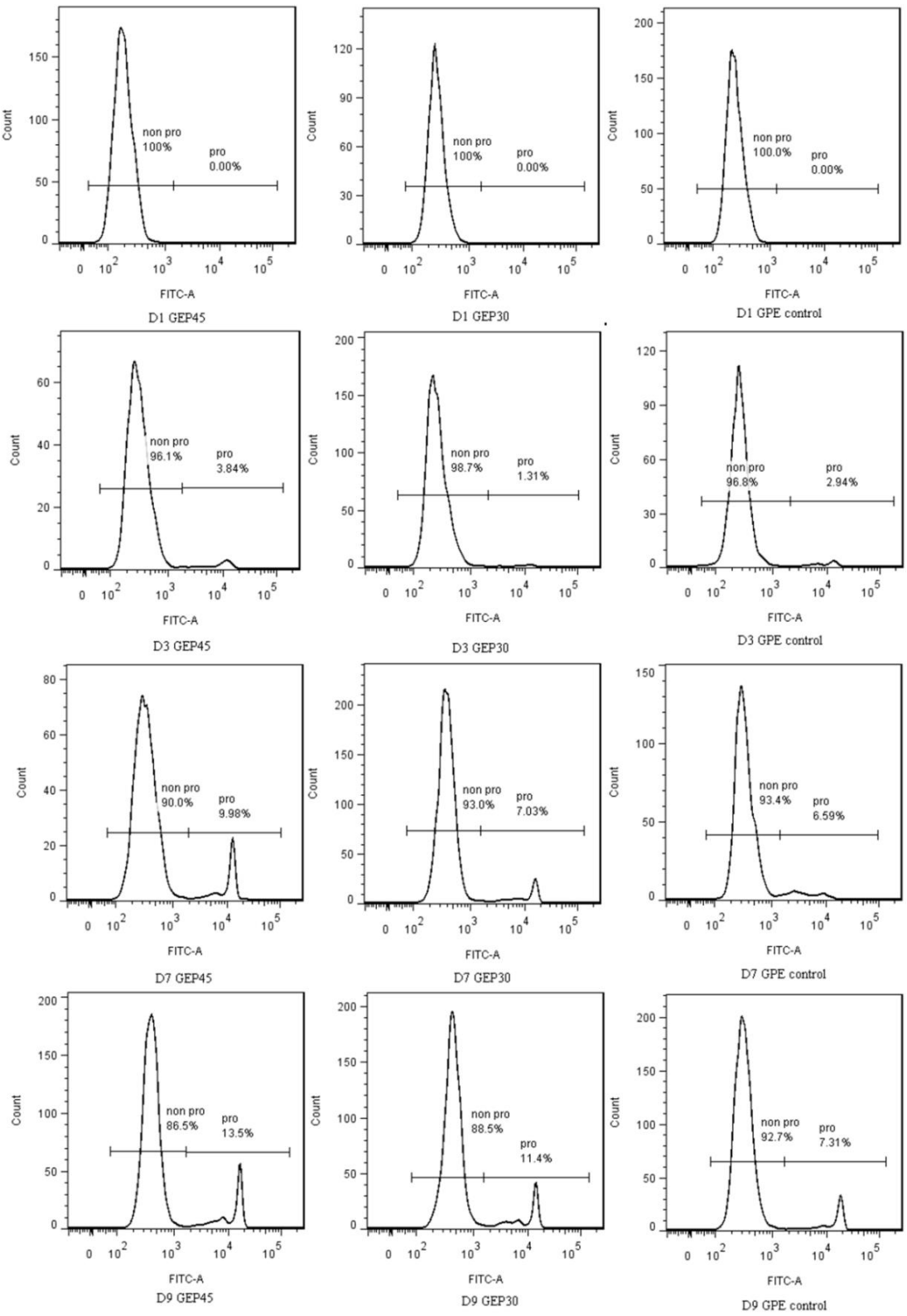

Figure 6.8 Cell proliferations of NHDFs encapsulated in GEP45, GEP30 and GPE control at day 0, 3, 7 and 9. The single-parameter histograms of fluorescence EdU-488 levels for flow

cytometry data was used to estimate the percentage of proliferation cells during 24hours EdU incubation. (Non pro represents the percentage of non-proliferation cells, while pro means the percentage of proliferation cells.)

6.3.5 ECM deposition

The biochemical matrix remodeling associated with cellular activity in the gelatin and elastin hybrid PEG hydrogel includes the production of structural proteins such as collagen, as well as the synthesis of elastin. Elastin synthesis is often an obstacle in tissue engineering, especilally in dermal substitutes.[37] In order to further delineate the ECM deposition and cellular morphogenesis in the three hydrogels, NHDFs cultured within each hydrogel sample were fixed after 10 days culture, stained for elastin (green), type I collagen (yellow), F-actin (red) and cell nuclei (blue) and finally imaged via confocal microscopy. As seen in Figure 6.9, NHDFs within all samples displayed a certain level of F-actin bundling; cells in GPE45 and GPE30 showed significant cytoplasmic spreading and F-actin bunding compared with GPE control hydrogels. This indicated a more active interaction between fibroblasts and GPE45 or GPE30 because of the existence of covalently conjugated soluble elastin. It should be particularly noted that the stretched morphology is extremely important for the survival and function of anchorage-dependent cells: for example, Chen et al. reported that the spheroidal anchorage-dependent cells were prone to apoptosis but streched cells survive and proliferate.[15] Higher elastin concentration in GPE45 provided more biological cues in the form of GXXPG peptide sequences such as VGVAPG[38], thus promoting the proliferation (Figure 6.8).

Subsequent immuno-staining analysis (Figure 6.9) confirmed the presence of newly synthesized ECM proteins, while the gene expressions of collagen and elastin (Figure 6.10) were quantiflied to explain the effect of added elastin. Fibroblasts cultured within all three hydrogels were stained for collagen type I, elastin and F-actin. Expression of elastin and collagen, the most abundant ECM proteins in elastic tissue, were more pronounced in GPE45 and GPE30 compared to GPE control. All ECM proteins were located near fibroblasts, and cohesive collagen and elastin fiber networks were formed

within the GEP45 and GEP30 constructs. Real-time PCR analysis (Figure 6.10) quantitatively proved that more collagen I A and elastin gene expression were found in the GEP45 hydrogel, indicating that covalently conjugating more elastin into gelatin-PEG hydrogel did promote cell proliferation and then increased more ECM protein deposition. The reason has been elaborated in the previous paragraph. This corresponds well to the work of Willeke et al. who have previously demonstrated that the addition of solubilized elastin was able to markedly improve the regeneration of collagen and elastin due to the biological effects of elastin.[23] Aleksander et al. also have previously reported that dermal fibrobalsts stimulated with proteolytic digest derive elastin injected into the skin of nude mice or human skin explants showed increased elastin gene expression compared to untreated cells.[39]

A

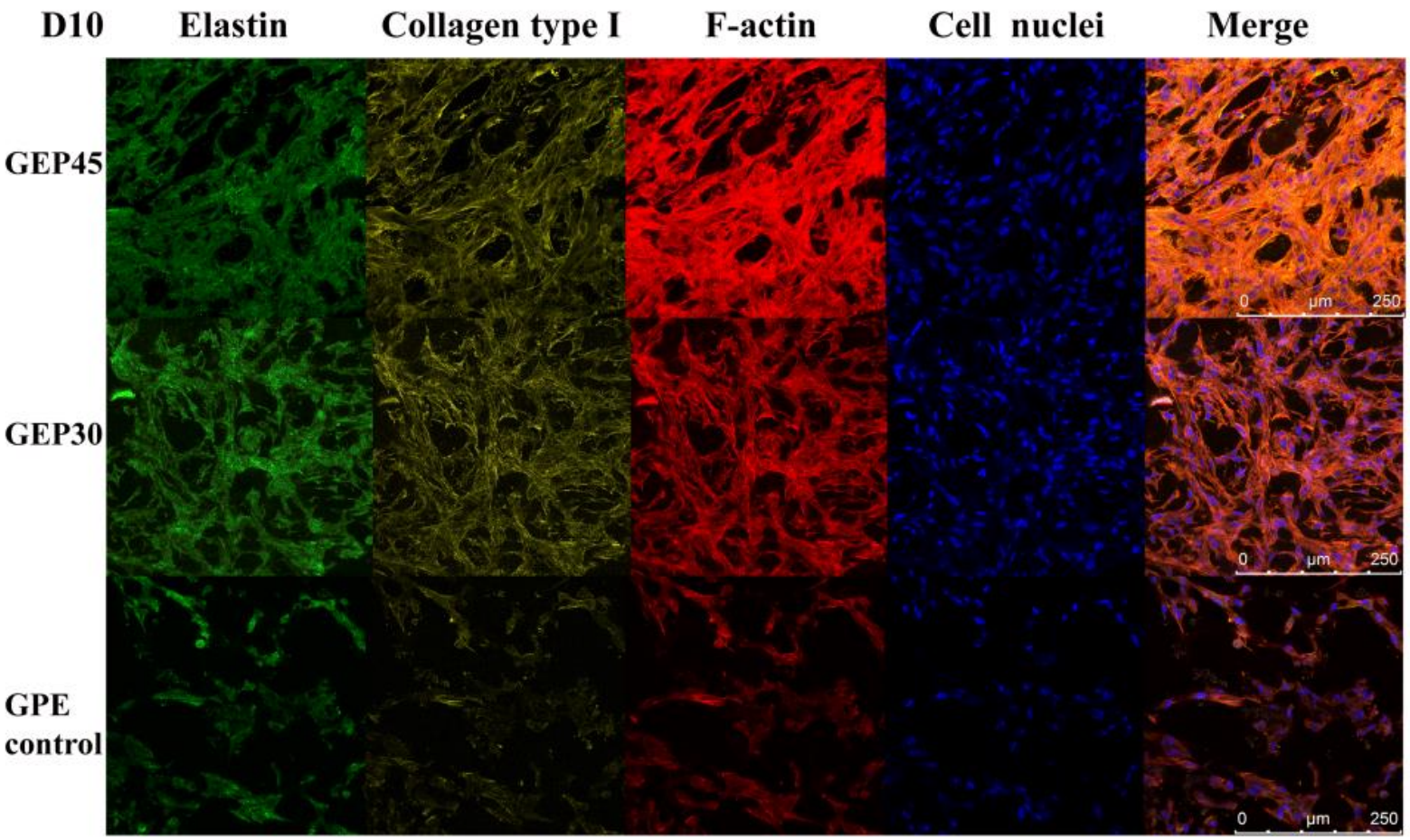
D10
Elastin
Collagen type I
F-actin
Cell nuclei
Merge
GEP45
GEP30
GPE control
0 µm 250
0 µm 250
0 µm 250

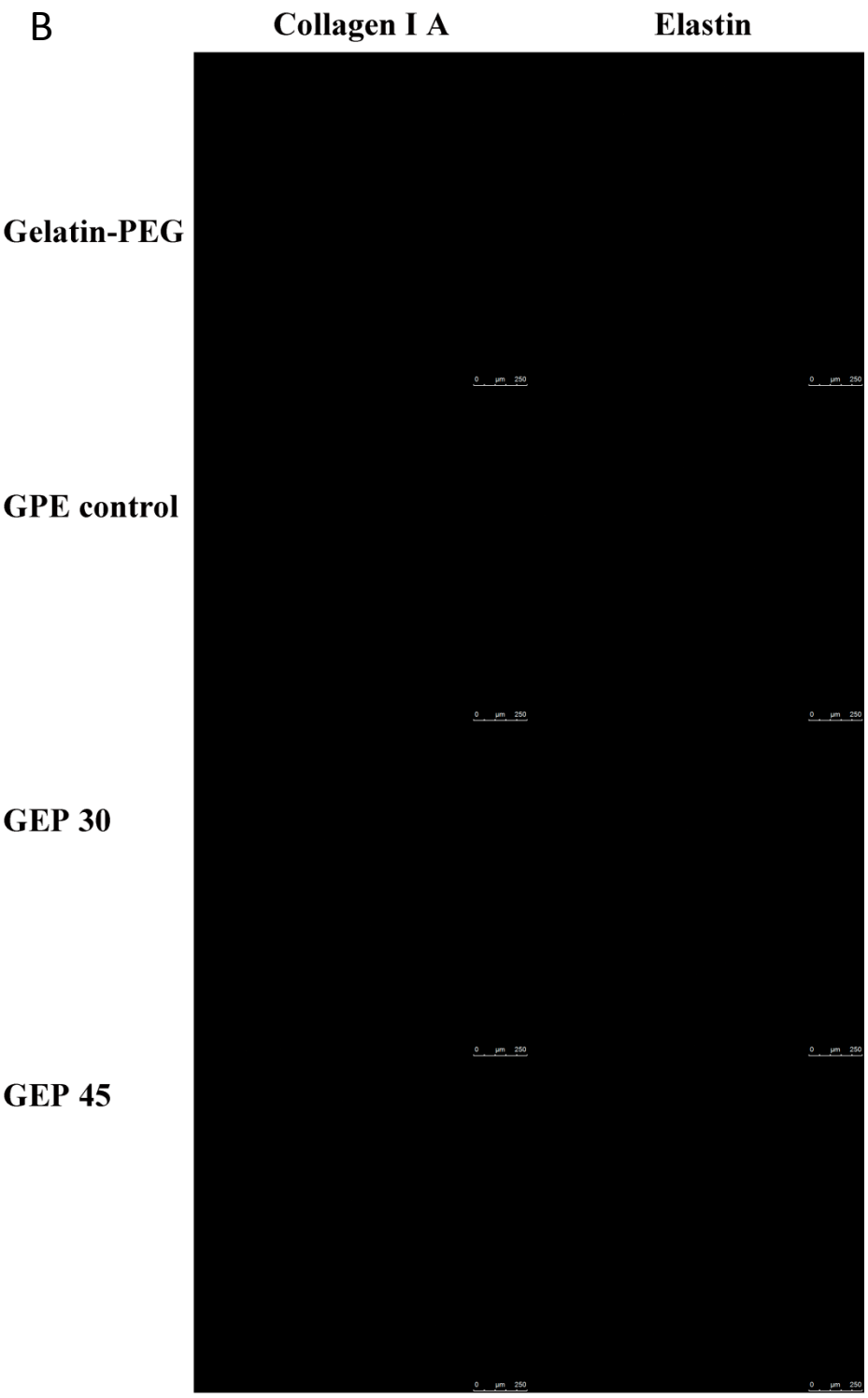

Figure 6.9 (A) Immunofluorescence staining for elastin, collagen type I, F-actin in GEP45, GEP30 and GPE control at day 10. Scale bar=250µm.The antibodies are only reactive with human specific collagen type I and elastin. (B) Immunofluorescence staining for elastin (green) and collagen type I A (yellow) in cell free GEP45, GEP30 and GPE control. Scale bar=250µm.

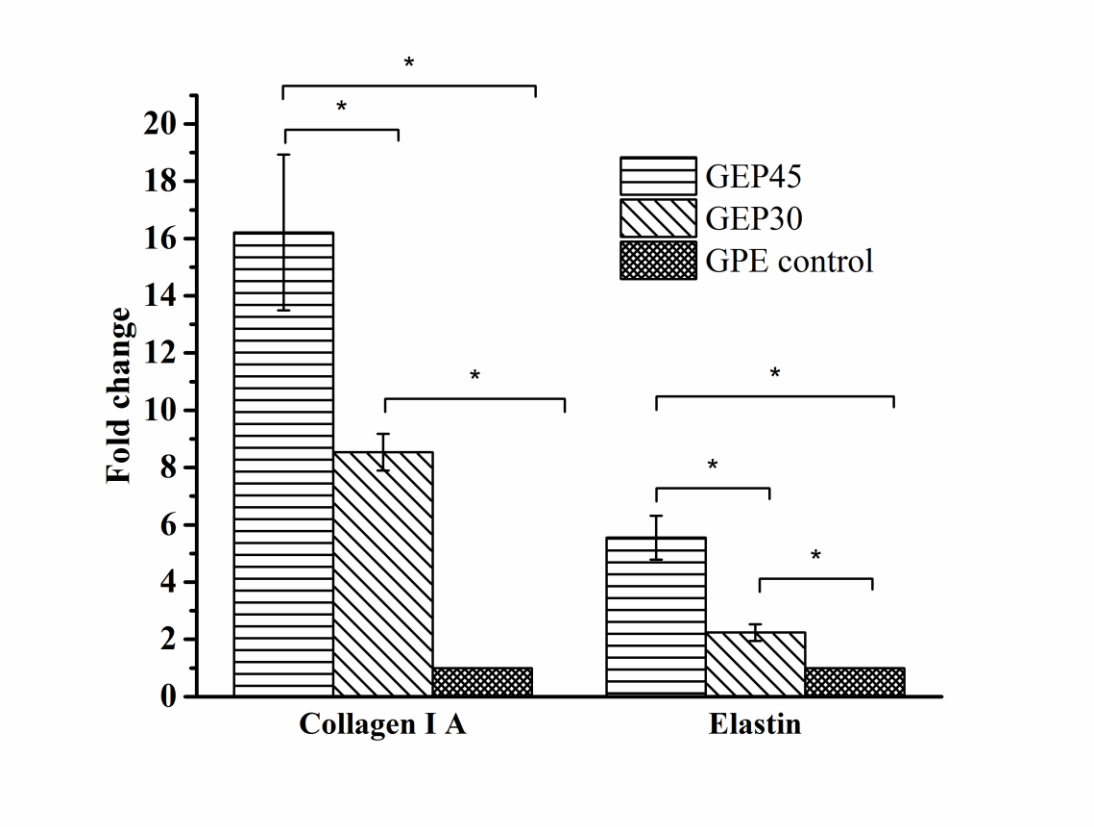

Figure 6.10 Effect of elastin addition on ECM proteins (collagen 1A and elastin) gene expression at day 9. Elastin addition resulted in a significant increase in collagen 1A and elastin at day 9. Gene expression was normalized to the housekeeping gene GAPDH and expressed as fold change versus NHDFs seeded GPE control hydrogels (considered as 1) at day 9. * denote $p<0.05$.n=4.

6.4 Summary

An ECM-mimicking hybrid hydrogel was fashioned out of crosslinkable gelatin and elastin molecules. By comparing the hybrid hydrogel to a gelatin hydrogel incorporating soluble elastin, we have shown quantitatively how covalent linking of elastin to the network is necessary for proliferation of dermal fibroblasts within these hydrogels in 3-D. Results confirmed that the chemical interpenetrating network of gelatin-PEG and elastin-PEG was an effective means of combining the beneficial properties of both proteins to better mimic the physical, mechanical and biological cues offered by the soft

tissue or skin dermis. In particular, despite the presence of cell binding motifs provided by gelatin, we found that a higher concentration of elastin-PEG in the biomatrix promotes dermal fibroblast proliferation and ECM deposition and performs better in remodeling their ECM microenvironments. Furthermore, our results indicated that these ECM protein and synthetic hybrid hydrogels, in contrast to a natural ECM single-component gel such as collagen, may be adapted to mimic the desired ECM microenvironments and to incorporate target biological cues.

References

[1] D. E. Ingber, V. C. Mow, D. Butler, L. Niklason, J. Huard, J. Mao, I. Yannas, D. Kaplan, G. Vunjak-Novakovic. *Tissue engineering*. **2006**, 12, 3265-3283.

[2] K. H. Nakayama, L. Hou, N. F. Huang. *Advanced Healthcare Materials*. **2014**, 3, 628-641.

[3] N. A. Peppas, J. Z. Hilt, A. Khademhosseini, R. Langer. *ADVANCED MATERIALS-DEERFIELD BEACH THEN WEINHEIM-*. **2006**, 18, 1345.

[4] M. A. Fernandez-Yague, S. A. Abbah, L. McNamara, D. I. Zeugolis, A. Pandit, M. J. Biggs. Advanced drug delivery reviews. 2015, 84, 1-29.

[5] K. Xu, Y. Fu, W. Chung, X. Zheng, Y. Cui, I. C. Hsu, W. J. Kao. Acta Biomaterialia. 2012, 8, 2504-2516.

[6] Y. Fu, K. Xu, X. Zheng, A. J. Giacomin, A. W. Mix, W. J. Kao. Biomaterials. 2012, 33, 48-58.

[7] M. Gonen-Wadmany, R. Goldshmid, D. Seliktar. Biomaterials. 2011, 32, 6025-6033.

[8] D. J. Munoz-Pinto, A. C. Jimenez-Vergara, T. P. Gharat, M. S. Hahn. Biomaterials. 2015, 40, 32-42.

[9] M. W. Tibbitt, K. S. Anseth. Biotechnology and bioengineering. 2009, 103, 655-663.

[10] B. H. Lee, S. P. H. Tin, S. Y. Chaw, Y. Cao, Y. Xia, T. W. Steele, D. Seliktar, H. Bianco-Peled, S. S. Venkatraman. Journal of Biomaterials Science, Polymer Edition. 2014, 25, 394-409.

[11] L. D. Amer, A. Holtzinger, G. Keller, M. J. Mahoney, S. J. Bryant. Acta Biomaterialia. 2015, 22, 103-110.

[12] S. Mahadevaiah, K. G. Robinson, P. M. Kharkar, K. L. Kiick, R. E. Akins. Biomaterials. 2015, 62, 24-34.

[13] H. Shih, C.-C. Lin. Biomacromolecules. 2015.

[14] M. A. Daniele, A. A. Adams, J. Naciri, S. H. North, F. S. Ligler. Biomaterials. 2014, 35, 1845-1856.

[15] C. S. Chen, M. Mrksich, S. Huang, G. M. Whitesides, D. E. Ingber. Science. 1997, 276, 1425-1428.

[16] J. A. Burdick, K. S. Anseth. Biomaterials. 2002, 23, 4315-4323.

[17] T. Loth, R. Hötzel, C. Kascholke, U. Anderegg, M. Schulz-Siegmund, M. C. Hacker. Biomacromolecules. 2014, 15, 2104-2118.

[18] J. Rnjak, S. G. Wise, S. M. Mithieux, A. S. Weiss. Tissue Engineering Part B: Reviews. 2011, 17, 81-91.

[19] A. Vasconcelos, A. C. Gomes, A. Cavaco-Paulo. Acta Biomaterialia. 2012, 8, 3049-3060.

[20] L. Buttafoco, P. Engbers‐Buijtenhuijs, A. Poot, P. Dijkstra, W. Daamen, T. Van Kuppevelt, I. Vermes, J. Feijen. Journal of Biomedical Materials Research Part B: Applied Biomaterials. 2006, 77, 357-368.

[21] C. N. Grover, R. E. Cameron, S. M. Best. Journal of the Mechanical Behavior of Biomedical Materials. 2012, 10, 62-74.

[22] A. J. Ryan, F. J. O'Brien. Biomaterials. 2015, 73, 296-307.

[23] W. F. Daamen, S. T. Nillesen, R. G. Wismans, D. P. Reinhardt, T. Hafmans, J. H. Veerkamp, T. H. Van Kuppevelt. Tissue Engineering Part A. 2008, 14, 349-360.

[24] W. Daamen, S. Nillesen, T. Hafmans, J. Veerkamp, M. Van Luyn, T. Van Kuppevelt. Biomaterials. 2005, 26, 81-92.

[25] N. Annabi, S. M. Mithieux, A. S. Weiss, F. Dehghani. Biomaterials. 2009, 30, 1-7.

[26] N. Annabi, S. M. Mithieux, E. A. Boughton, A. J. Ruys, A. S. Weiss, F. Dehghani. Biomaterials. 2009, 30, 4550-4557.

[27] D. V. Bax, U. R. Rodgers, M. M. Bilek, A. S. Weiss. Journal of biological chemistry. 2009, 284, 28616-28623.

[28] A. Fathi, S. M. Mithieux, H. Wei, W. Chrzanowski, P. Valtchev, A. S. Weiss, F. Dehghani. Biomaterials. 2014, 35, 5425-5435.

[29] G. T. Hermanson. *Bioconjugate techniques*, *Academic press*, **2013**.

[30] M. B. Browning, E. Cosgriff-Hernandez. *Biomacromolecules*. **2012**, 13, 779-786.

[31] R. Singh, L. Kats, W. A. Blättler, J. M. Lambert. *Analytical biochemistry*. **1996**, 236, 114-125.

[32] V. X. Truong, K. M. Tsang, G. P. Simon, R. L. Boyd, R. A. Evans, H. Thissen, J. S. Forsythe. *Biomacromolecules*. **2015**, 16, 2246-2253.

[33] E. H. Chung, M. Gilbert, A. S. Virdi, K. Sena, D. R. Sumner, K. E. Healy. *Journal of Biomedical Materials Research Part A*. **2006**, 79, 815-826.

[34] Y. Ariyoshi. *Trends in Food Science & Technology*. **1993**, 4, 139-144.

[35] C. Wang, R. R. Varshney, D.-A. Wang. *Advanced Drug Delivery Reviews*. **2010**, 62, 699-710.

[36] J. A. Bradford, S. T. Clarke, in *Current Protocols in Cytometry*, John Wiley & Sons, Inc., 2001.

[37] A.-T. N. Truong, A. Kowal-Vern, B. A. Latenser, D. E. Wiley, R. J. Walter. *Journal of burns and wounds*. **2005**, 4.

[38] J. F. Almine, D. V. Bax, S. M. Mithieux, L. Nivison-Smith, J. Rnjak, A. Waterhouse, S. G. Wise, A. S. Weiss. *Chemical Society Reviews*. **2010**, 39, 3371-3379.

[39] A. Hinek, Y. Wang, K. Liu, T. F. Mitts, F. Jimenez. *Journal of dermatological science*. **2005**, 39, 155-166.

Chapter 7

Discussion, Conclusions and Future Work

This chapter describes the discussion of the research findings and gives the conclusions of this work. In the last section, the recommendations on the possible future work have been explained according to the various findings of this work. Overall, the findings have several potential applications: 1) *guide vascular cells (SMCs, HUVECs) behavior within gelatin and elastin hybrid PEG hydrogel in 3-D; 2) comprehensive study of the vascularization of patterned gelatin and elastin hybrid PEG hydrogel on the surface of polymer conduits.*

7.1 Discussion and conclusions

7.1.1 Elastin-PEG hydrogel for cell encapsulation

3-D elastin hydrogels have been successfully fabricated and characterized, with and without cellular encapsulation. This work has successfully demonstrated the use of EDC/NHS based thiolation method, as well as thiol and PEGDA based Michael addition reaction, and finally a cell encapsulation method based on photo-polymerization and crosslinking. Two kinds of starting elastin materials (elastin soluble, ES and elastin peptides, EP) were studied. First, the conjugation of ES-PEG and EP-PEG were confirmed by FTIR and ^{1}H-NMR spectroscopy (Figure 4.3 and Figure 4.4). After PEG conjugation, the NMR and FTIR spectrums of ES-PEG and EP-PEG showed similarity to the original proteins and to PEGDA. The spectra confirm that PEGDA was successfully covalently connected to ES and EP, respectively. The amount of sulfhydryl groups could be adjusted by changing the amount of EDC and NHS. Accordingly, the constitution of hydrogel precursor was also changed as the PEG amount is depending on the amount of thiols. Finally, the stiffness of hydrogel can be controlled by the concentration of precursor to satisfy the requirements of the selected biomedical application.

2-D cell culture results showed that fibroblast and smooth muscle cells could grow very well in the presence of ES-PEG or EP-PEG, which demonstrated that ES-PEG and EP-PEG were non-toxic and biocompatible. However, SMCs encapsulated into hydrogels were not able to attach and maintained the round shape for five days; the reason could be due to lack of strong cell adhesion peptides or sequences in the elastin. Although SMCs are not able to attach in elastin based PEG hydrogel, thus non-ADCs (anchorage-dependent cells) may be a better choice for elastin-based PEG hydrogel. One such example are native cartilage cells which are spheroidal and may easily dedifferentiate; however, they may undergo osteogenesis or other morphogenesis after adhesion and finally lose their phenotype and function.[1] The results obtained show the feasibility of incorporating cells inside an elastin-only matrix, and point to its usefulness for incorporation of proliferating non-ADCs. 3-D cell encapsulation results showed that elastin cannot support the attachment of ADCs in 3-D microenvironments.

7.1.2 Gelatin-PEG hydrogel for cell encapsulation

A 3-D gelatin-PEG acrylate precursor was also successfully prepared and characterized. The gelatin-PEG acrylate precursor was fabricated by reacting thiolated gelatin with PEGDA. NHDFs were encapsulated into several kinds of gelatin-PEG hydrogels to study the relationship between cell growth and gel stiffness. The composition of gelatin-PEG precursor could be changed via adjusting the reaction ratio between Traut's reagent and gelatin molecules, which would affect the mechanical properties of hydrogel. The composition change of hydrogel would induce a large influence on the rheological properties, swelling properties and hydrogel network mesh size. Moreover, the bulk properties of the hydrogel, like swelling property and crosslinking density, possess a significant and direct influence on cell behavior. Besides, the size of hydrogel "porosity (hydrogel network mesh size)" is highly depending on the structure of hydrogel, which influence oxygen, nutrients, signal molecules diffusion and cell adhesion.

As is well known, higher storage modulus(smaller the mesh size) will cause less "porosity" available for the cells in the 3-D hydrogel, which will induce the cells more difficult to attach, elongate, migrate and proliferate; this is shown in Figure 5.8, following the trend in Figure 5.5. Other researches also demonstrated a similar phenomenon between the stiffness of hydrogel and cell actives, even with the existing of RGD in the hydrogels.[2, 3] Blau et al. proved that muscle stem cells could die and lose their pluripotency after seeding on the surface of plastic dishes, with elastic modulus above 106 kPa. In contrast, those cells would exhibit high proliferation ability and better integration with muscle tissue when they were grew on the surface of PEG hydrogel with elastic modulus around 12 kPa. [4]

Cell adhesion is one of the most crucial parameters for choosing a suitable tissue engineering scaffold as the cell attachment is the first phenomenon for ADCs before other cell activities, including elongation, migration, proliferation and new tissue formation. In this work, NHDFs were able to adhere within gelatin-PEG hydrogel only when the hydrogel possessed enough gelatin molecules (~ 2.3 w/v %) and suitable initial storage modulus (storage modulus <~100 Pa). There are two aspects to this issue. Firstly, pure PEG hydrogel lacks cells binding sites, thus the biomimetic gelatin-PEG hydrogel must possess adequate gelatin (RGD or other adhesion peptides) to facilitate cell adhesion.

Previous studies proved that RGD amount ranging from 25 to 3.5 mmol/mL could support cell attachment and elongation in 3-D PEG hydrogels.[5] Secondly, the binding of integrin to the attachment peptides on the nanoscale could be governed by the mechanical property of scaffold, which could finally mediate the fate of cells. In this work, it is hypothesized that in fact the mesh size (physically crucial property) is governing the interactions of cells and adhesion peptides, while the mesh size can be measured based on storage modulus and swelling.

Higher stiffness hydrogels possess several advantages such as easy handling, and longer degradation time, while they also have some shortcomings. Firstly, nutrients, wastes or biological cues are difficult to diffuse, which are important for cells maintaining their normal functions, for instance, remolding new ECM. Secondly, the better mechanical property can decrease degradation speed. The degradation speed of scaffold, should match the growth speed of cells for a tissue engineering application, otherwise the hydrogel can act as a barrier for cells growth. In this work, NHDFs were not able to attach within the control hydrogel, which is a mixture of physically blended gelatin PEG hydrogel (Figure 5.8). One of the possible reasons was its unsuitable mechanical property (<~100 Pa) or the minimum mesh size, while the other reason was lacking cell binding site due to the dissolution of gelatin overtime. Another interesting finding was that the storage modulus of GP30-55 decreased fast after the cells could attach on day 3, and a sudden spike exhibited in the mesh size change (shown in Figure 5.6(B)) from day 3 to 7. According to the cell proliferation results (Figure 5.9) and mesh size results (Figure 5.6(B)), it shows that a mesh size of ~150 nm is a threshold value above which the cells can proliferate. Thus, the GP30-45 hydrogel is a better scaffold than (for instance) the GP30-55 hydrogel.

The reason for this decrease could be explained from Figure 5.7, which schematically displayed the interactions between cells and gelatin-PEG hydrogel. Cells within gelatin-PEG hydrogels showed round shape at the beginning (left of the first row and left of the second row). In the 3-D scaffold, cells are able to adhere to the hydrogel, produce enzymes to disintegrate hydrogel network (middle of the first row), elongate, migrate and finally connect (right of the first row), while the other cells start to attach, spread, migrate and finally separate to two cells.

NHDFs are ADCs and can only survive after attachment to the hydrogel network in 3-D, therefore the survival of cells are depending on the binding between integrins on the surface of cells to the adhesive peptides of gelatin in PEG hydrogel. As shown in Figure 5.7, the NHDFs in GP30-45 could adhere at day 1, vastly elongated at day 7 and showed excellent intercellular networks at day 10. However, the NHDFs in GP30-55 exhibited delayed adhesions and elongations compared to GP30-45 probably because of higher storage modulus and lower mesh size. This finding is in accordance with the change of storage modulus (presented in Figure 5.5 and schematically in Figure 5.9) and cell viability results (shown in Figure 5.10). As mentioned earlier, Chen et al. proved that round shape ADCs were more inclined to undergo apoptosis and finally die but spread cells were able to grow and experience mitosis.[6] Thus, one of the benefits of this new fabrication method based gelatin-PEG hydrogel system is high cell viability since there were few dead cells within GP30-45 and GP30-55 hydrogels presented in Figure 5.7. Though UV polymerization did not lead to any direct cell damage in this work, future carcinogenesis and mutagenesis analyses are essence for proving that the UV-polymerized hydrogels is really cell safe.

Though both GP60-55 and GP30-55 hydrogels possess sufficient cell attachment motifs, higher stiffness of hydrogel (smaller mesh size) could lead to delayed cell adhesion, elongation and proliferation until a suitable mesh size is showed. Some other gelatin hydrogels such as gelatin-MA PEG hydrogel [7]exhibited similar results as GP30-55 and GP60-55. 5-10% of cells within above high stiffness gelatin-MA PEG hydrogel died during waiting for a suitable mechanical property (lower stiffness or larger mesh size), though this hydrogel has longer gel life. As we all know, the mechanical properties of hydrogel influence the cell behaviors meaningfully, which is in good agreement with a recent study claiming that 3-D hydrogel with high mechanical properties can be a physical barrier and a means of restriction for cells.[8]

The fate of cells is governed by cell attachment and elongation since the mechanical property of hydrogel is able to modulate the binding of integrin and reorganization of attachment ligands on the nanoscale. To further investigate cell morphology and behavior in 3-D microenvironment, NHDFs encapsulated within gelatin-PEG hydrogels were learned *via* analysis of cytoskeleton F-actin and nucleic acid (Figure 5.11). Those results

proved that gelatin-PEG hydrogels can support NHDFs attachment and growth effectually. The results also demonstrated that NHDFs encapsulated within gelatin-PEG hydrogels showed their typical spindle morphology and behavior well to this new artificial new 3-D microenvironment. Furthermore, Figure 5.9 revealed that hydrogel with higher mechanical property acted as a barrier for cell attachment and growth in 3-D microenvironment. Thus, this novel gelatin-PEG hydrogel encapsulation system could effectively help NHDFs to rebuild new ECM by promoting the secretion F-actin and cell proliferation. In light of these results we hypothesized that the growth of NHDFs encapsulated in gelatin-PEG hydrogels can be controlled by adjusting the mechanical property or hydrogel network mesh size.

Therefore, this new method (Traut's reagent based) fabricated biomimetic gelatin-PEG hydrogel with tunable mechanical property rendered gelatin-PEG hydrogel an effective and promising scaffold for tissue engineering and cell based therapy.

7.1.3 Hybrid crosslinked Gelatin/ elastin based PEG hydrogel for cell encapsulation

In Chapter 6, 3-D ECM protein based PEG hydrogel with variable geometrical features were fabricated to better mimic desired ECM microenvironments. Gelatin was selected due to provide an excellent matrix for cellular adhesion, while elastin was particularly chosen to modulate fibroblast behaviors to be similar as desired tissue. The results of this study demonstrate that a cell delivery system can be fabricated by covalently conjugating gelatin and elastin with PEGDA. The conjugation of Gelatin-PEG and Elastin-PEG were confirmed by ^{1}H-NMR spectroscopy (Figure 6.4). After PEG connection, the spectrum of gelatin-PEG and elastin-PEG showed similarity to the unmodified proteins and PEGDA. Thus the NMR results confirm the PEGDA was successfully modified to gelatin and elastin, respectively.

The extent of cell adhesion is one of the most crucial parameters for selecting a suitable scaffold for tissue regeneration; adequate cell adhesion must occur before cell spreading, migration, proliferation and new tissue formation. Cell behavior in 3-D microenvironments is markedly different from that on the 2-D microenvironments. As is known, fibroblasts are anchorage-dependent cells and their fate depends on the

attachment to the scaffold, whereas cells that fail to adhere to the scaffold will go through apoptosis and death in a couple of weeks.[9, 10] Cells in a 3-D hydrogel are constrained to a round shape, no matter what cell type or native morphology, because of a special 3-D enlacing mechanism of hydrogel encapsulation.[10] The bulk of the hydrogels possess a hydrophilic and bio-inert microenvironment in which integrin-protein binding is not able to be initiated. Moreover, the micron sized cells are holding in the highly aqueous polymeric network with nano-scale pores. Without strong biochemical cues, the cells are restricted from stretching or moving freely in any direction. In the three hydrogels studied here, significant differences were observed on day 10: NHDFs in gelatin and elastin hybrid PEG hydrogels (GEP45 and GEP30) showed extensive cell spreading and the formation of intercellular networks, whereas NHDFs encapsulated in GPE control with physically incorporated elastin showed limited spreading and intercellular networks. The reason for this phenomenon is the effect of elastin in the gelatin and elastin hybrid hydrogels as it has the capacity to promote cell chemotaxis, attachment and proliferation[11, 12]: GEP45 has more elastin than GEP30 and this caused better cell growth. Elastin peptides, hydrolyzed from hydrophobic domains, have been identified that can modulate cell behavior by most common permutation- GXXPG motif such as VGVAPG, GVAPGV.[13] Similarly, Annabi et al. reported that α-elastin hydrogel crosslinked by glutaraldehyde (at high pressure CO_2) supported attachment and proliferation of human dermal fibroblasts on the surface of hydrogel. [14, 15] The elastin in GPE control leached out from the hydrogel during the swelling and changing of cell culture medium and thus lost the effects of the favorable peptide motifs in elastin.

The proliferation of encapsulated NHDFs was quantified by directly measuring DNA synthesis as shown in Figure 6.8. We observed that covalently crosslinking soluble elastin into gelatin-PEG hydrogels facilitated faster proliferation rate compared to the control (Gelatin-PEG hydrogel with physically incorporated elastin). And GEP45 has more elastin than GEP30 and this caused higher proliferation rate. This phenomenon can be explained that elastin possesses chemotactic properties, induces fibroblast's proliferation and regulates cell differentiation.[16, 17]

The actin cytoskeleton has been widely investigated and proven to play a important effect in cell morphology and behaviors and connecting the ECM and cell interior *via* cell

attachments.[18] In Figure 6.7, our results indicated a more active interaction between fibroblasts and GPE45 or GPE30 because of the existence of covalently conjugated soluble elastin. Higher elastin concentration in GPE45 provided more biological cues, as mentioned earlier (GXXPG peptide sequences such as VGVAPG[13]), thus promoting the secretion of F-actin and proliferation (shown in Figure 6.9).It should be particularly noted that the stretched morphology is extremely important for the survival and function of anchorage-dependent cells: for example, Chen et al. reported that the spheroidal anchorage-dependent cells were prone to apoptosis but stretched cells survive and proliferate.[6]

The biochemical matrix remodeling associated with cellular activity in the gelatin and elastin hybrid PEG hydrogel includes the production of structural proteins such as collagen, as well as the synthesis of elastin. Elastin synthesis is often an obstacle in tissue engineering, especially in dermal substitutes.[19] As expected, more ECM proteins were found in GPE45 hydrogel, indicating that more covalently conjugating elastin into Gelatin-PEG hydrogel did promote cell proliferation and then increased more ECM proteins deposition.

In conclusions, this hybrid PEG/elastin-gelatin hydrogel system provides an improved 3-D scaffold that promotes ECM production and proliferation and is a superior substrate for soft tissue engineering in general and skin tissue engineering in particular.

7.2 Future work

Cell delivery-based therapies have been emerged as a major and promising approach in regenerative medicine, yet its therapeutic effect is depending on delivery efficiency and the growth of living mammalian cells. More specifically, the delivered cells can grow at the sites and exhibit therapeutic effects to repair damaged tissues or eliminate malignant neoplasms. Towards providing a better ECM mimicking 3-D microenvironment for cell therapy based tissue regeneration, continuous exploration in design and fabrication of cell delivery system is desired. More specifically, future work could be focused on the following three directions: i) guide vascular cells (SMCs, HUVECs) behavior within gelatin and elastin hybrid PEG hydrogel in 3-D; ii) comprehensive study of the

vascularization of patterned gelatin and elastin hybrid PEG hydrogel on the surface of polymer conduits.

Transplanted cells live *in vivo* in a complex and dynamic 3-D microenvironment, which should possess heterogeneous micro-structure that are able to facilitate dynamic delivery of signaling and biological cues like oxygen, nutrients and cell-secreted signaling molecules. However, the supply of nutrients and oxygen to transplanted cells is often limited *in vivo* by diffusion to cells within 100 - 200 μm *via* a capillary.[20] Although constructs fabricated with pore sizes between 0.8 and 8 μm were proven to allow full infiltration of host cells and neovascularization despite of material component, their inability to have enough blood supply immediately after transplantation can cause poor cellular integration or hypoxiarelated cell death in a scaffold.[21] While many scaffolds will be vascularized after several weeks, this phenomenon is often too slow to supply proper nutrition to the cells in the center of a large construct. Hence, it is necessary and crucial to design and fabricate new bio-inspired approaches for enhancing vascularization to promote survival of large tissue-engineered constructs. Elastin emerges as a potential approach to enhance vascularization while previous researches have been proven that the addition of elastin to vascular scaffolds can reduce thrombogenicity and support the growing of human vascular cells (SMCs, endothelial cells and embryonic palatal mesenchymal stem cells).[22] In addition, elastin has been proved to be able to activate pathways which dominate the proliferation and differentiation of vascular cells. More specifically, elastin can enhance gene expression of the SMC markers alpha-SMA and calponin for MSCs seeded on elastin coated biomaterials *in vitro*.[23] Elastin can bind to the 67 kDa elastin/laminin binding protein which has been proven to mediate mechanotransduction, the assembly of ECM, cell proliferation and chemotaxis.[22] Despite several advantages that elastin possesses, it has usually been ignored from synthetic vascular substitutes due to difficulty on achieving elastin and incorporating it into scaffold. As mentioned earlier, natural elastin and tropoelastin are difficult to source for biomaterials application due to its highly insolubility and complicated fabrication procedures. In this thesis, solubilized elastin overcame these problems and has been employed to guide fibroblast behavior for soft tissue engineering. Similar to the human dermal fibroblasts, this novel gelatin/elastin based PEG hydrogel system may be also

particularly fit for human artery smooth muscle cells related vascularization. Because several studies proved that elastin can modulate SMCs from a synthetic phenotype to a quiescent and contractile phenotype.[22] The ability to control SMC phenotype is an important characteristic for cardiovascular tissue engineering, which is necessary for vasoactivity and inhibition of intimal hyperplasia *in vivo*.[24] Thus, this gelatin/elastin hybrid PEG hydrogel system is capable of being utilized for soft tissue regeneration including skin, vascular tissue engineering.

The need for synthetic polymer based conduits to bypass or replace blocked arterial segments is particularly pressing, to overcome the dependence on patient derived vessels for the treatment of coronary artery related diseases. Autologous vessels collected from the patient are limited due to the shortage of suitable vessels due to reasons including previous harvest, venous disease, and anatomical variability. [22] Currently, the two clinically available synthetic vessels are polyethylene terephthalate (Dacron) and expanded polytetrafluoroethylene (ePTFE).[13] Both products show an unexpected immunity response and are highly thrombogenic, making them innately unsuitable for vascular tissue engineering.[25] Endothelial cells also cannot grow very well on these biomaterials, which can lead to chronic inflammation and hyperplasia. The shortage of autologous vessel sources and the disadvantages of current synthetic vascular grafts have driven the development of tissue-engineered vascular grafts, which mimic the structure and function of native blood vessels.[26] As mentioned above elastin has several natural advantages on enhancing vascularization. 3-D micropatterns on the polymer conduits may be employed to modulate the phenotype of SMCs, align SMCs on the surface and finally enhance the vascularization. More importantly, hydrogel can be printed, UV curing at the same time and finally patterned on the artificial conduits, while SMCs encapsulated into hydrogel.

References

[1] C. Wang, R. R. Varshney, D.-A. Wang. *Advanced drug delivery reviews*. **2010**, 62, 699-710.

[2] H. Liao, D. Munoz-Pinto, X. Qu, Y. Hou, M. A. Grunlan, M. S. Hahn. *Acta Biomaterialia*. **2008**, 4, 1161-1171.

[3] S. R. Peyton, C. B. Raub, V. P. Keschrumrus, A. J. Putnam. *Biomaterials*. **2006**, 27, 4881-4893.

[4] P. M. Gilbert, K. L. Havenstrite, K. E. G. Magnusson, A. Sacco, N. A. Leonardi, P. Kraft, N. K. Nguyen, S. Thrun, M. P. Lutolf, H. M. Blau. *Science*. **2010**, 329, 1078-1081.

[5] E. A. Phelps, N. O. Enemchukwu, V. F. Fiore, J. C. Sy, N. Murthy, T. A. Sulchek, T. H. Barker, A. J. García. *Advanced materials*. **2012**, 24, 64-70.

[6] C. S. Chen, M. Mrksich, S. Huang, G. M. Whitesides, D. E. Ingber. *Science*. **1997**, 276, 1425-1428.

[7] M. A. Daniele, A. A. Adams, J. Naciri, S. H. North, F. S. Ligler. *Biomaterials*. **2014**, 35, 1845-1856.

[8] K. Bott, Z. Upton, K. Schrobback, M. Ehrbar, J. A. Hubbell, M. P. Lutolf, S. C. Rizzi. *Biomaterials*. **2010**, 31, 8454-8464.

[9] F. G. Giancotti, E. Ruoslahti. *Science*. **1999**, 285, 1028-1033.

[10] C. Wang, R. R. Varshney, D.-A. Wang. *Advanced Drug Delivery Reviews*. **2010**, 62, 699-710.

[11] A. Kamoun, J.-M. Landeau, G. Godeau, J. Wallach, A. Duchesnay, B. Pellat, W. Hornebeck. *Cell Communication and Adhesion*. **1995**, 3, 273-281.

[12] R. M. Senior, G. L. Griffin, R. P. Mecham. *Journal of Clinical Investigation*. **1982**, 70, 614.

[13] J. F. Almine, D. V. Bax, S. M. Mithieux, L. Nivison-Smith, J. Rnjak, A. Waterhouse, S. G. Wise, A. S. Weiss. *Chemical Society Reviews*. **2010**, 39, 3371-3379.

[14] N. Annabi, S. M. Mithieux, A. S. Weiss, F. Dehghani. *Biomaterials*. **2009**, 30, 1-7.

[15] N. Annabi, S. M. Mithieux, E. A. Boughton, A. J. Ruys, A. S. Weiss, F. Dehghani. *Biomaterials*. **2009**, 30, 4550-4557.

[16] U. Rodgers, A. S. Weiss. *Biochimie*. **2004**, 86, 173-178.

[17] D. V. Bax, U. R. Rodgers, M. M. Bilek, A. S. Weiss. *Journal of biological chemistry*. **2009**, 284, 28616-28623.

[18] M. Vicente-Manzanares, C. K. Choi, A. R. Horwitz. *Journal of cell science*. **2009**, 122, 199-206.

[19] A.-T. N. Truong, A. Kowal-Vern, B. A. Latenser, D. E. Wiley, R. J. Walter. *Journal of burns and wounds*. **2005**, 4.

[20] S. J. Hollister. *Nat Mater*. **2005**, 4, 518-524.

[21] J. Rouwkema, N. C. Rivron, C. A. van Blitterswijk. *Trends in biotechnology*. **2008**, 26, 434-441.

[22] L. Nivison-Smith, A. Weiss. *Elastin based constructs*, *INTECH Open Access Publisher*, **2011**.

[23] S. Sundaram, L. E. Niklason. *Cells, Tissues, Organs*. **2011**, 195, 15-25.

[24] A. J. Ryan, F. J. O'Brien. *Biomaterials*. **2015**, 73, 296-307.

[25] M. R. Hoenig, G. R. Campbell, B. E. Rolfe, J. H. Campbell. *Arteriosclerosis, thrombosis, and vascular biology*. **2005**, 25, 1128-1134.

[26] L. Wang, J. Hu, C. E. Sorek, E. Y. Chen, P. X. Ma, B. Yang. *Expert opinion on biological therapy*. **2016**, 16, 317-330.

Publications

1. Ye Cao, Bae Hoon Lee, Havazelet Bianco Peled, Subbu S Venkatraman. Synthesis of Stiffness-Tunable and Cell-Responsive Gelatin-Poly (ethylene glycol) Hydrogel for 3-Dimensional Cell Encapsulation. Journal of Biomedical Materials Research Part A , DOI: 10.1002/jbm.a.35779.

2. Ye Cao, Bae Hoon Lee, Havazelet Bianco Peled, Subbu S Venkatraman. Hybrid Crosslinked Gelatin/Elastin Based PEG Hydrogel: An Injectable and Tunable Platform for in situ Cell Delivery. Under review.

3. Xinxin Zhao, Scott Alexander Irvine, Animesh Agrawal, Ye Cao, Pei Qi Lim, Si Ying Tan, Subbu S. Venkatraman. 3D Patterned Substrates for Bioartificial Blood Vessels-the Effect of Hydrogels on Aligned Cells on a Biomaterial Surface. Acta Biomaterialia, 26, 2015; 159–168.

4. Rongcong Luo, Ye Cao, Peng Shi, Chia-Hung Chen. Near-Infrared Light Responsive Multi-Compartmental Hydrogel Particles Synthesized Through Droplets Assembly Induced by Superhydrophobic Surface. Small, 23, 2014; 4886–4894.

5. Lee, Bae Hoon, Stella Poh Hui Tin, Su Yin Chaw, Ye Cao, Yun Xia, Terry WJ Steele, Dror Seliktar, Havazelet Bianco-Peled, and Subbu S. Venkatraman. "Influence of soluble PEG-OH incorporation in a 3D cell-laden PEG-fibrinogen (PF) hydrogel on smooth muscle cell morphology and growth." Journal of Biomaterials Science, Polymer Edition 25, NO. 4, 2014; 394-409.

Conferences

2015 The 2015 European Materials Research Society Spring Meeting, France.
Topic: 3-D Cell Encapsulation in ECM Mimicking Poly (ethylene glycol) Hydrogel for Tissue Engineering. Oral presentation

2015 The International Conference on Materials for Advanced Technologies, Singapore. Topic: Synthetic and ECM-Mimicking Gelatin-PEG Hydrogel for 3-D Living Cell Culture. Oral presentation